Development of an Analytical Method for the Quantification of Saturated Monoacylglycerols in Biodiesel

Master Thesis

to obtain the academic degree

Diplomingenieur (Dipl.-Ing.)

at the Faculty of Technical Chemistry, Chemical and Process Engineering, Biotechnology

Graz University of Technology

Lena Hirschegger, BSc.

Supervised by

Ao. Univ.-Prof. Dr. rer. nat. Martin Mittelbach

Dr. rer. nat. Sigurd Schober

Working group Renewable Resources

Institute of Chemistry, University of Graz

2013

Danksagung

Ich möchte mich ganz herzlich bei meiner lieben Arbeitsgruppe für die tolle fachliche und menschliche Unterstützung bedanken. Danke für eure Hilfsbereitschaft und Motivation. Ihr seid die Besten!

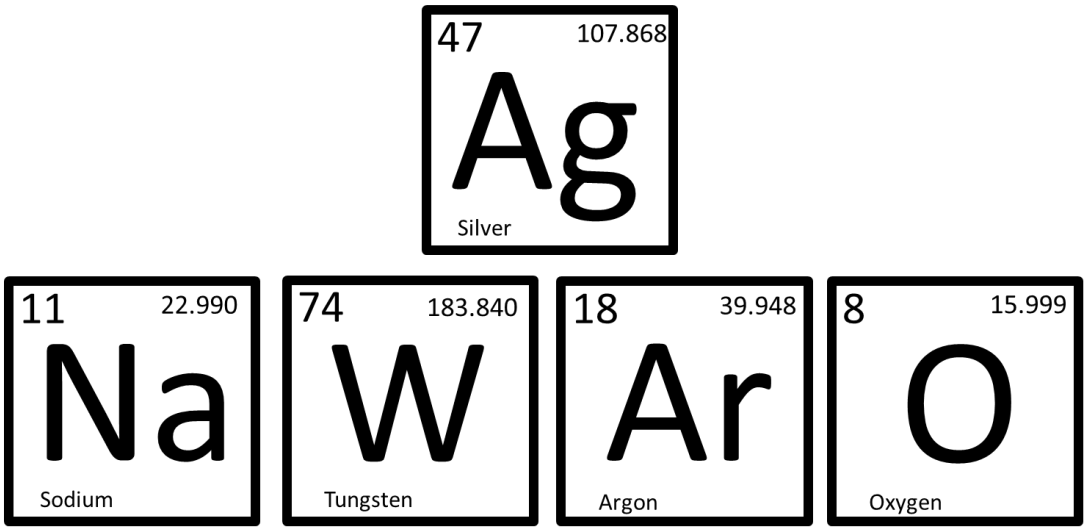

Danke Mama und Papa.

Danke Patrick.

Deutsche Fassung:

Beschluss der Curricula-Kommission für Bachelor-, Master- und Diplomstudien vom 10.11.2008

Genehmigung des Senates am 1.12.2008

EIDESSTATTLICHE ERKLÄRUNG

Ich erkläre an Eides statt, dass ich die vorliegende Arbeit selbstständig verfasst, andere als die angegebenen Quellen/Hilfsmittel nicht benutzt, und die den benutzten Quellen wörtlich und inhaltlich entnommene Stellen als solche kenntlich gemacht habe.

Graz, am …… ……..

(Unterschrift)

Englische Fassung:

STATUTORY DECLARATION

I declare that I have authored this thesis independently, that I have not used other than the declared sources / resources, and that I have explicitly marked all material which has been quoted either literally or by content from the used sources.

…… ……..

date (signature)

Abstract

In this work the challenges of insufficient cold flow properties of biodiesel, due to saturated monoacylglycerols, and corresponding approaches as well as an overview of existing analytical methods for monoacylglycerols are elucidated. The experimental aim was to develop a method for the quantification of saturated monoacylglycerols in biodiesel using gas chromatography-mass spectrometry (GC-MS), due to the fact that so far no feasible method for this problem has been described in the literature. The method follows a simple analytical procedure in which the biodiesel sample is mixed with the internal standard (glyceryl monononadecanoate) and a silylating agent (N-Methyl-N-(trimethylsilyl)-trifluoroacetamide) before applying GC-MS analysis. The acquisition mode used was single ion monitoring (SIM), which allows the specific investigation of target components via their characteristic ions. This analysis mode enhances on the one hand the sensitivity of the measurements and on the other hand enables to exclude interfering substances (which elute at a similar retention time) by only detecting certain quantitation ions. The linearity between signal and concentration was investigated (R^2>0.99) and the limits of detection and quantification (LOD: 8 - 20 ng/g, LOQ: 26 - 61 ng/g) were determined. The biodiesel samples analysed with this method derived from waste animal fats and used cooking oil.

Content

List of abbreviations

1-MAG-TMS	*sn*-1-monoacylglycerol-trimethylsilylether
2-MAG-TMS	*sn*-2-monoacylglycerol-trimethylsilylether
APCI	atmospheric pressure chemical ionisation
BR-ME	methyl ester from bacon rind
CFPP	cold filter plugging point
CP	cloud point
CSFT	cold soak filtration test
CSO	cottonseed oil
DSC	differential scanning calorimetry
ECN	equivalent carbon number
EI	electron ionisation
ELSD	evaporative light scattering detection/detector
FAME	fatty acid methyl esters
FFA	free fatty acids
FID	flame ionization detection
FMT	final melting temperature
FTIR	Fourier transform infrared spectroscopy
GC	gas chromatography
HPLC	high performance liquid chromatography
HT	high temperature
IS	internal standard
LOD	limit of detection
LOQ	limit of quantification
MAG	monoacylglycerol
MS	mass spectrometry/spectrometer
MSTFA	N-Methyl-N-(trimethylsilyl)-trifluoracetamide
NP	normal phase
PF	poultry fat
PP	pour point
RID	refractive index detection/detector
RME	rapeseed oil methyl esters
RP	reversed phase

rsd	relative standard deviation
RT	room temperature
SBO	soybean oil
SEC	size exclusion chromatography
SIM	single ion monitoring
THF	tetrahydrofuran
UCO-ME	methyl ester from used cooking oil
WAF-ME	methyl ester from waste animal fat

1 Introduction

Biodiesel, as one of the most deployed renewable liquid biofuels accompanies certain quality concerns at low temperature operations. In general, the cold flow properties depend on the fatty acid composition of the particular biodiesel. However, contaminants like monoacylglycerols, especially saturated monoacylglycerols, may cause crystallization problems in biodiesel due to their high melting points and even polar characteristics [1]. The currently valid European standard method EN 14104 for the determination of free glycerol, mono-, di- and triacylglycerol (MAGs, DAGs, TAGs) contents does not include the specific quantification of saturated MAGs, which have generally been identified as one of the most harmful individual components affecting fuel quality issues and leading to filter plugging [2]. Especially blending with non-polar (hydrophobic) petro diesel decreases the solubility of the MAGs, which may accelerate precipitation [3].

The transesterification reaction of TAGs to produce biodiesel and glycerol, as a by-product, involves three steps. DAGs and MAGs are the intermediates of these reaction steps. The reaction rate of MAGs to yield fatty acid methyl esters (FAME) is significantly lower than the corresponding rates of DAGs and TAGs [4].

Achieving an acceptable fuel quality is essential for the commercial success of biodiesel. Unfortunately, there are still challenges to overcome with respect to the ability to compete economically with petro-derived diesel. One way to increase the economic viability of biodiesel is the use of inexpensive triglyceride feedstocks such as used cooking oils (UCO) and waste animal fats (WAF). These wastes do not compete with the food market, reduce production costs, and therefore, enhance the profitability of biodiesel [5].

However biodiesel from animal fats contains significantly more saturated components than biodiesel from vegetable oils like soybean- or rapeseed oil. Saturated MAGs with long chain fatty acids (C_{16}-C_{18}) have relatively high melting points, which may cause formation of solid precipitates and affect the cold flow properties [6]. A list of melting points and -ranges for saturated FAME and MAG is presented in Table 1-1.

Table 1-1 Melting points/ranges of saturated FAME and MAG

FAME	T_m [C°] [7]
Methyl laurate	4 - 5
Methyl myristate	18°C
Methyl palmitate	32 - 35
Methyl heptadecanoate	29.8 - 30.3
Methyl stearate	37 - 41 °C
Methyl arachidate	45 - 48 °C
Methyl behenate	54 - 58 °C

MAG	T_m [C°] [8]
Monolaurin	63.6
Monomyristin	72.4
Monopalmitin	78.0
Monostearin	82.7
Monoarachidin	86.1
Monobehenin	87.3

In contrast to methanol, free glycerol, salts and soaps, MAGs cannot be removed completely by washing the biodiesel with water, due to their poor water solubility [9]. Furthermore, as mentioned above, blending FAMEs with non-polar fossil diesel leads to a decrease of MAG solubility which may accelerate precipitation [3].

The European Committee for Standardization (CEN) contemplates to establish a limit value specifically for saturated MAG in biodiesel, which primarily requires a specific analysis method. At present there is no suitable test method for the determination of saturated monoglyceride content in FAME [10]. In order to be able to estimate the saturated MAG content in pure FAME, two calculation models have been introduced in the informative annex C of the European Standard EN 14214:2012.

1) The industry-based model was developed on the correlation between the saturated FAME content and the cloud point (CP) of the FAME, allowing the calculation of the saturated MAG content as follows:

$$\mu_{SMG} = \mu_{MG} \times \left(\frac{(2.248 * CP) + 17.657}{100} \right)$$

μ_{SMG} = saturated MAG content, in % (m/m)
μ_{MG} = MAG content as measured via EN 14105, in % (m/m)
CP = cloud point in °C as measured via EN 23015

2) The second model is based on the calculation of the saturated MAG content of the FAME from measurements made by EN 14103 (Fat and oil derivatives - Fatty Acid Methyl Esters - Determination of ester and linolenic acid methyl ester contents) and EN 14105 (Fat and oil derivatives - Fatty Acid Methyl Esters - Determination of free and total glycerol and mono-, di-, triglyceride contents). The model is based on the assumption that saturated fatty esters, saturated fatty acids and saturated MAGs are present in the same proportions.

$$\mu_{SMG} = \mu_{MG} \times \left({}^{\mu_{satFA}}/_{100} \right)$$

μ_{SMG} = saturated MAG content, in % (m/m)
μ_{MG} = MAG content as measured via EN 14105, in % (m/m)
μ_{satFA} = total saturated FAME content measured via EN 14103, in % (m/m)

The uncertainty of this correlation has been estimated, using the guidance set out in EN ISO 4259, and can vary from about -50 % to +50 % of the estimated content of the saturated MAGs. Because of this high level of uncertainty this correlation cannot be used to precisely specify saturated MAG content in the FAME [10].
Due to these rather imprecise approaches, the purpose of this work was the development of an adequate analysis method for the determination of saturated MAGs in FAME by gas chromatography-mass spectrometry (GC-MS).

2 Theoretical Part

2.2 MAGs in biodiesel

Biodiesel consists mainly of mono-alkyl fatty acid esters, which are produced by a transesterfication reaction of a TAG source like a fat or oil with an alcohol such as methanol or ethanol, usually in the presence of a catalyst. The process of converting the TAGs of the fats and oils to biodiesel and glycerol generally follows three steps schematically shown in Figure 2-1.

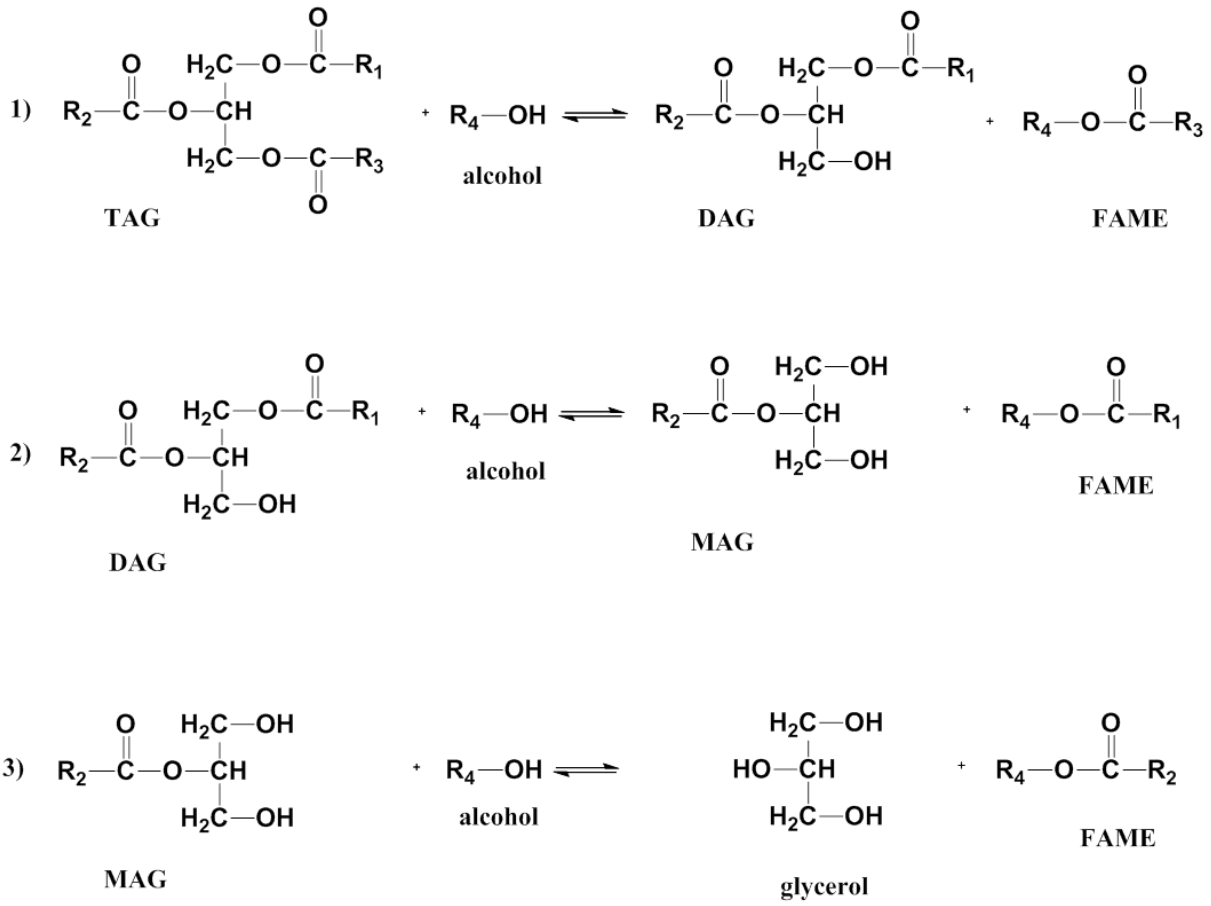

Figure 2-1 Reaction scheme of transesterification reaction to yield biodiesel from TAGs. R_1, R_2, R_3 = long-chain saturated or unsaturated hydrocarbon moiety, R_4= alkyl moiety (e.g. CH_3)

The reactions shown in Figure 2-1 are consecutive and reversible and a molar excess of alcohol as well as an increased reaction temperature and the use of a catalyst is necessary to drive the reaction [6].

Pinzi et al. studied the influence of the fatty acid composition on the optimization of the reaction temperature as one of the main parameters involved in the transesterification process. Therefore, the conversion progress of glycerides (MAGs, DAGs, TAGs) over time under optimal reaction conditions was investigated, using different feedstocks (olive-, sunflower-, maize-, linseed-, coconut and palm oil). They concluded that the MAG conversion to FAME depends on the chemical- and physical properties of the oils. It was found that the optimal reaction temperature depends on both length and the degree of unsaturation of the fatty acid chains of the vegetable oil. Vegetable oils with a higher degree of unsaturation exhibit faster conversion of monoglycerides to biodiesel [11].

2.2.1 General- and climate-related requirements for FAME

Biodiesel does not consist of 100% FAME due to impurities such as water, free glycerol, glycerides, alcohol, free fatty acids (FFA), soaps, residual catalyst and unsaponifiable matter. Unsaponifiable matter includes mainly plant sterols, tocopherols and hydrocarbons as well as very small quantities of pigments and minerals [1]. The process of the transesterification of a TAG source and an alcohol (methanol, ethanol) leaves behind small concentrations of minor constituents including MAGs that are only poorly soluble in water and can therefore not be removed by water washing of the biodiesel [9].

The currently valid quantitative limit values for glycerol and glycerides as well as other general requirements for FAME are listed in Table 2-1.

Table 2-1 Abstract of general requirements and test methods for biodiesel according to EN 14214 [10]

Property	Unit	Limit	Test method
FAME content	% (m/m)	min. 96.5	EN 14103
Density	kg/m^3	860-900	EN ISO 3675 EN ISO 12185
Viscosity at 40°C	mm^2/s	3.50-5.00	EN ISO 3104
Water content	mg/kg	500	EN ISO 12937

Total contamination	mg/kg	24	EN 12662
Monoglyceride content	% (m/m)	0.70[a]	EN 14105
Diglyceride content	% (m/m)	0.20	EN 14105
Triglycerid content	% (m/m)	0.20	EN 14105
Free glycerol	% (m/m)	0.02	EN 14105
Total glycerol	% (m/m)	0.25	EN 14105

In the currently valid version EN 14214:2012 climate-related requirements and test methods for FAME were further refined. The limits of these requirements, the cold filter plugging points (CFPP), are divided into two sections, one for temperate climates and one for arctic climates, both listed in Table 2-2.

Table 2-2 Climate-related requirements and test methods for FAME fuel [10]

Property	Unit	Limits for temperate climates						Test method
		Grade A	Grade B	Grade C	Grade D	Grade E	Grade F	
CFPP	°C, max.	+5	0	-5	-10	-15	-20	EN 116

Property	Unit	Limits for arctic climates					Test method
		Class 0	Class 1	Class 2	Class 3	Class 4	
CFPP	°C, max.	-20	-26	-32	-38	-44	EN 116

The national provisions required in EN 14214 are being given in the National Annex. In Austria the climate-dependent requirements for FAME being used as 100 % as automotive diesel fuel have to meet the specifications as follows:

Climate-dependent behaviour (CFPP grades):

Summer grade	(April 1st to September 30th),	maximum	+5°C (Class A)
Winter grade	(October 1st to February 28th),	maximum	-20°C (Class F)
	(March 1st to March 31st),	maximum	-15°C (Class E)

[a] For use as an extender to diesel fuel Table 2-3 applies

When FAME is being used as blend component in diesel fuel, for each period of the year specific combinations of CP and CFPP maximum temperature and maximum monoglyceride content shall be chosen to ensure trouble free operation of vehicles and fuel distribution systems [10]. Climate-related requirements and test methods for FAME as blend component are shown in Table 2-3.

Table 2-3 Climate-related requirements and test methods for FAME as blend component [10]

Property	Unit	Limits for cold flow property choices						Test method
		Grade a	Grade b	Grade c	Grade d	Grade e	Grade f	
CP	°C, max.	16	13	9	5	0	-3	EN 23015
CFPP	°C, max.	13	10	5	0	-5	-10	EN 116

Property	Unit	Limits for monoglyceride content choices						Test method
		Grade 1	Grade 2	Grade 3	Grade 4	Grade 5	Grade 6	
MAG content	% (m/m) max.	0.15[b]	0.30	0.40	0.50	0.60	0.70	EN 116

The national provisions required in EN 14214 are being given in the National Annex. In Austria the climate-dependent requirements for FAME being used as blend component have to meet the following specifications for the production of automotive diesel fuel:

– for summer products the requirements of grade b (CP max. +13 °C, CFPP max. +10 °C) apply,
– for winter products the requirements of grade d (CP max. +5 °C, CFPP 0 °C) apply.

The monoglyceride content according to Table 2-3 is specified with grade 6 (max. 0.70 % m/m) throughout the whole year. For Austria, the limits for saturated monoglycerides for Northern Europe winter and Northern Europe summer, i.e. 55 mg/l and 90 mg/l, respectively, are recommended [10].

[b] Meant for 100% distilled FAME, limit to be established by further test method

2.3 Effects of saturated MAGs on biodiesel quality

Saturated MAGs with long chain fatty acids (C_{16}-C_{18}) have relatively high melting points (78°C for glycerol monopalmitate and 83°C for glycerol monostearate [8]), which may cause formation of solid precipitates during storage at low temperatures and affect the cold flow properties [6].

Cold flow properties of diesel fuels are usually characterised by the cloud point (CP), cold filter plugging point (CFPP) and pour point (PP). The CP is defined as temperature at which crystals in the FAME become visible. The PP is defined as the temperature at which agglomeration of crystals is sufficiently extensive to prevent free pouring of the fluid [12].

The CFPP accords to the highest temperature at which a given volume of fuel fails to pass through a standardised filtration device in a specified time, when cooled under standardised conditions [13].

The composition of the biodiesel affects its cold flow properties. Especially the quantities of saturated compounds have a significant impact on the quality of FAME at low temperature conditions. Beef tallow possibly contains up to 5% myristic acid chains, 25-35% palmitic acid, and 20-25% stearic acid [14]. Therefore the CP, PP and CFPP of tallow-FAME respectively at 17°C (CP), 15°C (PP) and 9°C (CFPP) [15] are significantly higher compared to FAME from rapeseed oil (RME) at -3°C (PP), -9°C (PP) and -9°C (CFPP) [16]. FAME from lard shows also significantly higher values for the cold flow parameters at 11°C (CP), 12°C (PP) and 8°C (CFPP) [17]. The values for CP, PP and CFPP of the three FAMEs are listed in Table 2-4.

Table 2-4 Comparison of the cold flow properties of RME, FAME from lard and FAME from beef tallow

	RME	FAME from tallow	FAME from lard
CP [C°]	-3	17	11
PP [C°]	-9	15	12
CFPP [C°]	-9	9	8

Van Gerpen et al. investigated a paste-like material that was extracted from a plugged fuel filter which had been used with a blend of 20% biodiesel in diesel fuel (B20). The analysis of the paste showed that it consisted of MAGs and DAGs. 95% of the MAGs found in the precipitate were saturated. This led to a study in which *Van Gerpen and his co-workers* spiked methyl esters that had been distilled twice, with monopalmitin, monostearin and monoolein as well as with dipalmitin and analysed the effects on the crystallisation of the methyl esters via Differential Scanning Calorimetry (DSC). The addition of only 0.05% saturated MAGs significantly increased the CP, compared to a neat control sample, from -6°C to -4°C of the spiked methyl ester and adding 0.5% saturated MAGs led to an increase of the CP from -6°C to 10°C. The methyl esters spiked with monoolein up to 2% did not show any increase of the CP which confirmed their results from the analysis of the fuel filter paste. They concluded that unsaturated MAGs did not affect the crystallisation behaviour of the fuels [1].

There have been publications on the polymorphic characteristics of monoglycerides [18] [19]. *Chupka et al.* investigated the effect of saturated monoglycerides on the CP and the final melting temperature (FMT) of pure biodiesel (B100) as well as their polymorphic behaviour. They spiked B100 samples with saturated monoglycerides and the onset of crystallisation (CP) and the disappearance of the final solids (FMT) were analysed with a Phase Technology 70X Analyzer (diffuse light scattering). It was observed that a monopalmitin concentration of 0.2% and a monostearin concentration of 0.1% in B100 from soybean oil significantly affected the CP (increase from -0.9 to 4.8 and 6.7 °C) and FMT (increase from 0.8 to 10.2 and 10.0°C) compared to neat control samples. The polymorphic behaviour of saturated monoglycerides was investigated via DSC. MAG samples were tempered at 40°C and then heated up to 110°C [14]. They showed melting points consistent with the stable β polymorph reported by *Vereecken et al*., who additionally confirmed the assumption that β polymorph is present during the initial melting, by X-ray diffraction [8].

Chupka et al. proceeded their experiment by cyclic heating/cooling/heating of the samples. The observable re-crystallisation of the MAGs proved that the stable β form only develops during long-time storage and was not formed upon reheating of less

stable forms [14]. *Vereecken et al.* concluded that the three peaks observable during cooling of monostearin correspond to an α- and two sub-α polymorphic forms. The re-crystallisation occurred at around 75°C for the α form an at around 45 °C for the sub-α form. The melting points of different polymorphic forms of saturated MAGs, determined by DSC are presented in Table 2-5 [8].

Table 2-5 Melting points of different polymorphic forms of saturated MAGs determined by DSC [8]

	Sub-α [C°]	α [C°]	β [C°]
monolaurin	29.0	45.9	63.6
monomyristin	37.1	58.7	72.4
monopalmitin	42.5	67.1	78.0
monostearin	49.4	73.6	82.7
monoarachidin	58.3	82.1	86.1
monobehenin	65.2	86.6	87.3

These changes in crystal characteristics indicate that precipitates of saturated MAGs form upon rapid cooling the α form with a lower melting temperature and over time or upon slow heating it can transform into the higher melting β polymorph, possibly leading to fuel filter plugging above CP [14].

Tang et al. investigated the composition and the cold flow properties of precipitates in biodiesel blends from soybean oil (SBO), cottonseed oil (CSO), and poultry fat (PF) after storage at 23°C, 4°C and -15°C for 24 hours. They concluded that the higher the degree of saturation in PF- and CSO derived biodiesel blends, the higher the CP and PP compared to SBO based blends. Further they found out that the storage temperature, storage time, biodiesel blend level and feedstock affect the amount of precipitate formed. Thereby SBO based biodiesel blends at 4°C showed more precipitate than CSO- and PF based blends. The composition of the precipitates was analysed with gas chromatography-flame ionisation detection (GC-FID) and fourier transform infrared spectroscopy (FTIR), revealing that precipitates from SBO biodiesel blends mainly consist of steryl glucosides whereas precipitates from PF

biodiesel blends are due to MAGs. Precipitates of CSO based biodiesel blends apparently consist of both steryl glucosides and MAGs [20].

Lin et al. presented a study evaluating the impact of saturated MAGs, glycerine and soap on cold soak filterability [21].
The cold soak filtration test (CSFT) is a method that determines the suitability of a biodiesel (B100) blend stock for blending with middle distillates, by filtration time after cold soak, to provide adequate low temperature operability performance to at least the CP of the finished blend. 300 ml of B100 are stored at 4.4°C for 16 hours, allowed to warm to 20-22°C, and are then vacuum filtered through a single 0.7 µm glass tube. The filtration time is reported in seconds. Fuels that give short filtration times are expected to give satisfactory operation down to the CP of biodiesel blends. The test method can be used in specification as means of controlling levels of minor filter plugging components in biodiesel and biodiesel blends. [22].

In the work of *Lin et al*. refined biodiesel was spiked with different quantities of saturated MAGs, the CSFT was carried out as described above and the amount of precipitate formed was determined. They found out that MAG spiking above 0.16% increased the filtration time significantly. In their opinion a downscaling of the CSFT with a reduced biodiesel volume (instead of 300 ml) was necessary in order to develop a high-throughput screening method [21].

2.4 Methods for separation of MAGs

2.4.1 Winterization - MAG removal

In order to avoid the MAG-related quality problems mentioned above, elimination of saturated MAGs can be achieved by cooling the biodiesel followed by filtration [23]. This fractional crystallization is referred to as winterization and usually used to remove saturated FAME in order to improve the cold flow properties of the particular biodiesel [12] [24]. Generally the FAME sample is cooled down to temperatures between the known CP and the PP at rates of about 0.2 to 1.0°C.

Pérez at al. used additionally agitation at 140 rpm to improve the mass transfer and the phase-based thermodynamic equilibrium and yield [12] whereas *Sahlabji et al.* allowed the crystal structures to form for about 2 days [25]. Subsequently the crystals are filtered under low-pressure and under constant cooling, obtaining a solid precipitate and a liquid phase. To maximize the yield of saturated compounds and therefore significantly reduce the PP, several winterization steps or winterizing in various solvents is required [12]. Solvent fractionation, e.g. in the presence of methanol reduces crystallization times and facilitates the separation process but accompanies increased costs. Winterization removes solid contaminants indeed, but involves the loss of the biodiesel product and results in a solid by-product that needs to be disposed or subsequently processed (12).

2.4.2 Enhancing reaction rate of transesterification by CO_2

Another approach to minimize MAG interference is to enhance the reaction rate of the transesterification of MAGs and methanol by CO_2. *Song et al.* studied the effect of CO_2 on the reaction rate of transesterification of glycerol monostearate and methanol to form methyl stearate. Their experimental procedure involved 0.01 mol of glycerol monostearate, 0.045 mol of methanol and 0.03 g of concentrated sulphuric acid, serving as a catalyst. The reaction mixture was loaded into the reactor, which was warmed up by a water bath at a constant temperature and charged with CO_2 to a suitable pressure under stirring. After a certain reaction time the reactor was cooled on ice, CO_2 was released and the amount of produced methyl stearate was investigated by gas chromatography using dimethylformamide as internal standard. They observed that the reaction rate could indeed be enhanced in the presence of CO_2, proportionally to the increasing CO_2 pressure. The presumed reasons for the enhancement of the reaction rate are that CO_2 increases the miscibility and the diffusion coefficients of the reactants and reduces the viscosity of the reaction mixture [26]. *Song et al.* believe that CO_2 may be used to enhance the efficiency of the final conversion step in biodiesel production.

2.4.3 Enzymatic transesterification of MAG

Another way to improve the MAG transesterification balance is the lipase-catalyzed transesterification of saturated MAGs to FAME and glycerol. *Padhi et al.* used a lipase from *Penicillium camemberti* (lipase G) due to its preference for MAG transesterification. They mixed glycerol monopalmitate and glycerol monostearate with biodiesel and dissolved the MAGs by heating the mixture at 60°C. Then methanol and lipase G were added and stirred for 24h in which two extra doses of methanol as well as lipase G were added. To investigate the residual MAG levels during incubation, aliquots of the mixture were silylated and analysed by GC-MS. Quantification was carried out with an external calibration obtained by standard curves of glycerol monopalmitate and glycerol monostearate in biodiesel. The enzymatic transesterification of MAGs resulted in decreasing concentrations from initially 2.0% (w/v) of each MAG to a level of 0.22% (w/v) glycerol monopalmitate and to 0.14% (w/v) glycerol monostearate after 24h [23].

2.5 Analytical methods for MAGs with HPLC

Numerous methods for the determination of MAGs have been developed in combination with high-performance liquid chromatography (HPLC) such as analysing biodiesel mixtures using non-aqueous reversed phase high-performance liquid chromatography (RP-HPLC) with a UV detector, via an evaporative light-scattering detection (HPLC-ELSD), RP-HPLC coupled with mass spectrometry (HPLC-MS), as well as approaches with HPLC based on size-exclusion chromatography (SEC) with a differential refractive index (RI) detector. Furthermore using a single HPLC chiral column in combination to a photodiode array detector and a RID or ELSD was used to investigate the separation of regioisomers and enantiomers of MAG-derived fatty acids.

2.5.1 RP-HPLC

Di Nicola et al. optimized statistically a binary gradient method for analysing biodiesel mixtures using non-aqueous RP-HPLC with a UV detector at 210 nm. It was performed on a RP C_{18} column with two mobile phases (A: acetonitrile/methanol 4:1 (v/v), B: n-hexane/isopropanol 8:5 (v/v)). Identification was achieved by separately

analysing pure reference standards. Their work resulted in a robust qualitative analysis with a high resolution of all biodiesel compounds in less than 30 minutes [27].

A review article of *Hellmuth et al.*, describes advantages and disadvantages of different strategies for the analysis of acylglycerols and elucidates the fact that in the range of wavelengths at which the chromophore of the ester bond absorbes UV-light (200-230 nm), lipids only show low absorbance. Thus certain solvents (acetone, ethylacetate, toluene or chloroform) that absorb strongly in this wavelength range cannot be used for the analysis. Instead methanol, isopropanol and acetonitrile are suitable. The limited choice of solvents restricts the applications of UV detection mode [28].
Mercato and Cecchin developed a method for the separation and identification of saturated glycerides, glycerol and saturated fatty acids simultaneously and in a single run, based on the use of ternary-gradient HPLC with ELSD and a reversed-phase RP-8 end capped column. They stated that ELS detection was sensitive just to the mass of the vaporized analyte and was not limited by the absorption characteristics of the individual components and/or the nature of the eluent. For the analysis, standard and sample solutions resulting in a final concentration of 2500 ppm (w/v) were prepared. The identification of the individual compounds was achieved by matching the corresponding retention times of the pure standards. MAGs were quantified by an external calibration. This method even allowed the identification and quantification of positional isomers such as *sn*-1 and *sn*-2 MAGs [29].

Türkan A. and Kalay S. proposed analytical methods that enable the quantitation of compounds (TAGs, DAGs, MAGs, FAME, glycerol and methanol) involved in the transesterification of a vegetable oil and an alcohol during a lipase-catalyzed biodiesel production. They developed two RP-HPLC methods with UV detection to qualitatively analyse samples taken at certain time intervals from the transesterification reaction. Here, only the first, more successful method will be discussed. The individual TAGs, DAGs, MAGs as well as the fatty acids and their corresponding methyl esters were separated using acetonitrile/acetone as a mobile phase and performing the analyses on a C_{18} column at 10°C with a flow-rate of 1

ml/min. UV detection was carried out at 210 nm. The method used a combined linear gradient elution (from 100% acetonitrile to 50% acetonitrile + 50% acetone) followed by an isocratic elution (at 50% acetonitrile + 50% acetone), a step gradient (to 30% acetonitrile + 70% acetone) and a final isocratic elution at the final composition. This method further completely resolved *sn*-2 and sn-1 isomers of MAGs as well as *sn*-1,2 and *sn*-1,3 isomers of DAGs. Quantitative analyses were obtained by calibration curves for the compounds linoleic acid methy ester, 1,3-dilinolein, oleic acid methyl ester, 1-monoolein and 1,3 diolein. HPLC-MS was used to identify each compound, supplied with an ion trap analyser and an atmospheric pressure chemical ionisation (APCI) source. The saturated MAGs monopalmitin and monostearin were identified in the negative-ion mode of APCI, allegedly resulting in more distinct signals [30].

2.5.2 SEC-chromatography

Arzamendi et al. presented a method based on size exclusion chromatography (SEC) that allows the simultaneous determination of the total amounts of several compounds involved in the methanolysis reaction of sunflower oil, including methanol and glycerol. The SEC system featured a differential refractive index detector (RID) and a dual detector (light scattering and viscometry) and the mobile phase was ultrapure tetrahydrofuran (THF). Identification and calibration of the MAG peaks was performed by calibration mixtures of monostearin, monoolein, monolinolein and monolinolenin within a range of concentrations as in the transesterification reactions. Their developed method was applied to evaluate the effects of the catalyst (NaOH, KOH) concentration and the methanol/oil molar ratio and has turned out to be a simple, robust and relatively fast method, which provided accurate and reproducible results. With this method the total MAG amount can be determined [31].

Hellmuth et al. pointed out the disadvantages of RI detection in this context, referring to the fact that the functionality of the RID does not allow eluent gradients, which limits the method [28].

2.5.3 Enantioselective-HPLC

L. Deng et al. established a method for the direct separation of the positional isomers (regioisomers) and enantiomers of monostearoylglycerols, monopalmitoylglycerols,

monooleoylglycerols and monolinoleoylglycerols without any derivatisation steps to investigate the stereoselectivity of *Candida antarctica* lipase B. The method was based on a tandem column HPLC system, in which a normal phase silica gel column and a enantioselective column were connected in series, the mobile phase consisted of n-hexane/2-propanol (97:7-97:3 v/v) and the peak detection was carried out using evaporative light scattering [32].
A similar method was presented by *García et al.* achieving the separation of regioisomers and enantiomers of MAGs using a single chiral column and hexane/2-propanol eluent mixtures without prior derivatisation and a photodiode array detector (at 210 nm). The method was stated to be suitable for MAGs with different fatty acid chain lengths and various degrees of unsaturation, resulting in shorter retention times than previously reported methods, such as *L. Deng et al*. described above [33].

Petrosino et al. proposed a procedure to separate the three isomeric MAG classes (*sn*-1-, *sn*-2-, *sn*-3-MAG). This was achieved by derivatisation of the MAGs with (S)-(+)-1-(1-naphtyl)-ethyl-isocyanate and the separation on a normal-phase HPLC (NP-HPLC). This method allows the resolution of the two enantiomeric classes (*sn*-1-MAG and *sn*-3-MAG) as diastereomers without the requirement of a chiral column, as well as the separation of the isomeric 2-*sn*-MAGs. Derivatisation results in chromophoric moieties on the MAGs and enables UV-detection. The NP-HPLC system was equipped with two detectors in-series (diode array detector, mass spectrometer: APCI, positive ion mode). Coupling the UV detector with MS allowed the confirmation of identified peaks. The purpose of this work was to obtain the stereospecific analysis of the TAG fraction of extra virgin olive oil [34].

2.5.4 Comparison of HPLC detectors

Holcapek et al. developed a RP-HPLC method suitable for the separation of TAGs, DAGs and MAGs, combining aqueous-organic and non-aqueous gradient elution. Further they compared UV-, ELS and APCI-MS detectors in terms of their sensitivity, compatibility with gradient elution and possibility of peak identification without authentic standards. Their work focused on the monitoring of oleic-, linoleic- and linolenic fatty acid methyl esters and the corresponding acylglycerols, including the respective positional isomers, during biodiesel production from rapeseed oil. They

concluded that the determination of TAGs with a differing equivalent carbon number (ECN) was possible using UV detection at 205 nm, ELSD and APCI-MS but that APCI-MS was the best suited detection mode for the analysis of all individual compounds in sample mixtures. All detectors showed comparable reproducibility but MS showed a better or at least comparable sensitivity compared to UV, while the limit of detection (LOD) for ELSD was at least one magnitude higher. APCI-MS features valuable structural information and enables investigating overlapping chromatographic peaks, using extracted ion chromatograms [35].

2.6 Analytical methods for MAGs with GC

2.6.1 GC-FID

Plank and Lorbeer developed a gas chromatographic (GC) method with flame ionization detection (FID) for simultaneous determination of glycerol, mono-, di- and triglycerides in vegetable oil methyl esters. They introduced an approach that allowed the determination of all analytes in a single GC run using a 10 m capillary column coated with (5% phenyl)-methylpolysiloxane (DB-5). Calibration was carried out by standard solution containing glycerol, mono-, di-, and triolein as well as the two internal standards 1,2,4-butanetriol and tricaprin [36].

EN 14105:2011

Based on the work of *Plank and Lorbeer*, the currently valid European standard method EN 14105:2011 [37], for free glycerol, MAGs, DAGs and TAGs, was established [38].

The principle of the method was the transformation of glycerol, mono-, and diglycerides into more volatile and stable silyl derivatives in presence of pyridine and N-trimethylsilyltrifluoroacetamide (MSTFA). The analysis of the sample after silylation is carried out by gas chromatography on a short capillary column with thin film thickness, with an on-column injector or equivalent device, a temperature-programmable oven and flame ionization detection (FID). After a calibration procedure, the quantification of the glycerol is carried out in presence of the internal standard 1,2,4-butantriol. MAGs, DAGs and TAGs are directly evaluated in presence of an internal standard for each glyceride category: glyceryl monononadecanoate for

MAGs, glyceryl dinonadecanaoate for DAGs and glyceryl trinonadecanoate for TAGs [37].

This method is suitable for determining the collective acylglycerol content but is limited in terms of identifying the detailed distribution of MAGs, DAGs and TAGs congeners [38].

2.6.2 SPE-GC-FID

Giacometti et al. presented a procedure for the separation of polar lipids, MAGs, DAGs and TAGs and the determination of the corresponding fatty acid compositions. The separation of the lipid classes was achieved by solid-phase extraction (SPE) using an aminopropyl silica column and for elution of the neutral lipids, chloroform was applied on the column. Further separation of steryl esters (eluent: hexane), TAGs (eluent: hexane/$MeCl_2$/$CHCl_3$ 88:10:2), sterols (eluent: hexane/ethyl acetate 5:95), DAGs (eluent: hexane/ethyl acetate 15:85) and finally MAGs (eluent $CHCl_3$/MeOH 2:1). Fatty acid compositions of the obtained fractions were determined with a GC equipped with a capillary column and FID using split-injection (100:1) and a temperature programme from 140°C to 220°C at which the detector temperature was held at 350°C. They concluded that the proposed methodology is appropriate even for limited amounts of sample (<200 mg) [39].

Bondioli et al. submitted a work for publication, which introduces a technique for the determination of total monoglyceride content and the separate quantification of glycerol monopalmitate and -stearate. The method is based on acetylation (instead of trimethylsilyl derivatisation) followed by micro column solid phase separation, isolation of polar fraction containing all acetylated glycerides and GC quantification with glycerylmononononadecanoate as IS. The SPE was carried out by pre-conditioning the micro silica column with hexane/diethyl ether 99:1 and eluting the first fraction (non-polar fraction) with the same mixture of solvents. The second fraction (polar fraction), containing all acetylated glycerides was recovered by using pure diethyl ether. The experimental conditions of the gas chromatographic analysis were chosen according to EN 14105. The new procedure (acetylation/SPE) yielded in systematically lower results than the standard procedure (EN 14105:2011). They observed that the chromatogram of the polar fraction is very clean and that the

corresponding peaks for monoglycerides C_{16} and C_{18} are easily identified. Additionally they mentioned that possible squalene interferences can be avoided, due to the fact that they elute in the non-polar fraction of the SPE [40].

2.6.3 GC-MS

Linck, Teller and Petrovic developed a method for the analysis of 1-MAGs in hamster tissue using GC with a mass spectrometer (MS). The lipids were extracted from adipose tissue and blood plasma and submitted to thin-layer chromatography (TLC) for further separation. 1-monopalmitin was used as a reference for the MAG fraction. The MAG fraction was silylated and GC-MS analysis applied. In the mass spectra of the samples, the ions at m/z 371 for monopalmitin and m/z 397 for monoolein (both equivalent to $[M-103]^+$) were present, which are characteristic for the corresponding 1-MAGs. Additionally, for 1-monopalmitin the fragments m/z 459, 371, 239, 73 were observed, which were also outlined in the experimental part of this thesis, see 4.1.1 [41].

Myher et al. also developed a very early work on the GC-MS analysis of monacyl- and monoalkylglycerols. The analysis of the mass spectra of the positional isomers (*sn*-1 and *sn*-2) of monopalmitin and monostearin were especially of interest in correlation with this thesis. They also converted the monoacylglycerols into the corresponding trimethylsilyl ethers by derivatisation prior to GC-MS analysis. Their work demonstrated that the fragment $[M-103]^+$ was only present in the mass spectra of the 1-MAGs and not in the corresponding mass spectra of the *sn*-2-isomers. On the other hand they found out that m/z 218 was highly favoured by all *sn*-2-isomers, although it was not involving the characteristic fatty acid moiety. They also found out that the 1-MAGs gave a significantly higher proportion of the molecular ion [42].

A more recent work, presented by *Yang et al.*, focused on the development of a unified method for polar oxygenates in biodiesel, including free fatty acids (FFAs), free glycerol, MAGs and free sterols, based on SPE, silylation and GC-MS analysis. Their analytical procedure started with the isolation and enrichment of minor polar components of biodiesel, using a 3 g silica gel column conditioned with n-hexane followed by sequentially rinsing the column with dichloromethane and methanol to

obtain the fatty acid esters and polar fractions. The polar compounds were analysed using a GC-MS system equipped with a SAC 5 GC column (5%phenyl/95% dimethylpolisiloxane) and 5973 mass selectivity detector, performing in the splitless mode and under a temperature programme from 50°C to 275°C. Mass spectra were obtained by electron impact (EI) ionisation at 70 eV in full scan and SIM modes. The identification of the analytes were based on retention time and spectral data of silylation derivatives of target analytes with those of authenticated standards and a positive match of mass spectra of target analytes with that of NIST (the U.S. national Institute of Standards and Technology) 2008 Mass Spectral Library. The target analytes were quantified by the single ion with the highest abundance or characterised fragment ions. The quantitation ions for sixteen MAGs were presented including 2-$C_{16:0}$ (m/z 218), 1-$C_{16:0}$ (m/z 371), 1-$C_{17:0}$ (m/z 385) and 1-$C_{18:0}$ (m/z 399) [38].

3 Experimental Part

3.2 Chemicals and Materials

3.2.1 Monoacylglycerols

- 2-Monopalmitoyl-glycerol ($C_{16:0}$) approx. 99%, Sigma
- DL-α-Palmitin purum ≥98%, Sigma
- Monoheptadecanoin >99%, NU-CHECK PREP, INC.
- 1-Stearoyl-rac-glycerol, approx. 99%, Sigma
- Monononadecanoin >99%, NU-CHECK PREP, INC.
- Monopalmitolein >99%, NU-CHECK PREP, INC.

3.2.2 Chemicals and solvents

- N-Hexane, HPLC-grade, ≥97%, VWR International, MW= 86g/mol,
- Pyridine, ReagentPlus®, ≥99%,Sigma-Aldrich, MW= 79,10 g/mol
- N-Methyl-N-(trimethylsilyl)-trifluoracetamide (MSTFA), ≥97%, Carl Roth GmbH + Co. KG, MW= 199,25 g/mol

3.2.3 Biodiesel samples

- Fatty acid methyl esters from used cooking oil (UCO-ME: samples UCO-ME 1-UCO-ME 2 and UCO-ME 3) were supplied by SEEG Mureck reg. Gen.m.b.H. (Mureck, Austria)
- Fatty acid methyl esters from waste animal fats (WAF-ME, samples: WAF-ME 1 to WAF-ME 6) and FAME from UCO (UCO-ME 4 to UCO-ME 9) were supplied by BDI-BioEnergy International AG (Grambach/Graz, Austria)
- Fatty acid methyl esters from bacon rind (BR-ME) were supplied by the Institute of Chemistry, University of Graz

3.2.4 Sample preparation

- Manual syringes (100 µL, 1 ml), Agilent Technologies
- Analytical balance (max 210g, min 10 mg, e=1mg, d=0.1 mg), Sartorius
- GC vials: Macherey-Nagel GmbH&Co. KG, 1.5 ml/11.6x32mm/clear
- GC Vials: Agilent Technologies, screw vial, fixed insert, amber
- Vortex: Stuart Scientific Autovortex SA6

3.2.5 Instruments

- GC-MS: performed on a HP 6890 Series GC System equipped with an Agilent HP-5MS column (30 m × 250 µm × 0.25 µm), an Agilent 7683 Series AutoSampler, a HP 7689 Series Injector and a HP 5973 MSD. The data were analysed with a MSD ChemStation E.0200.493.

- GC-FID for determination of fatty acid compositions: performed on an Agilent Technologies 7890 GC System equipped with a flame ionisation detector (FID), a CTC Analytics Autosampler, split inlet, J&W Scientific 122-7031 DB-WAX PEG column (20-260°C, 30 m x 250 µm x 0.15 µm).

- High temperature- (HT) GC-FID for total MAG quantification (EN 14105): performed on a HP 6890 GC System equipped with a FID, a HP 7683 Series Injector, a cold-on-column inlet and an Agilent Technologies 123-5711 DB-5HT column (60-400°C, 15m x 320 µm x 0.1 µm) for the determination of total MAGs in the biodiesel. (Preliminary tests for method development were performed on the same instrument but partly with a different column: 122-5731 DB-5HT. For details see Table 6-1 and Table 6-2)

3.3 Method development

3.3.1 Preliminary tests

The first step in the development of the new analytical method for the quantification of saturated MAGs was to find the right GC column as well as a suitable temperature programme for an optimal separation. The answers to these questions were worked out by a few preliminary tests. The separation of the MAGs, especially from their unsaturated counterparts and positional isomers was checked on the 123-5711 DB-5HT column (60-400°C, 15m x 320 µm x 0.1 µm) of the HT-GC-FID. In order to see if a separation of the unsaturated MAGs from the saturated MAGs could be achieved and also to investigate if a separation of the positional isomers 2-$C_{16:0}$ and 1-$C_{16:0}$ was satisfactory on that particular column, solutions of the C_{16} MAGs were prepared. Therefore 26.2 mg 2-$C_{16:0}$, 24.7 mg 1-$C_{16:0}$ and 25.0 mg 1-$C_{16:1}$ were weighed in three different 5 ml volumetric flasks and made up to the mark with pyridine. The resulting MAG concentrations were 5.24 mg/ml 2-$C_{16:0}$, 4.94 mg/ml and 1-$C_{16:0}$, 5 mg/ml 1-C16:1. 20 µl of each MAG were transferred in a sample tube, 100 µl MSTFA were added, and thorough mixing was ensured by adequate vortexing. The silylation took 1h at room temperature (RT). After that about 1 ml of the mixture was transferred in a GC vial and the analysis of the obtained solution was performed on a HP 6890 GC System equipped with a FID, a HP 7683 Series Injector, a cold-on-column inlet and an Agilent Technologies 123-5711 DB-5HT column (60-400°C, 15m x 320 µm x 0.1 µm). The same solution was also measured on the same instrument with a different column: 122-5731 DB-5HT column (60-400°C, 30 m × 0.25 mm × 0.25 µm). The methods used (Lena1 and Lena lang) are listed in detail in Table 6-1 and Table 6-2 in the appendix.

3.3.2 GC-MS conditions

The GC-MS parameter mentioned conditions in Table 3-1 were developed to achieve separation and quantitation of all target MAGs. The temperature programme was chosen referring to a previous publication by *Yang et al.* [38].

Table 3-1 Detection conditions for GC-MS analyses of saturated MAGs

Parameter	Condition
Column	HP-5MS (Agilent Technologies, USA)
Type	5% phenyl methyl siloxane (30 m × 0.25 mm × 0.25 μm)
Pressure	52.2 kPa
Gas Type	Helium
Oven	
Initial temperature	50°C
Initial time	1 min
Rate	15°C/min to 275°C hold for 10 min
Injection	
Volume	1μl
Mode	Split
Split ratio	10:1
Split Flow	9.9 ml/min
Temperature	250°C
MS parameters	
Acquisition mode	SIM
SIM parameters	Group 1 Ions: 218, 371, 385, 399 Group 2 Ions: (start time 19 min) 218, 371, 385, 399, 413
Solvent delay	4 min
Quadrupole temperature	150°C
Source temperature	230°C

3.3.3 Quantitation ions for SIM Mode

Therefore 24.5 mg 1-$C_{16:0}$, 24.6 mg 2-$C_{16:0,}$ 99.9 mg 1-$C_{17:0}$, 99.5 mg 1-$C_{18:0}$ and 99.8 mg 1-$C_{19:0}$ were weighed in 25 ml and respectively in 100 ml volumetric flasks. The reason why some MAGs were weighed in 25 ml flasks and others in 100 ml flasks was simply due to a partially low available MAG amount at that time. The flasks then were filled up to the mark with pyridine and shaken well to ensure thorough mixing of the solutions. The resulting MAG concentrations were 0.984 mg/ml 2-$C_{16:0}$, 0.980 mg/ml 1-$C_{16:0,}$ 0.999 mg/l 1-$C_{17:0}$, 0.995 mg/ml 1-$C_{18:0}$ and 0.998 mg/ml 1-$C_{19:0.}$ In order to obtain measuring solutions containing all five MAGs, the stock solutions were further diluted and combined by transferring 500 µl of each stock solution in one 20 ml volumetric flask and made up to the mark with pyridine. Thereof 250 µl were transferred to a GC vial and dried under a nitrogen stream by evaporating the solvent with a heated water bath at about 120°C ($bp_{(pyridine)}$:115°C). The dried residue was silylated with 100 µl MSTFA for 1h at room temperature (RT) and afterwards the excessive silylating agent was evaporated as described above with a water bath at about 140°C ($bp_{(MSTFA)}$:130-132°C). 0.5 ml hexane (HPLC grade) were added to the dried content in the vial and measured with GC-MS in scan mode (scan mass range 20-700) using the method described in Table 3-1.

3.3.4 Limit of detection and quantification

The limit of detection (LOD) and the limit of quantification (LOQ) were determined by diluting the stock solutions from the determination of quantitation ions by transferring 250 µl of each stock solution in separate 100 ml volumetric flasks, making them up to the mark with pyridine and mixing thoroughly. The obtained concentrations of about 2.5 mg/ml were further diluted 25-fold, 50-fold and 100-fold to give concentrations of approximately 0.1 µg/ml, 0.05 µg/ml and 0.025 µg/ml. 500 µl of each dilution was transferred in a GC vial and 40 µl MSTFA were added. After vortexing and 30 minutes of derivatisation at RT the mixtures were analysed in triplicates with the corresponding GC-MS method.

3.3.5 Linearity

In order to obtain standard curves of the saturated MAGs, all target MAGs were serially diluted in the range of 1.0 to 0.1 mg/ml. Stock solutions of 1-$C_{17:0}$, 1-$C_{18:0}$ and 1-$C_{19:0}$ with concentrations of about 1 mg/ml were prepared by weighing 10.4 mg 1-$C_{16:0}$, 10.2 mg 1-$C_{17:0}$, 9.7 mg 1-$C_{18:0}$ and 9.7 mg 1-$C_{19:0}$ in individual 10 ml volumetric flasks and making them up to the mark with pyridine. Thus, concentrations of 1.04 mg/ml 1-$C_{16:0}$, 1.02 mg/ml 1-$C_{17:0}$, 0.97 mg/ml 1-C18:0 and 0.97 mg/ml 1-$C_{19:0}$ were obtained. For 2-$C_{16:0}$ the existing stock solution from the previous analyses was used at 0.948 mg/ml due to the lack of available 2-$C_{16:0}$ standard. Then five serial dilutions in the range of 1.0 to 0.1 mg/ml were prepared. Therefore 100, 80, 60, 40, 20 and 10 µl of the particular stock solution were transferred in separate interlock GC vials and respectively 0, 20, 40, 60, 80 and 90 µl of pyridine were added leading to concentrations of 1 mg/ml, 0.8 mg/ml, 0.6 mg/ml, 0.4 mg/ml, 0.2 mg/ml and 0.1 mg/ml. Drivatisation was carried out by adding 10 µl MSTFA into each GC vial and subsequent thorough vortexing. After 30 minutes at RT the serial dilution was analysed in triplicates with the corresponding GC-MS method. The layout for the serial dilution is shown in Table 3-2 and the resulting accurate concentrations are summarised in Table 3-3.

Table 3-2 Layout for the serial dilution of the MAGs

MAG_x c= 1 mg/ml [µl]	**pyridine [µl]**	**MSTFA [µl]**	**resulting concentration [mg/ml]**
100	0	10	1.0
80	20	10	0.8
60	40	10	0.6
40	60	10	0.4
20	80	10	0.2
10	90	10	0.1

Table 3-3 Accurate concentrations of the MAG serial dilutions

Ideal concentration	**Accurate concentration**				
	2-$C_{16:0}$	1-$C_{16:0}$	1-$C_{17:0}$	1-$C_{18:0}$	1-$C_{19:0}$
[mg/ml]	[mg/ml]	[mg/ml]	[mg/ml]	[mg/ml]	[mg/ml]
1.0	0.984	1.04	1.02	0.97	0.97
0.8	0.787	0.832	0.816	0.776	0.776
0.6	0.590	0.624	0.618	0.582	0.582
0.4	0.394	0.416	0.408	0.388	0.388
0.2	0.197	0.208	0.204	0.194	0.194
0.1	0.098	0.104	0.102	0.097	0.097

3.4 Analysis of biodiesel samples

The solutions of MAGs from the LOD and LOQ quantification at 2.5 mg/ml were used as stock solutions. 500 µl of each stock were transferred in a 10 ml volumetric flask. After making the flask up to the mark with pyridine and thoroughly mixing, 500 µl were transferred in a GC vial, mixed with 100 µl MSTFA and vortexed adequately. After 30 minutes at RT, the sample was measured with the GC-MS. The analysis, including preparation of measuring solutions, was repeated three times in the same way and the average value for each MAG peak area was used for the calculation of the CFs. The equations 3-1 to 3-3 for the calculation of the CFs are shown below, whereby RF_x refers to the response factor of the target peak, A_x refers to the peak area of the target MAG, c_x refers to the concentration of the target peak, RF_{IS} refers to the response factor of the IS, A_{IS} refers to the peak area of the IS, c_{IS} refers to the concentration of the IS, CF_x refers to the correction factor of the target MAG.

Equation 3-1 $$\boldsymbol{RF_x = \frac{A_x}{c_x}}$$

Equation 3-2 $$\boldsymbol{RF_{IS} = \frac{A_{IS}}{c_{IS}}}$$

Equation 3-3 $$\boldsymbol{CF_x = \frac{RF_{IS}}{RF_x}}$$

3.4.1 Saturated MAGs in FAME

To quantify saturated MAGs in biodiesel, methyl esters from used cooking oil (UCO-ME), waste animal fats (WAF-ME) and bacon rind (BR-ME), were analysed with the developed GC-MS method and the target MAGs were quantified via glycerol mononononadecanoate (1-$C_{19:0}$), which served as an internal standard (IS). The IS with a concentration of about 50 µg/ml was prepared by transferring 5 ml of the IS stock solution, with a concentration of 0.998 mg/ml (see 3.2.3) in a 100 ml volumetric flask and making it up to the mark with pyridine (20-fold dilution). The resulting accurate concentration of the IS was 49.9 µg/ml.

The general procedure for the analysis of saturated MAGs in biodiesel was established as follows:

- Accurately weighing approximately 10-30 mg of FAME,
- adding 1 ml IS (c= 50 µg/ml),
- adding 100 µl MSTFA,
- adequate vortexing,
- and 30 minutes of derivatisation at RT.

The samples were analysed with the GC-MS method described in Table 3-1. The quantities of the individual saturated MAGs were calculated according to Equation 3-4 and Equation 3-5. A_x refers to the peak area of the target MAG, A_{IS} refers to the peak area of the IS, c_{IS} refers to the concentration of the IS, CF_x refers to the correction factor of the target MAG and FAME refers to the inserted weight of FAME.

Equation 3-4

$$\boldsymbol{MAG_x}\ \left[\frac{\mu \boldsymbol{g}}{\boldsymbol{ml}}\right] = \left(\frac{\boldsymbol{A_x \times c_{IS}}}{\boldsymbol{A_{IS}}}\right) \times \boldsymbol{CF_x}$$

Equation 3-5

$$\boldsymbol{MAG_x}\ \left[\frac{\mu \boldsymbol{g}}{\boldsymbol{g}}\right] = \frac{\boldsymbol{MAG_x}\left[\frac{\mu \boldsymbol{g}}{\boldsymbol{ml}}\right]}{\boldsymbol{FAME}\ [\boldsymbol{g}]}$$

FAME from used cooking oil

Ten samples of each UCO-ME 1, UCO-ME 2 and UCO-ME 3 were weighed in GC vials and mixed with 1 ml 1-$C_{19:0}$ IS (c=49.9 µg/ml). The samples of UCO-ME 1 were

silylated with respectively 100 µl MSTFA and the samples of UCO-ME 2 and UCO-ME 3 were silylated with respectively 50 µl MSTFA.
The sample weights are listed in Table 3-4.

Table 3-4 Sample weights of UCO-ME 1, UCO-ME 2, UCO-ME 3

	UCO-ME 1	**UCO-ME 2**	**UCO-ME 3**
sample	[mg]	[mg]	[mg]
a	24.6	25.1	17.4
b	24.7	23.7	15.7
c	24.6	22.8	20.2
d	22.7	24.6	22.7
e	26.1	24.5	21.2
f	26.3	24.6	24.8
g	28.2	22.3	30.1
h	28.2	19.7	22.0
i	24.3	21.5	20.4
j	21.7	21.5	20.0

Three samples of each UCO-ME 4, UCO-ME 5, UCO-ME 6, UCO-ME 7, UCO-ME 8 and UCO-ME 9 were weighed in GC vials and mixed with 1 ml 1-$C_{19:0}$ IS (c= 49.9 µg/ml). The samples UCO-ME 4 to UCO-ME 9 were silylated with respectively 40 µl MSTFA and the samples of UCO-ME 9 were silylated with respectively 20 µl MSTFA. The sample weights are listed in Table 3-5 and Table 3-6.

Table 3-5 Sample weights of UCO-ME 4, UCO-ME 5, UCO-ME 6

	UCO-ME 4	**UCO-ME 5**	**UCO-ME 6**
sample	[mg]	[mg]	[mg]
a	27.4	26.8	30.8
b	27.8	27.8	26.8
c	24.5	26.3	25.1

Table 3-6 Sample weights of UCO-ME 7, UCO-ME 8, UCO-ME 9

	UCO-ME 7	UCO-ME 8	UCO-ME 9
sample	[mg]	[mg]	[mg]
a	24.4	34.7	30.5
b	16.0	26.8	22.0
c	21.1	25.1	22.9

The reason why ten samples were taken for UCO-ME 1 to UCO-ME 3 was to check the precision of the method, further explained in 4.3.1.

FAME from waste animal fats

Three samples of the particular FAME were weighed in GC vials and mixed with 1 ml 1-$C_{19:0}$ IS (c= 49.9 µg/ml). The samples of WAF-ME 1 to WAF-ME 6 were silylated with respectively 40 µl MSTFA. The sample weights are listed in Table 3-7 and Table 3-8.

Table 3-7 Sample weights of WAF-ME 1, WAF-ME 2, WAF-ME 3

	WAF-ME 1	WAF-ME 2	WAF-ME 3
sample	[mg]	[mg]	[mg]
a	26.3	23.8	22.0
b	25.4	24.9	24.3
c	22.0	24.3	23.7

Table 3-8 Sample weights of WAF-ME 4, WAF-ME 5, WAF-ME 6

	WAF-ME 4	WAF-ME 5	WAF-ME 6
sample	[mg]	[mg]	[mg]
a	25.4	25.3	24.5
b	26.9	20.5	23.5
c	24.2	28.4	23.8

FAME from bacon rind

Three samples of the FAME from bacon rind were weighed in GC vials and mixed with 1 ml of 1-$C_{19:0}$ (IS) (c=49.9 µg/ml). The samples were silylated with respectively 100 µl MSTFA for 30 minutes at RT. The sample weights are listed in Table 3-9.

Table 3-9 Sample weights of BR-ME

	BR-ME
sample	[mg]
a	24.9
b	29.1
c	25.7

3.4.2 Fatty acid profile

The fatty acid methyl ester profile of all biodiesel samples was investigated on an Agilent Technologies 7890 GC System equipped with a flame ionisation detector (FID), a CTC Analytics Autosampler, split inlet and a J&W Scientific 122-7031 DB-WAX PEG column (20-260°C, 30 m x 250 µm x 0.15 µm). The sample preparation involved transferring 1-2 drops of FAME into a GC vial and adding 1.5 to 2 ml hexane. The method used for identification and quantification of FAME featured a temperature gradient of 5 C°/min from a starting temperature of 150 to 220°C and holding that temperature for 15 min. The method is listed in detail in Table 6-4 in the appendix. The identification of the target peaks was achieved by comparison of the retention times with a chromatogram of a reference material (GLC-462, Nu Check Prep Inc) containing 28 different FAMEs. The data evaluation was carried out with Agilent ChemStation (2008).

3.4.3 Total MAG content

The total MAG content of all biodiesel samples was analysed in the course of a standard determination of free and total glycerol as well as mono-, di-, and triglycerides. The experimental procedure and the quantification of the analyses were

carried out by Ms Heike Feichtinger, chemical engineer at the Institute of Chemistry, Graz University.The MAGs, DAGs and TAGs were directly evaluated in presence of an IS for each glyceride category, according to the European standard method EN 14105 [37] for the determination of free glycerol, MAGs, DAGs, TAGs and total glycerol. Glyceryl monononadecanoate (1-$C_{19:0}$) served as an IS for monoglycerides and respectively glyceryl dinonadecanoate and glyceryl trinonadecanoate for di-, and triglycerides. After a calibration procedure the quantification of glycerol is carried out in presence of the IS 1,2,4-butantriol.

Preparation of solutions

Approximately 50 mg of 1,2,4-butantriol were accurately weighed in a 50 ml volumetric flask and made up to the mark with pyridine. Approximately 50 mg of each reference glyceride (monononadecanoate, dinonadecanoate, trinonadecanoate) were accurately weighed in a 20 ml volumetric flask and made up to the mark with tetrahydrofurane. The sample preparation involved accurately weighing approximately 100 mg of the biodiesel sample in a 10 ml vial and adding 80 µl of the butantriol solution, 200 µl of the mono-, di- and triglyceride solution, 200 µl pyridine and 200 µl MSTFA. After thorough mixing and 15 minutes at RT, 8 ml hexane were added to the vial. The analysis of the obtained solution was performed on a HP 6890 GC System equipped with a FID, a HP 7683 Series Injector, a cold-on-column inlet and an Agilent Technologies 123-5711 DB-5HT column (60-400°C, 15m x 320 µm x 0.1 µm°C, at). The column temperature was programmed as follows: 50°C for 1 min, at 15 C°/min up to 180°C, at 7 C°/min up to 230°C, at 10 C°/min up to the final temperature of 370°C. The final temperature was held for 15 min. The method is listed in detail in Table 6-3 in the appendix.

Quantification of MAGs

Mass percentage of the MAGs in % (m/m) was calculated using Equation 3-6, whereby A_{MAG} refers to the peak area of the MAGs, $A_{monoC19}$ refers to the peak area of the IS for the MAGs (glyceryl monononadecanoate), $M_{monoC19}$ [mg] refers to the mass of the IS, m [mg] refers to the mass of the sample inserted.

Equation 3-6

$$\%\boldsymbol{MAG}\ (\boldsymbol{m/m}) = \left(\frac{\boldsymbol{A_{MAG}}}{\boldsymbol{A_{monoC19}}}\right) \times \left(\frac{\boldsymbol{M_{monoC19}}}{\boldsymbol{m}}\right) \times \mathbf{100}$$

4 Results and Discussion

4.2 Method development

4.2.1 Preliminary tests

It turned out that the 15 m column (123-5711 DB-5HT) achieved a clear separation of the regioisomers 2-$C_{16:0}$ and 1-$C_{16:0}$ as well as the saturated and unsaturated counterparts (1-$C_{16:0}$ and 1-$C_{16:1}$). Unfortunately there was an overlap of the unsaturated 1-$C_{16:1}$ and the 2-$C_{16:0}$ regioisomer due to their similar boiling points and polarity. Given that we were also interested in testing the new method on a *sn*-2-isomer, the overlap was unacceptable. Based on that fact it was decided to run the same test on the 30 m column (122-5731 DB-5HT) which featured the same polarity. Further, the method was optimized from “Lena1” to “Lena lang” (see Table 6-1 and Table 6-2 in appendix) as follows: initial temperature 50°C for 1 min, at 15 C°/min up to 180°C, at 7 C°/min up to 230°C and hold for 10 min at that temperature then at 7°C/min to the final temperature 250°C and hold for 5 min. This time the separation of all three target MAGs succeeded. Figure 4-1 presents the comparison between the measurement with the 15 m column using method “Lena1” (chromatogram above) as well as the measurement with the 30 m column using method “Lena lang” (chromatogram below) and therefore demonstrates the successful separation of 1-$C_{16:0}$, 2-$C_{16:0}$ and 1-$C_{16:1}$.

Due to the preliminary tests it was concluded that the 30 m column fits excellent for this application and was therefore used for further experiments. The aim of this work was to develop a highly sensitive method, which allows precise identification of saturated MAGs among similar, possibly interfering, compounds. GC-MS analyses enable the specific investigation of target components via their characteristic ions in SIM mode. This analysis mode enhances on the one hand the sensitivity of the measurements and on the other hand enables to exclude interfering substances (which elute at a similar retention time) by only detecting certain quantitation ions. That was the crucial factor to develop the analysis method for saturated MAGs for the GC-MS (with an equivalent column as tested before: HP-5MS, 30 m) and not for the HT-GC-FID.

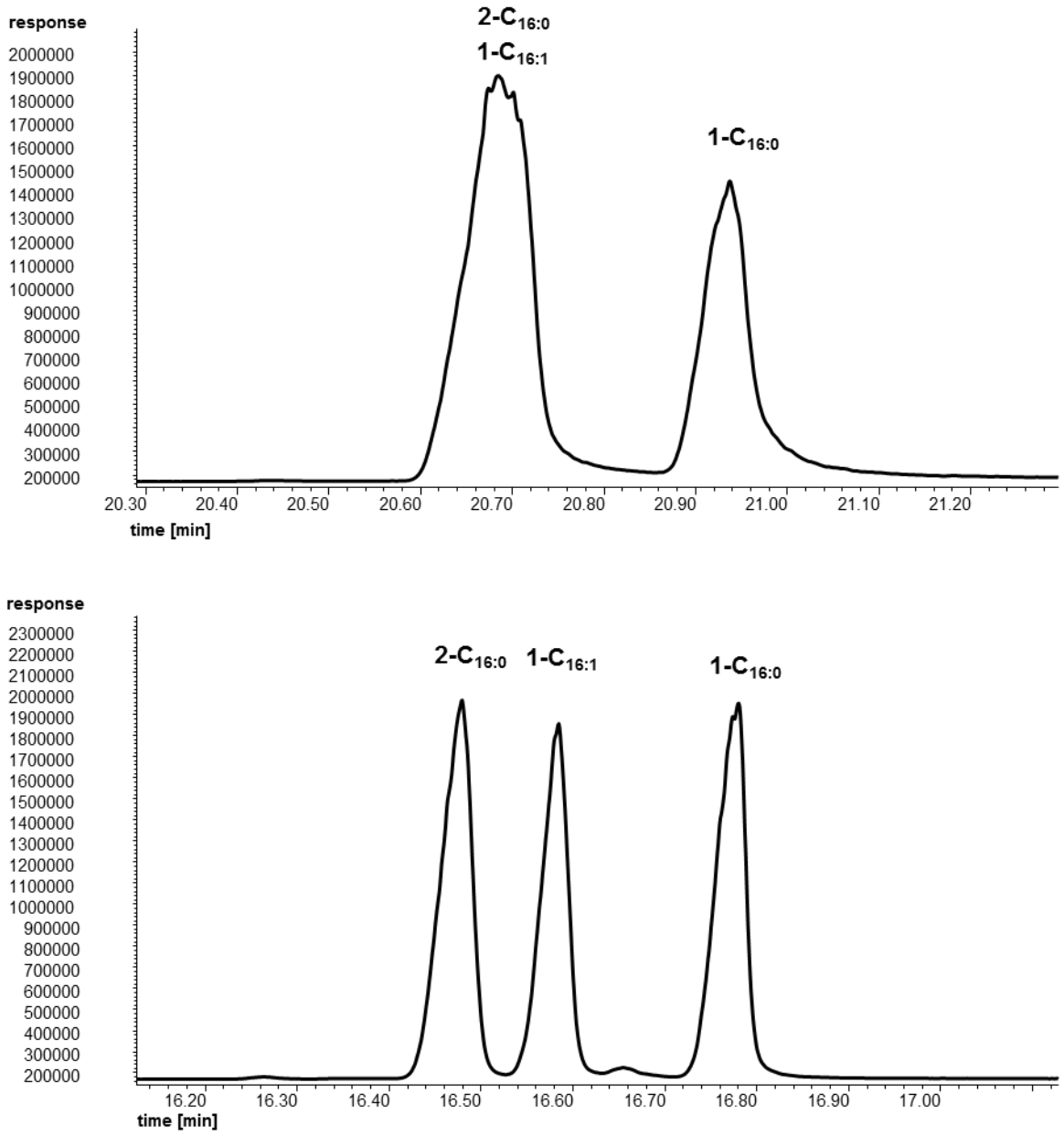

Figure 4-1 Comparison of the gas chromatograms demonstrating the separation benefits from the 30 m column and the optimized temperature programme

4.2.2 Quantitation ions for SIM mode

In order to be able to identify the target MAGs among other components in a biodiesel sample, GC-MS analyses were carried out in single ion monitoring mode (SIM Mode). To determine the characteristic ions of the target MAGs, fresh solutions of each MAG with concentrations of 1 mg/ml were prepared. At this time additionally the MAGs 1-$C_{17:0}$ and 1-$C_{19:0}$ were analysed. 1-$C_{17:0}$ was chosen because it occurs in

certain animal fats which might be interesting for biodiesel production. Due to the fact that 1-$C_{19:0}$ would serve as an internal standard in the quantification of MAGs in biodiesel, it was also necessary to investigate the characteristic ion of 1-$C_{19:0}$. (The unsaturated MAGs 1-$C_{16:1}$ and 1-$C_{18:1}$ were also analysed but later it was decided that the focus of this work was on the saturated counterparts exclusively. 1-$C_{16:1}$ and 1-$C_{18:1}$ were not considered in the further method development and are therefore presented in brackets in Figure 4-2.)

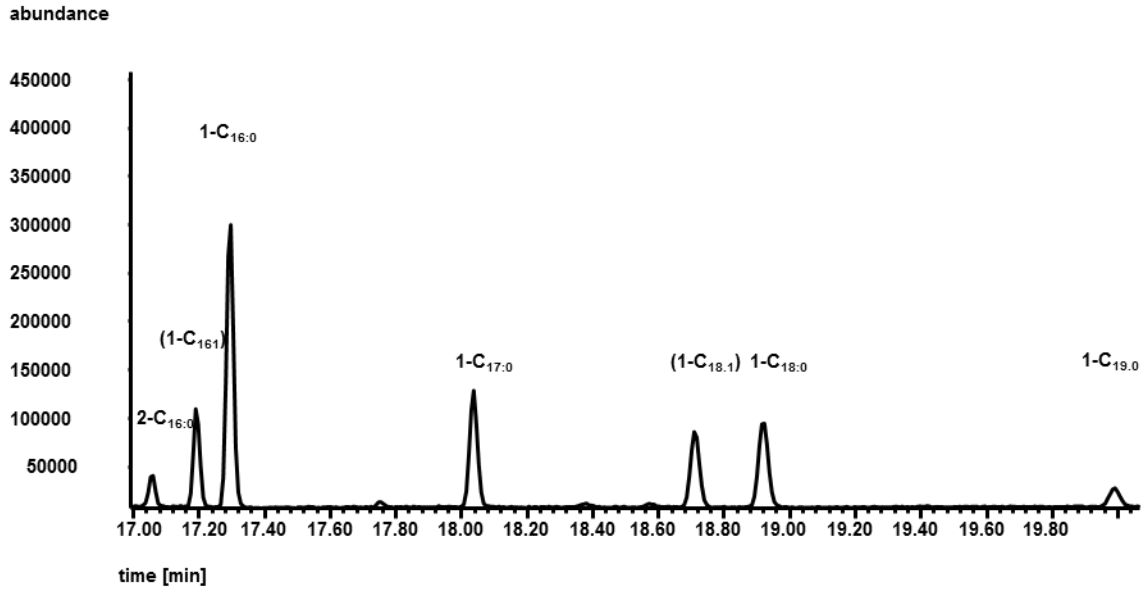

Figure 4-2 Gas chromatogram of standard solutions of MAGs at 1 mg/ml

The mass spectra of the MAGs were interpreted and a previous work of *Yang et al.* [38] was consulted to compare the characteristic ions for 2-$C_{16:0}$, 1-$C_{16:0}$, 1-$C_{17:0}$ and 1-$C_{18:0}$. The characteristic fragments of all MAGs are clearly the molecular ions (parent ions) $[M]^+$, which were however not measured with the ionisation at 70 eV, possibly because of immediate fragmentation. In addition to the molecular ions, other characteristic ions are formed by fragmentation as follows:
$[M\text{-}CH_3]^+$, $[M\text{-}103]^+$, $[RCO]^+$ for the MAGs with the fatty acid residue on position 1 of the glycerol structure (1-MAG-TMS: 1-$C_{16:0}$, 1-$C_{17:0}$, 1-$C_{18:0}$, 1-$C_{19:0}$) and $[RCO+74]^+$, $[RCO]^+$ and $[M\text{-}OCOR]^+$ for the MAG with the fatty acid residue on position 2 of the glycerol structure (2-MAG-TMS: 2-$C_{16:0}$). The m/z fragments for the MAGs are listed in Table 4-1 and Table 4-2.

The corresponding proposed fragment structures are shown in Figure 4-3 to Figure 4-9.

Table 4-1 EI fragments of 1-MAG-TMS

	$[M]^+$	$[M-CH_3]^+$	$[M-103]^+$	$[RCO]^+$
	m/z	m/z	m/z	m/z
1-monopalmitin (1-$C_{16:0}$)	474	459	371	239
monoheptadecanoin (1-$C_{17:0}$)	488	473	385	253
monostearin (1-$C_{18:0}$)	503	487	399	267
monononadecanoin (1-$C_{19:0}$)	517	501	413	281

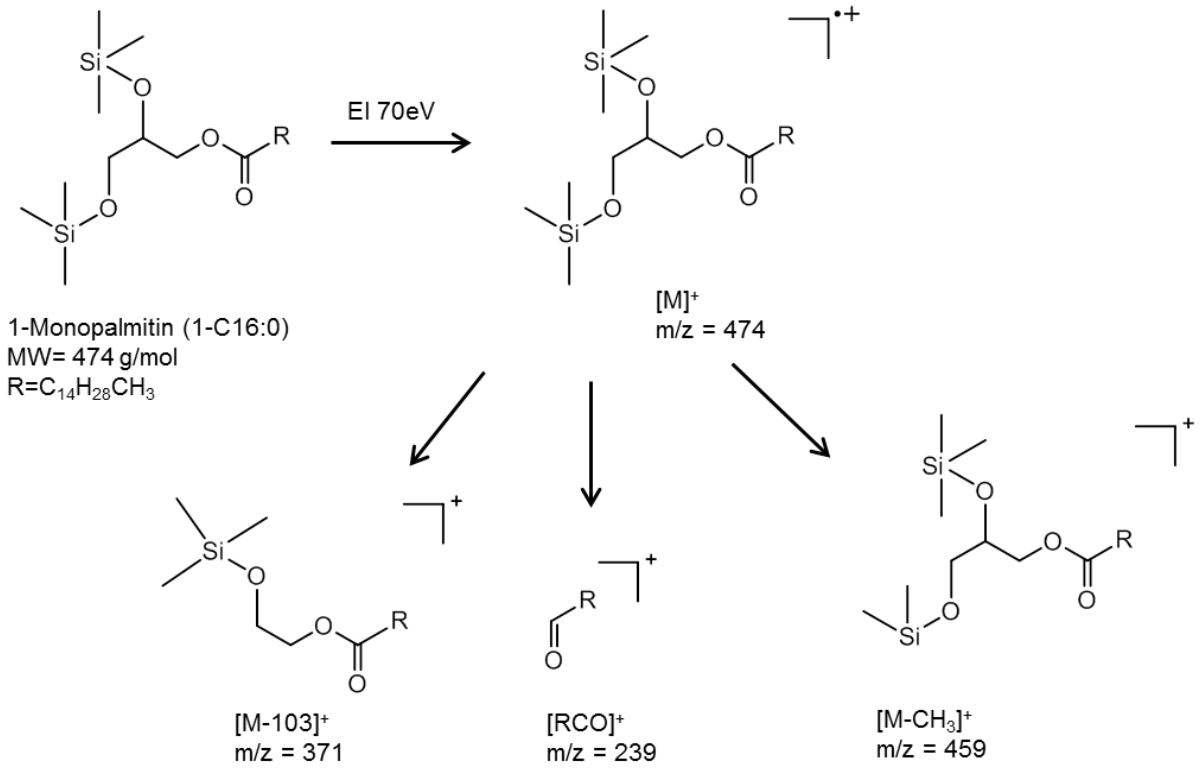

Figure 4-3 Possible fragmentation patterns of EI m/z of 1-monopalmitin

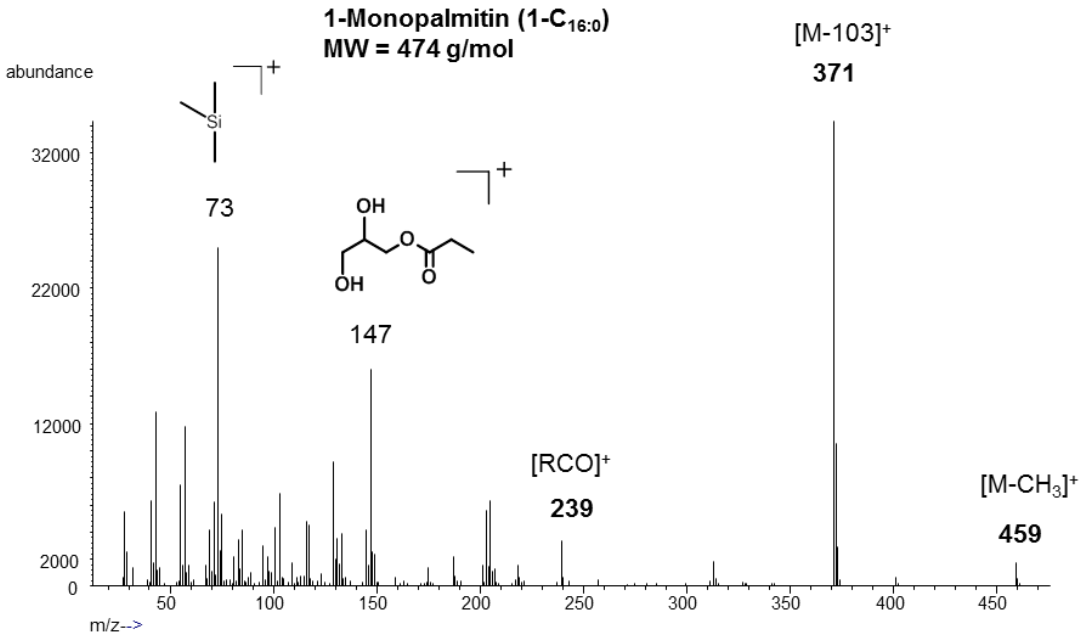

Figure 4-4 EI fragmentation mass spectrum of 1-monopalmitin

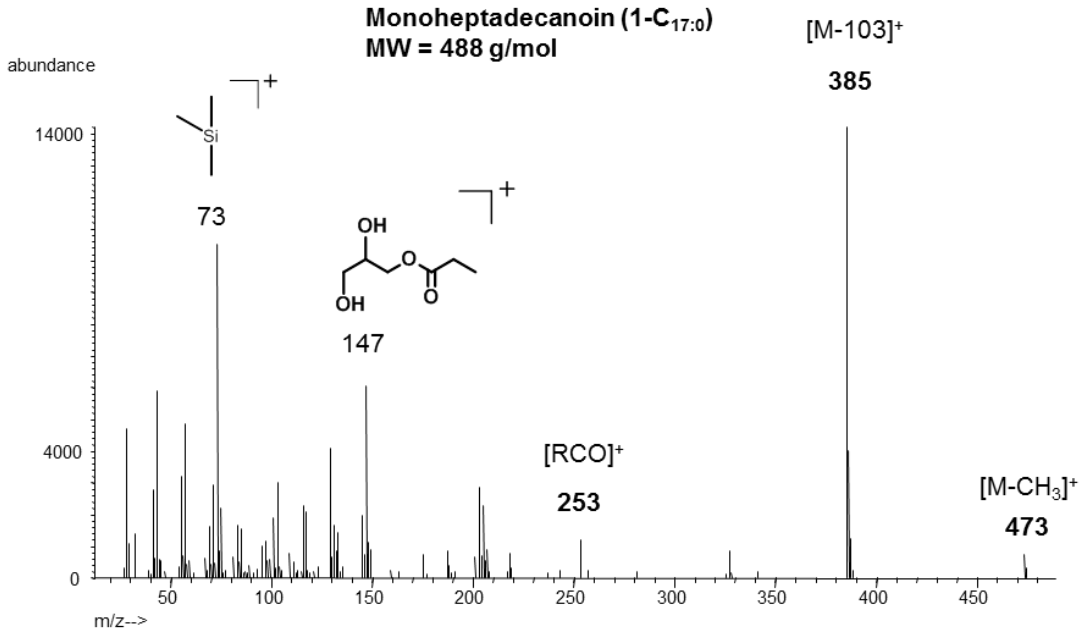

Figure 4-5 EI fragmentation mass spectrum of monoheptadecanoin

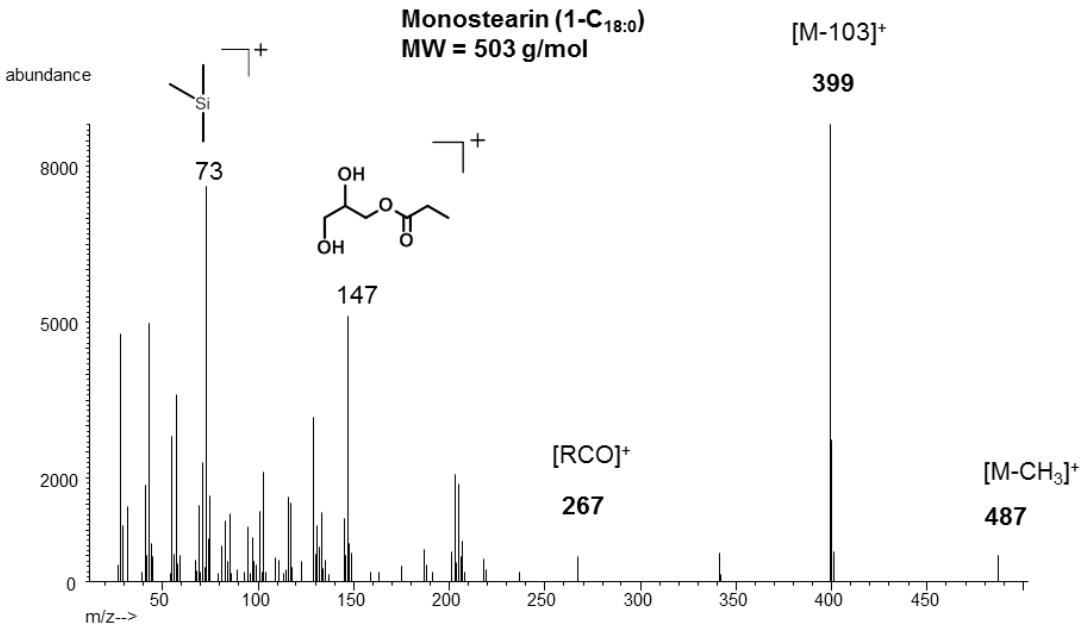

Figure 4-6 EI fragmentation mass spectrum of monostearin

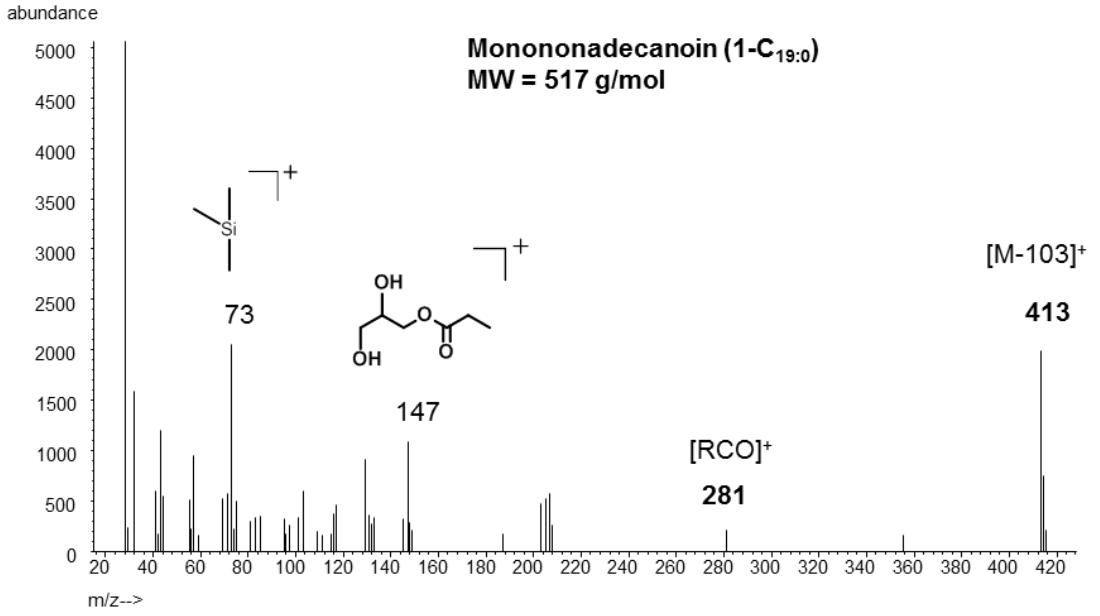

Figure 4-7 EI fragmentation mass spectrum of Monononadecanoin

Table 4-2 EI fragments of 2-MAG-TMS

	$[M]^+$	$[RCO+74]^+$	$[RCO]^+$	$[M-OCOR]^+$
	m/z	m/z	m/z	m/z
2-monopalmitin (2-$C_{16:0}$)	474	313	239	218

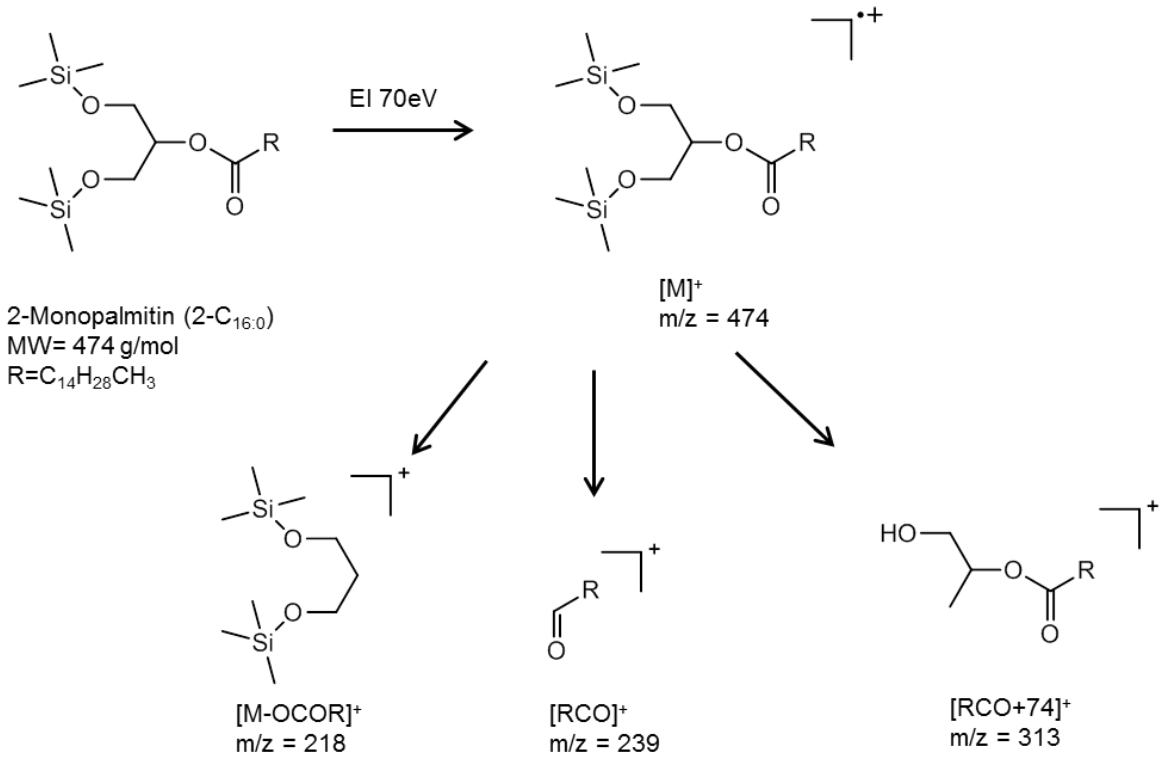

Figure 4-8 Possible fragmentation patterns of EI m/z of 2-monopalmitin

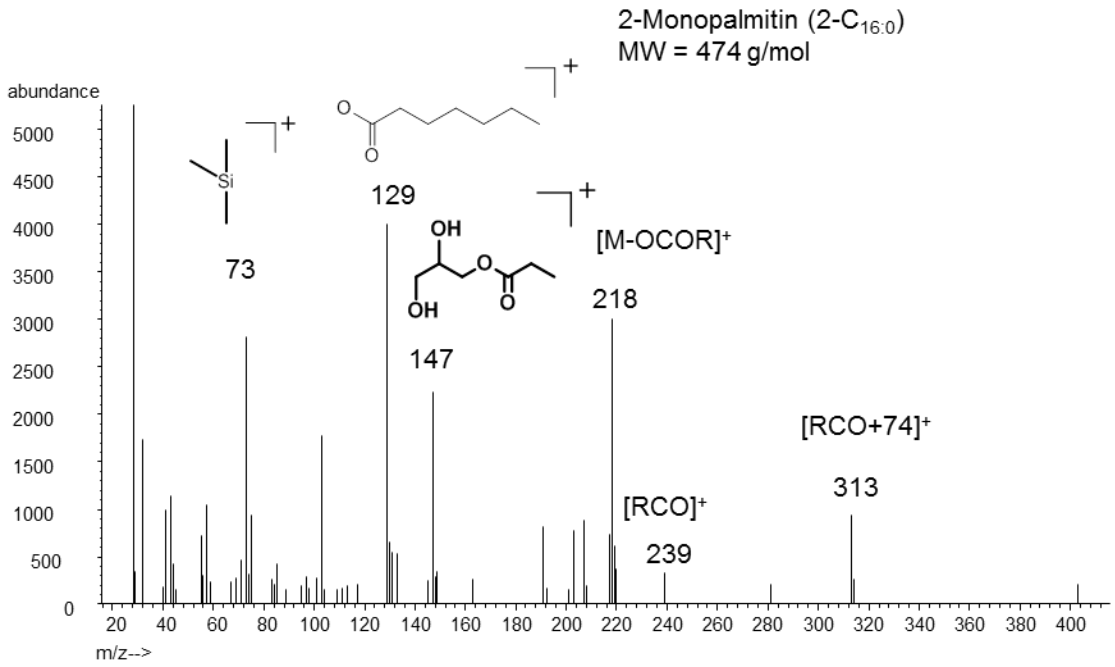

Figure 4-9 EI fragmentation mass spectrum of 2-Monoplamitin

The shaded columns in Table 4-1 and Table 4-2 contain the quantitation ions that were chosen for the subsequent quantification of each MAG in biodiesel. These quantitation ions $[M-103]^+$ result from the individual molecular ion $[M]^+$ less an ion m/z 103 which was assigned to the methoxytrimethylsilane-fragment as proposed in Figure 4-3. These quantitation ions were chosen due to their high abundance compared to the other characteristic fragments. *Linck et al.* also found the ions at m/z 459, 371, 239, 147 and 73 for 1-monopalmitin observing m/z 371 (respectively $[M-103]^+$) with the highest abundance [41].

For the 2-MAG-TMS the quantitation ion m/z 218 (shaded column Table 4-2) was chosen based on the literature [38] and due to its relative high abundance in the mass spectrum. Although this ion does not involve the fatty acid residue, and is therefore not a unique fragment, it is still a highly favoured ion for this positional isomer due to the fact that the chemical bond between the fatty acid chain and the glycerol moiety is apparently favourable for fragmentation. The ion $[M-103]^+$ m/z 371 which would be characteristic for the palmitic acid residue was not observed in the mass spectrum of 2-$C_{16:0}$ (see Figure 4-9). The fact that this particular ion only appears in the 1-MAG-TMS, was already demonstrated by *Myher, Marai, and Kuksis* [42].

The proposed structures of other fragments (m/z 73, 147 and 129) that show relatively high abundances, but are not characteristic for the individual MAG, are labelled in the mass spectra at the corresponding mass peak.

4.2.3 Limit of detection and quantification

The limit of detection (LOD) and the limit of quantification (LOQ), both relevant validation parameters, were determined by analysing the saturated MAGs with the new method, at three very low concentrations in triplicates and measuring the signal-to-noise-ratio (S/N) of each MAG.

The limits of quantification and detection of each MAG peak were determined by the Agilent ChemStation tool “signal-to-noise ratio”. It is used by drawing a baseline along the target peak and then drawing another baseline about 10 times the peak width along a region where no peaks are present. The first baseline catches the signal region and the second baseline catches the noise region. The ratio of these two regions in the chromatogram, at a known concentration allows the calculation of the corresponding concentrations for LOD at a signal-to-noise ratio of three (S/N=3), and LOQ at a signal-to-noise ratio of nine (S/N=9). The equations mentioned below (Equation 4-1, Equation 4-2, Equation 4-3) explain the calculation method: At a given concentration of 0.025 µg MAG per ml, the ChemStation tool determines a S/N of 5.3. The calculation of the concentration at a S/N of 3 and respectively 9 can easily be done using the rule of three. To obtain the corresponding parts per billion (ppb) by weight and respectively ng/g, the density of pyridine (0.98 g/ml) was taken into consideration. The results of the determination of LOD and LOQ for three different concentrations are shown in Table 4-3 and the averaged values for LOD and LOQ of each MAG are listed in Table 4-4. Figure 4-10 presents the corresponding gas chromatogram. For the detailed reports of the signal-to-noise determination with Agilent ChemStation see appendix. The obtained values for LOD and LOQ are significantly lower than comparable values proposed in the literature. For example *Yang et al.* claimed that for monoolein LOD was 0.3 µg/ml and LOQ respectively 1.00 µg/ml [38]. In contrast to the present work, they expressed LOQ by 10 times above the chromatographic backround instead of 9 times. Still the limits presented here are at least one magnitude lower, possibly due to measuring in SIM mode. However in terms of scan or SIM mode, the work of *Yang et al*. does not present specific

information about the analysis conditions for the LOD, LOQ determination. The LOD and LOQ for 1-$C_{16:0}$ show the lowest values compared to those of the other target MAGs. This can be explained by the fact that the quantitation ion for 1-$C_{16:0}$ (m/z 371) has the highest abundance compared to the signal from the other MAGs which can be observed in Figure 4-2 or Figure 4-10. The highest signal therefore accounts for the lowest LOD and LOQ because it is still distinguishable from the noise, whereas the other MAGs would not be distinguishable anymore.

$$0.0246\ \mu g/ml \cong {}^{S}/_{N} = 5.3$$

Equation 4-1 $$\boldsymbol{LOD = \frac{5.3 \cdot 0.0246\ g/ml}{3} = 0.0139\ \mu g/ml}$$

Equation 4-2 $$\boldsymbol{LOQ = \frac{5.3 \cdot 0.0246\ g/ml}{9} = 0.0418\ \mu g/ml}$$

Equation 4-3 $$\boldsymbol{LOQ = \left(\frac{0.0246\ g/ml}{0.98}\right) \times 1000 = 14.2\ ppb}$$

Table 4-3 Averaged values for LOD- and LOQ from measurements of the target MAGs at three different concentrations

	2-$C_{16:0}$	**1-$C_{16:0}$**	**1-$C_{17:0}$**	**1-$C_{18:0}$**
Conc. [µg/ml]	0.025	0.025	0.025	0.025
S/N	5.6	10.3	5.6	4.5
LOD (S/N=3) [µg/ml]	**0.0126**	**0.0072**	**0.0114**	**0.0166**
LOQ (S/N=9) [µg/ml]	**0.0377**	**0.0215**	**0.0341**	**0.0498**
Conc. [µg/ml]	0.05	0.05	0.05	0.05
S/N	14.0	24.4	14.6	10.7
LOD (S/N=3) [µg/ml]	**0.0127**	**0.0077**	**0.0126**	**0.0175**
LOQ (S/N=9) [µg/ml]	**0.0383**	**0.0230**	**0.0370**	**0.0527**
Conc. [µg/ml]	0.1	0.1	0.1	0.1
S/N	17.35	31.3	18.8	12.9
LOD (S/N=3) [µg/ml]	**0.0173**	**0.0097**	**0.0160**	**0.0236**
LOQ (S/N=9) [µg/ml]	**0.0520**	**0.0290**	**0.0480**	**0.0707**

Table 4-4 Averaged values for LOD and LOQ as ppb by weight and respectively ng/g

	Limit of detection (LOD)		Limit of quantification (LOQ)	
	[ng/g] [ppb]	rsd [%]	[ng/g] [ppb]	rsd [%]
2-$C_{16:0}$	14.4	3.0	45.1	8.9
1-$C_{16:0}$	8.4	1.7	26.3	5.0
1-$C_{17:0}$	13.5	2.8	42.9	8.4
1-$C_{18:0}$	19.4	4.6	61.2	13.8

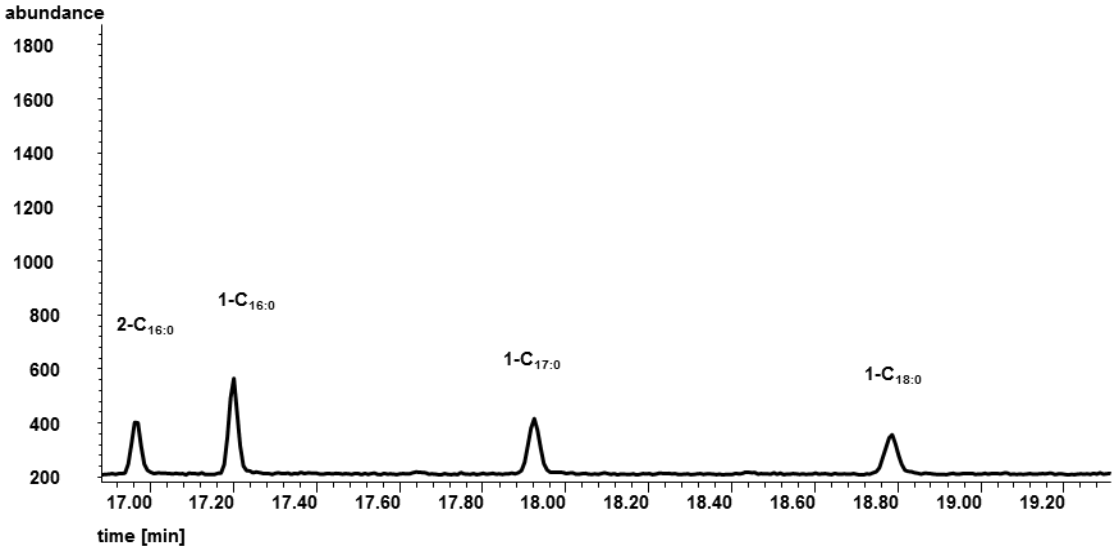

Figure 4-10 Representative chromatogram used for the determination of LOD, LOQ at 0.1 µg/ml

4.2.4 Linearity

The next step in the development of the method involved testing the linear relation between concentration and signal. The linearity is an important validation parameter and primarily the basis for a successful quantification of target analytes.

The resulting peak areas were plotted against the known MAG concentrations to get the linear regression lines and demonstrate the linearity of the new method. The coefficients of determination R^2 of all target MAGs are > 0.99 which was considered to be acceptable for this application.

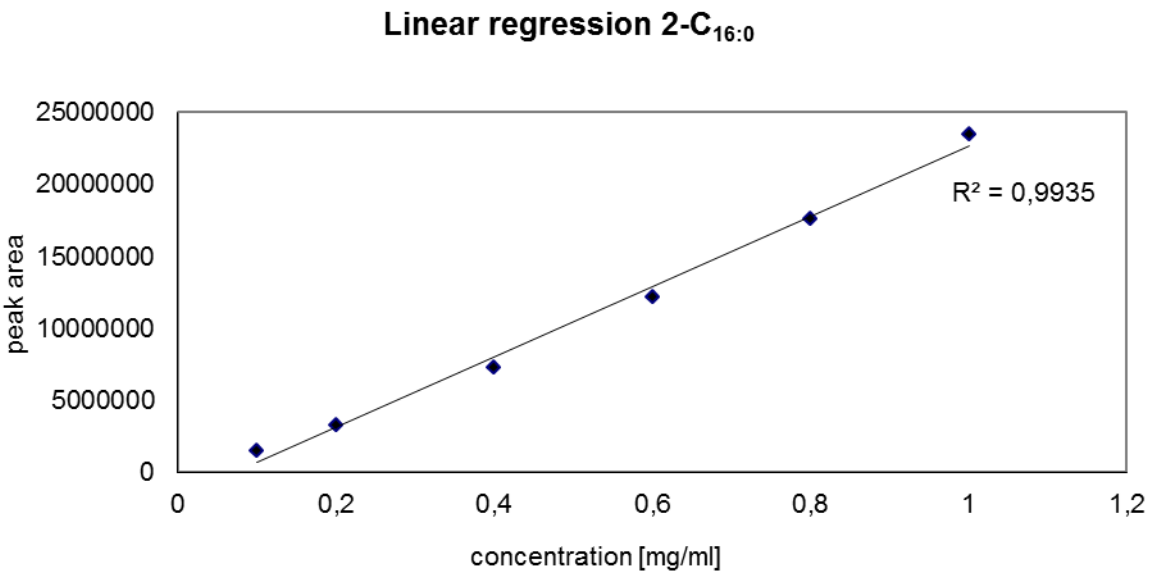

Figure 4-11 Linear regression of 2-$C_{16:0}$

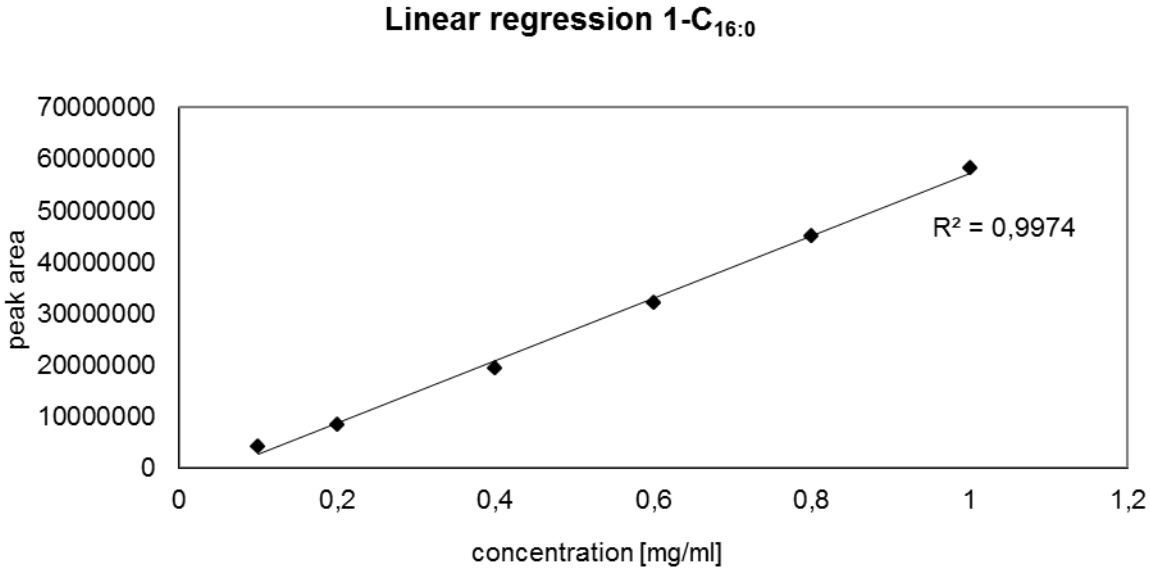

Figure 4-12 Linear regression of 1-$C_{16:0}$

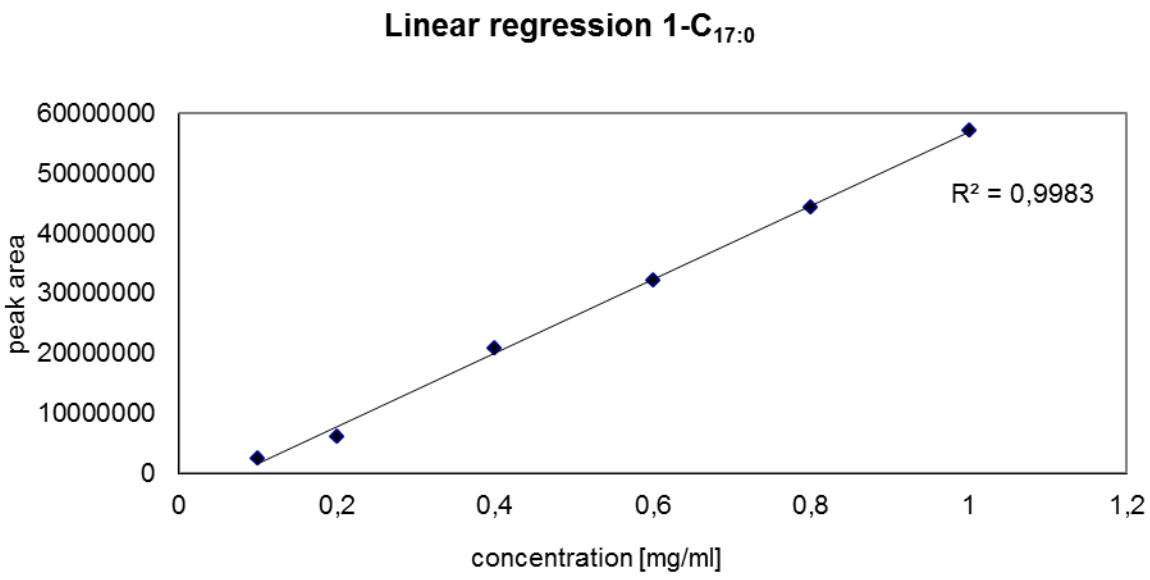

Figure 4-13 Linear regression of 1-$C_{17:0}$

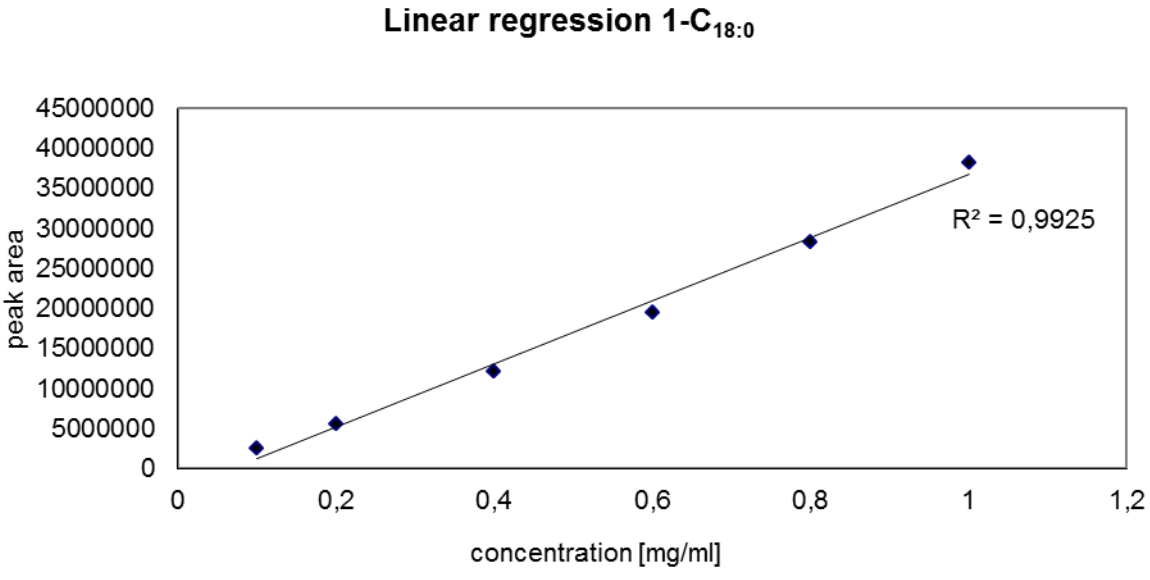

Figure 4-14 Linear regression of 1-$C_{18:0}$

4.3 Analysis of biodiesel samples

Prior to the quantification of the saturated MAGs in biodiesel samples, their response factors (RFs) and consequential correction factors (CFs) had to be determined, due to differing signal intensities of the individual MAGs at the same concentration. These differences of the signal intensities derive from the individual quantitation ions whose abundances vary, disregarding the concentration. Determination of the RFs and respectively CFs was carried out by analysing all four target MAGs and 1-$C_{19:0}$ at once and at the same concentration. 1-$C_{19:0}$ was intended to serve as IS in the following quantification analyses and therefore served here as IS as well. The CFs were calculated using the formulas of Equation 4-1, Equation 4-2 and Equation 4-3, quoted in 4.2.3.

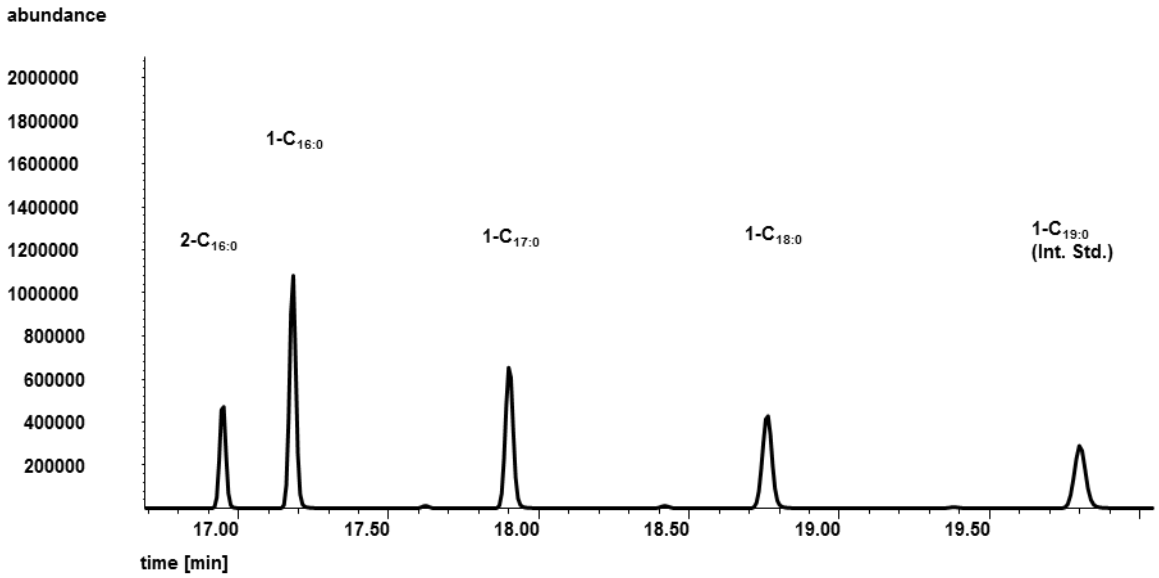

Figure 4-15 Determination of correction factors of the MAGs corresponding to the IS (1-$C_{19:0}$)

Table 4-5 Correction factors for the MAGs corresponding to the IS (1-$C_{19:0}$)

	Peak area	RF	CF
2-$C_{16:0}$	6718118	134632	1.11
1-$C_{16:0}$	15659086	313809	0.48
$C_{17:0}$	11500504	230471	0.65
$C_{18:0}$	9423765	188853	0.79
IS ($C_{19:0}$)	7440614	149111	1.00

The calculated values for the CFs ranged between 0.48 and 1.11 depending on whether the signal of the particular MAG compared to that of the IS was smaller (resulting CF>1) or greater (resulting CF<1).

After the general development of the method involving quantification strategy, linearity as well as investigating its limits, real biodiesel samples were analysed. Therefore it was important to design the analytical procedure as simple as possible in order to increase the efficiency of the method. Figure 4-16 presents the elaborated concept for the analytical procedure, which is carried out by weighing accurately about 10-30 mg of the biodiesel sample (theoretically similar fat derivatives are possible as well) into a GC vial and adding 1 ml IS (1-$C_{19:0}$, c= 50 µg/ml). After transferring 100 µl MSTFA into the vial, thorough vortexing is necessary to ensure successful mixing and silylation. Then, the vial is allowed to stand at RT for about 30 minutes to complete the derivatisation and yield the MAG-TMS. Subsequent GC-MS analyses were directly performed and the interpretation of the data and respectively the calculation of the results were carried out under consideration of the particular CFs. The results of the quantification of MAGs in biodiesel had to be multiplied with the respective CFs to correct the numerical value due to the differing signal intensities.

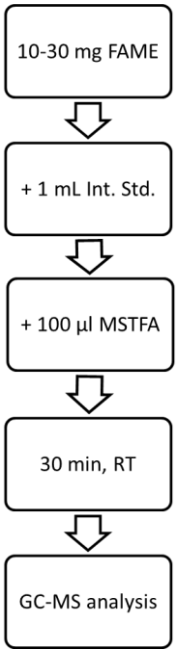

Figure 4-16 Scheme of the simple analytical procedure for the analysis of saturated MAGs in FAME

4.3.1 Saturated MAGs in FAME

All biodiesel samples were analysed following the scheme of the analytical procedure for the analysis of saturated MAGs shown in Figure 4-16 and using the developed method previously described.

FAME from used cooking oil

The FAME samples deriving from used cooking oil all resulted in very similar gas chromatograms, so that only one representative chromatogram is presented in Figure 4-17. The corresponding results of the MAG quantification are listed in Table 4-6. For all other UCO-ME chromatograms see appendix.

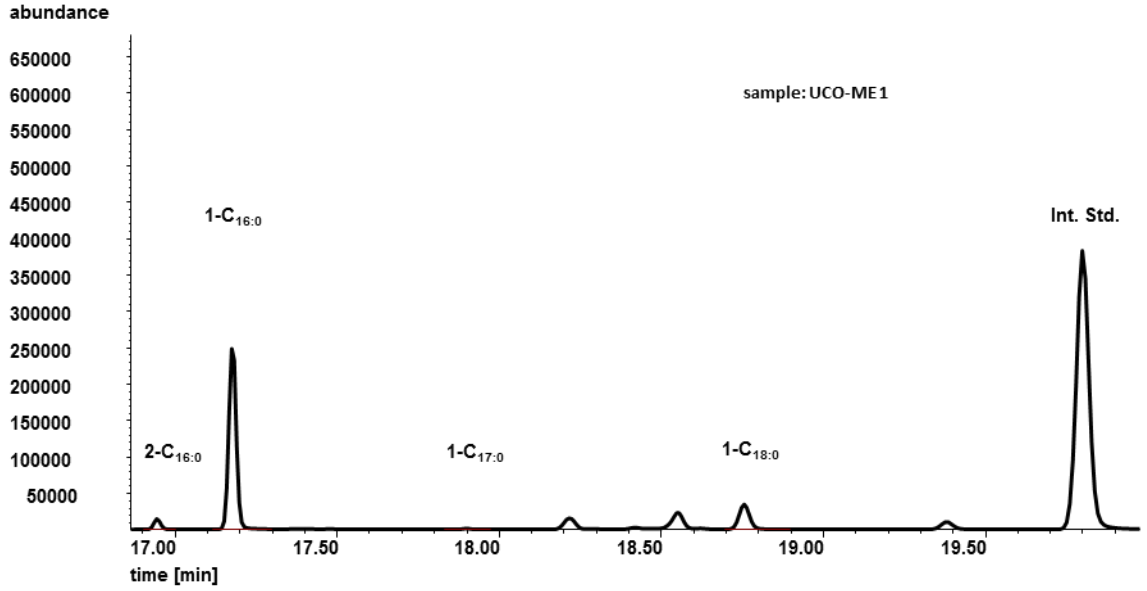

Figure 4-17 Representative gas chromatogram of biodiesel from UCO (sample: UCO-ME 1)

Table 4-6 MAG contents of UCO-ME 1

UCO-ME 1	2-$C_{16:0}$	1-$C_{16:0}$	1-$C_{17:0}$	1-$C_{18:0}$	Total
[µg/g]	45	370	3	118	536
RSD [%]	0.97	1.08	3.72	1.59	1.12

The MAGs were clearly identified by their retention times and quantitation ions. The chromatogram shows that 1-$C_{16:0}$ with 370 µg per g biodiesel was definitely the substantial component compared to the other saturated MAGs in the sample. 1-$C_{17:0}$ in contrast cannot be viewed in this scaling of the chromatogram. Only zooming in on the time area, where 1-$C_{17:0}$ was expected, enabled the observation of a small signal peak which was integrated and thus taken into account. The particular section was labelled in the chromatogram even if there is no visible peak.

Additionally the precision of the method was tested with the UCO-ME samples. Ten independent weighted samples (UCO-ME 1,2,3) and respectively three independent weighted samples (for UCO-ME 5,6,7) were analysed with the developed method according to the analytical procedure described in the previous chapter and the coefficients of variation were determined. The comparison of the coefficients of variation allows conclusion on the reproducibility of the method. The calculation followed Equation 4-4 whereby v_c refers to the coefficient of variation, x refers to the mean value of one test series, and s refers to the relative standard deviation.

Equation 4-4

$$\boldsymbol{v_c}[\%] = \frac{\bar{\boldsymbol{x}}}{\boldsymbol{s}} * \mathbf{100}$$

The coefficients of variation for all UCO-ME samples are presented in Table 4-7. The precision of the method is a measure that involves the variation of results caused by all steps of the analytical procedure (weighing, sample preparation, measurement, interpretation,…). It can be observed that the variance of the results for UCO-ME 1,2,3 (each ten samples measured) is not significantly lower (better) than for UCO-ME 5,6,7 (each three samples tested) and that therefore the measurement of three independent weighted samples was sufficient for the subsequent analyses (WAF-MEs, BR-ME). However it is noticeable that the coefficients for UCO-ME 8,9 are significantly higher, which implies that the corresponding results of these series are less precise due to a very high variation.

Table 4-7 Coefficients of variation for UCO-ME samples

v_c [%]	UCO-ME								
	1	**2**	**3**	**4**	**5**	**6**	**7**	**8**	**9**
2-$C_{16:0}$	1.13	0.70	0.84	2.19	0.55	0.30	0.77	4.67	16.2
1-$C_{16:0}$	1.59	1.01	0.73	2.30	0.35	0.32	1.48	4.33	10.6
1-$C_{17:0}$	3.60	5.41	6.83	-	-	-	1.53	-	10.4
1-$C_{18:0}$	1.68	0.78	1.27	1.00	0.83	0.39	0.87	4.41	11.9
Total	1.50	0.83	0.75	2.01	0.21	0.33	0.99	4.37	5.17

FAME from waste animal fats

The FAME samples deriving from waste animal fats all resulted in very similar gas chromatograms, so that only one representative chromatogram is presented in Figure 4-18. The corresponding results of the MAG quantification are listed in Table 4-8. For all other WAF-ME chromatograms see appendix.

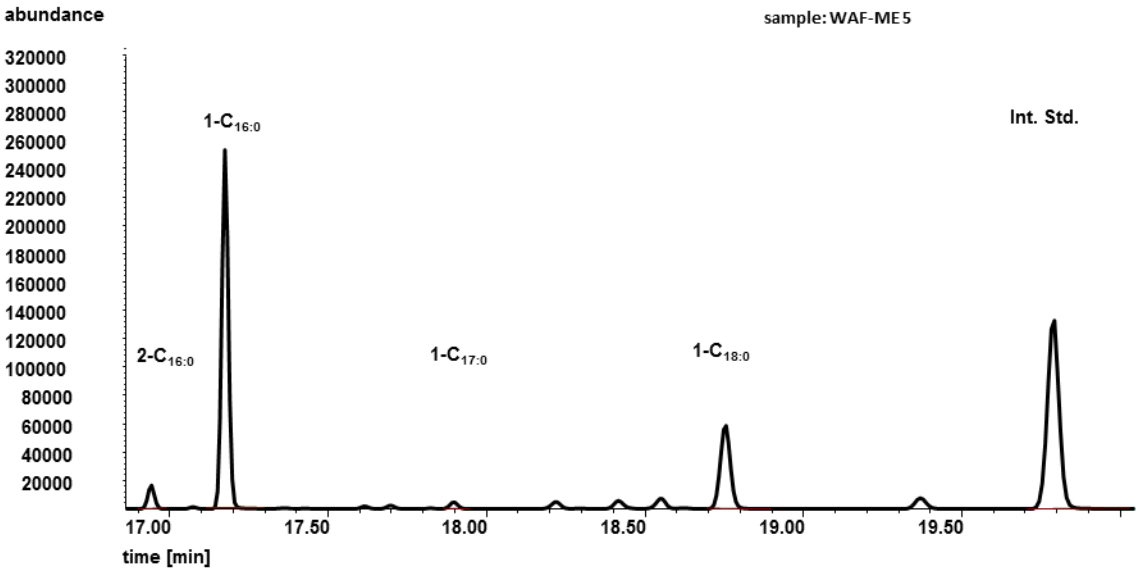

Figure 4-18 Representative gas chromatogram of biodiesel from WAF (sample: WAF-ME 5)

Table 4-8 MAG contents of WAF-ME 5

WAF-ME 5	2-$C_{16:0}$	1-$C_{16:0}$	1-$C_{17:0}$	1-$C_{18:0}$	Total
[µg /g]	136	886	28	520	1569
RSD [%]	0.32	0.21	0.38	0.52	0.30

The observation of the chromatogram (Figure 4-18) shows that 1-$C_{16:0}$ and 1-$C_{18:0}$ are definitely present in the sample, which was expected due to the animal derived feedstock of the biodiesel, that is known to contain more saturated fats than vegetable oil feedstocks. That fact can also be confirmed by comparing the amount of 1-$C_{16:0}$ and 1-$C_{18:0}$ in WAF-ME with the corresponding amounts in UCO-ME. 886 µg of 1-$C_{16:0}$ per g WAF-ME is more than twice as much compared to 370 µg of 1-$C_{16:0}$ per g UCO-ME. And 520 µg of 1-$C_{18:0}$ per g WAF-ME is almost five times as much as 118 µg 1-$C_{18:0}$ per g UCO-ME. This definitely shows that FAME from waste animal fats accompanies a significantly higher level of unfavourable saturated MAGs. Also the concentration of 1-$C_{17:0}$ in WAF-ME at 28 µg/g is about 9 times higher than the corresponding concentration of 3 µg/g in UCO-ME.

FAME from bacon rind

Figure 4-19 presents the gas chromatogram of FAME from bacon rind.

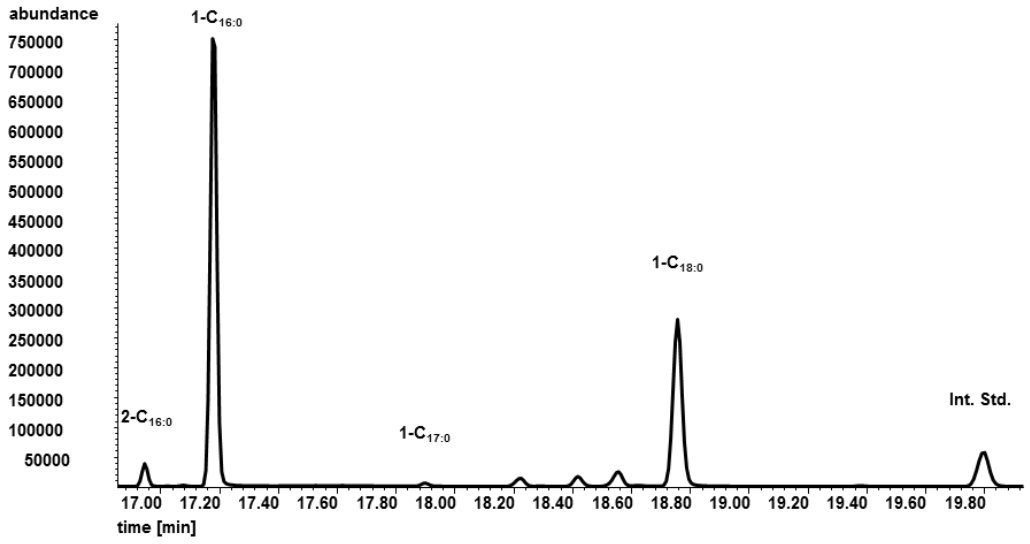

Figure 4-19 Gas chromatogram of biodiesel from bacon rind

Table 4-9 MAG contents of BR-ME

Bacon rind-ME	2-$C_{16:0}$	1-$C_{16:0}$	1-$C_{17:0}$	1-$C_{18:0}$	Total
[µg MAG/g]	168	1540	19	1326	3053
RSD [%]	2.72	2.58	8.27	2.73	2.61

The gas chromatogram shows the largest peaks for 1-$C_{16:0}$ and 1-$C_{18:0}$ compared to the other animal fat derived samples. Due to the fact that the exact composition of the WAF samples is unknown, these comparisons cannot be used to conclude that bacon rind derived biodiesel accompanies more quality issues than biodiesel from waste animal fats in general.

A qualitative observation of all chromatograms showed that there were more peaks than target MAGs which is probably caused by positional isomers of monostearin, monoolein and maybe even of monolinoleate that were present in the sample as well as a positional isomer of monononadecanoate respectively deriving from the IS. As explained and illustrated in 4.2.2 the quantitation ion for m/z 218 does not involve the characteristic fatty acid residue but is a fragment characteristic for substitutes on the carbon at position 2 of the glycerol structure. Therefore all 2-MAGs are measured with this ion even if the individual fatty acid chain differs. The mass spectra of the unidentified peaks exhibited all the fragment m/z 218, which confirmed the assumption that the additional peaks at about 18.22 and 18.55 minutes belong to positional isomers like 2-monostearate, 2-monooleate or 2-monolinoleate. They were not further investigated due to the fact that the peaks only represented impurities in the MAGs standards and therefore their size was too small to be able to determine the corresponding response factors.

Summary of results: MAGs in FAME

Table 4-10 Summary of results from the quantification of saturated MAGs with GC-MS in several FAME samples

FAME	**2-$C_{16:0}$** [µg/g]	**rsd** [%]	**1-$C_{16:0}$** [µg/g]	**rsd** [%]	**1-$C_{17:0}$** [µg/g]	**rsd** [%]	**1-$C_{18:0}$** [µg/g]	**rsd** [%]	**Sum** [µg/g]	**rsd** [%]
UCO-ME 1	45.1	0.97	370	1.08	2.58	3.72	118	1.59	536	1.12
UCO-ME 2	36.0	0.70	321	1.01	2.33	5.40	96.0	0.78	455	0.83
UCO-ME 3	35.5	0.84	318	0.73	2.39	6.78	94.6	1.27	450	0.75
UCO-ME 4	62.9	2.19	435	2.30	<0	-	121	1.00	620	2.01
UCO-ME 5	11.2	0.55	75.1	0.35	<0	-	11.0	0.83	97	0.21
UCO-ME 6	150	0.30	958	0.32	4.94	0.72	214	0.39	1327	0.33
UCO-ME 7	278	0.77	1669	1.48	9.69	1.53	460	0.87	2416	0.99
UCO-ME 8	50.8	4.67	327	4.33	<0	-	39	4.41	417	4.37
UCO-ME 9	699	16.2	2057	10.6	12.7	10.4	528	11.9	3296	5.17
WAF-ME 1	95.0	1.57	606	1.13	21.3	1.37	426	1.20	1148	1.17
WAF-ME 2	95.9	8.79	612	9.21	21.5	8.88	430	9.60	1159	9.31
WAF-ME 3	100	9.81	637	10.2	22.3	9.89	448	10.6	1206	10.3
WAF-ME 4	91.4	5.31	583	5.79	20.5	5.46	410	6.11	1105	5.86
WAF-ME 5	136	0.32	886	0.21	27.9	0.38	520	0.52	1569	0.30
WAF-ME 6	150	0.30	958	0.32	28.8	0.72	214	0.39	1327	0.33
BR-ME	168	2.72	1540	2.58	19.3	8.27	1326	2.73	3053	2.61

The most striking fact about the summarised results in Table 4-10 probably is the great variation of particular MAG contents within one group of biodiesel samples. When looking at the results of 1-$C_{16:0}$ in UCO-ME samples for instance, it can be observed that the values range between 318 and 2057 µg/g. One has to consider that the samples come from different suppliers, which could explain the fact that UCO-ME 1,2,3 contain significantly less MAGs than most of the other UCO-ME samples. The two exceptions within the UCO derived biodiesels, which show significantly higher MAG values, are UCO-ME 7 and UCO-ME 9. For UCO-ME 8,9 it has to be considered the great variation of the results presented in Table 4-7 which

led us to the assumption that the results are not directly comparable to the other UCO-ME results, due to the low precision.

UCO-ME 5 shows an exceptionally low level of MAGs due to the fact that this particular sample underwent a distillation process in which the MAGs were largely removed. Nevertheless the results show a clear tendency regarding the concentrations of 1-$C_{16:0}$ and 1-$C_{18:0}$: In all UCO-ME samples, the concentration of 1-$C_{16:0}$ is significantly higher than the concentration of 1-$C_{18:0}$.

The results of the WAF-ME samples are, compared to those of the UCO-ME samples, more constant with a smaller range of the MAG values. Due to the fact that waste animal fats can consist of a variety of animals for slaughter, including poultry whose fat composition differs significantly from pork and beef, it can be assumed that the samples are all composed of the same animal fats in equal parts. More detailed information about the WAF composition was obtained by analysing their fatty acid profiles, see Table 4-12.

BR-ME contains more saturated MAGs than the WAF-ME samples although they are made of similar feed material. Yet there are no sample specific details available to reasonably interpret this discrepancy.

4.3.2 Fatty acid profile

The fatty acid compositions of all biodiesel samples were analysed to investigate the concentrations of saturated FAMEs and to get information of the expected prominent MAGs. The aim was to test if the fatty acid compositions of the MAGs mirror that of the parent FAMEs. The gas chromatographic separation is based on the boiling points and polarity of the FAMEs. Short-chained FAMEs elute before long-chained FAMEs and less polar FAMEs (saturated FAMEs) elute before polar FAMEs (unsaturated FAMEs). The identification of the target peaks was achieved by comparison of the retention times with a chromatogram of a reference material (GLC-462, Nu Check Prep Inc) containing 28 different FAMEs.

FAME from used cooking oil

A representative gas chromatogram of a biodiesel from UCO is shown in Figure 4-20. The predominant fatty acids in FAME from UCO are $C_{16:0}$, $C_{18:1}$ and $C_{18:2}$. Additionally there are also significant amounts of $C_{18:0}$ and $C_{18:3}$ in the samples as well as quite

low concentrations of $C_{12:0}$, $C_{14:0}$, $C_{16:1}$ and $C_{20:0}$, $C_{20:1}$ and $C_{22:0}$. The accurate area per cents of the corresponding peaks are listed in

Table 4-11.

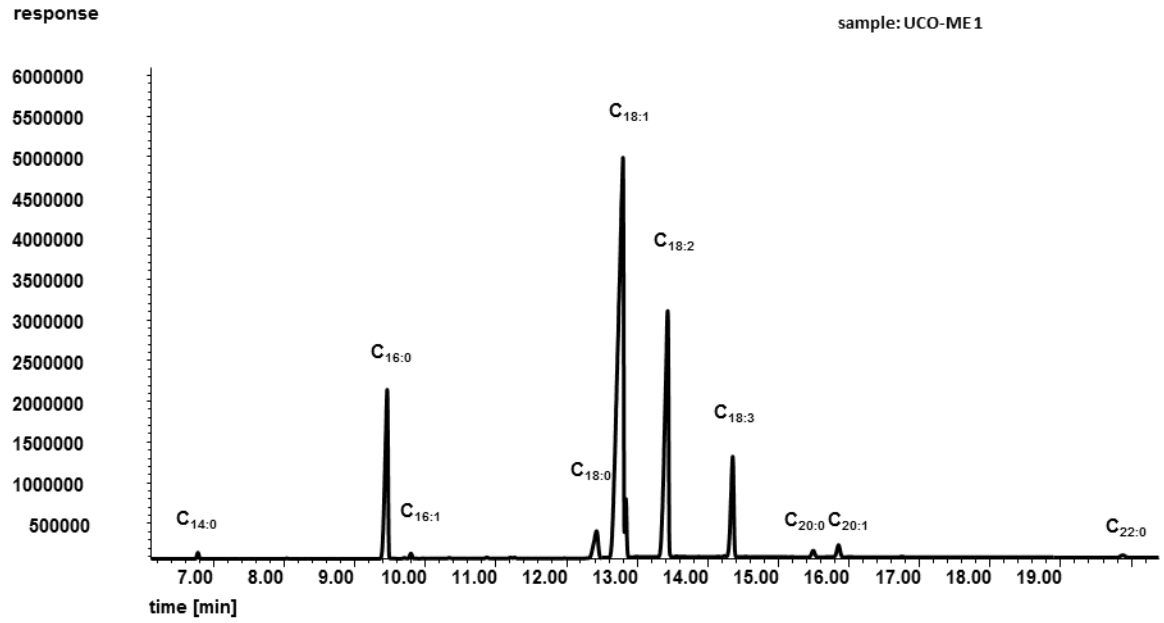

Figure 4-20 Representative gas chromatogram presenting the fatty acid profile of UCO-ME

The fact, that the results for $C_{16:0}$ turned out much higher than the results for $C_{18:0}$ was in accordance to the results from the MAG quantification, in which 1-$C_{16:0}$ also appeared at much higher levels than 1-$C_{18:0}$. In addition the very low concentration of 1-$C_{17:0}$ could be confirmed with the corresponding fatty acid profile. The 1-$C_{17:0}$ peak of the fatty acid profile was too small to be observed in Figure 4-20 but the accurate result is listed in Table 4-11.

An interesting fact about the UCO-ME samples is that all of them show (more or less) rather high levels of palmitic acid ranging between 8 to 16%. According to the "German Society for Fat Science" (Deutsche Gesellschaft für Fettwissenschaft) these levels for palmitic acid are too high that the samples could possibly derive exclusively from rapeseed oil (2.5 to 7 % C16:0) or sunflower oil (5.0-6.7% C16:0). It is more likely that they are a mixture of vegetable oils probably also containing fat sources that include higher levels of palmitic acid such as animal fat (20-30% C16:0) [43].

Table 4-11 Fatty acid composition of FAMEs from used cooking oil

FAME	UCO-ME								
	1	**2**	**3**	**4**	**5**	**6**	**7**	**8**	**9**
	[%]	**[%]**	**[%]**	**[%]**	**[%]**	**[%]**	**[%]**	**[%]**	**[%]**
$C_{10:0}$	-	0.06	0.05	0.02	-	-	-	0.03	0.02
$C_{12:0}$	0.11	0.34	0.31	0.12	0.17	0.03	0.12	0.13	0.12
$C_{14:0}$	0.31	0.51	0.49	0.39	0.53	0.14	0.39	0.45	0.39
$C_{14:1}$	-	0.01	-	-	0.02	-	-	0.04	-
$C_{15:0}$	0.03	0.04	0.04	0.03	0.05	0.02	-	0.04	0.03
$C_{15:1}$	-	-	-	-	0.03	-	-	0.01	-
$C_{16:0}$	**11.9**	**15.3**	**15.2**	**14.3**	**17.4**	**8.75**	**14.3**	**15.9**	**14.5**
$C_{16:1}$	0.35	0.44	0.43	0.42	0.53	0.24	0.42	0.47	0.43
$C_{17:0}$	**0.08**	**0.08**	**0.08**	**0.08**	**0.08**	**0.07**	**0.07**	**0.08**	**0.09**
$C_{17:1}$	0.05	0.05	0.09	0.08	0.1	0.06	0.08	0.09	0.09
$C_{18:0}$	**2.85**	**3.78**	**3.77**	**3.82**	**3.51**	**4.50**	**3.90**	**3.70**	**3.40**
$C_{18:1}$	53.6	46.6	46.9	44.5	43.0	47.2	44.7	44.14	44.5
$C_{18:2}$	21.9	28.3	28.3	32.0	31.3	33.2	31.7	31.2	31.4
$C_{18:3}$ n-6	6.97	2.77	2.79	2.85	2.75	3.06	2.77	2.70	2.71
$C_{18:3}$ n-3	0.47	0.40	0.40	-	-	-	-		-
$C_{20:0}$	0.91	0.53	0.61	0.38	0.21	0.70	0.42	0.27	0.422
$C_{20:1}$	-	0.04	-	0.50	0.32	0.90	0.53	0.44	0.60
$C_{20:2}$	0.08	-	0.04	-	0.03	-	-	0.03	-
$C_{22:0}$ n-3	-	0.46	0.45	0.46	-	1.09	0.61	0.23	0.53
$C_{22:1}$	0.12	-	0.09	-	-	-	-	0.04	-
$C_{22:2}$	-	0.08	-	-	-	-	-	-	-
$C_{16:0}$ + $C_{17:0}$ + $C_{18:0}$	**14.8**	**19.2**	**19.1**	**18.2**	**21.0**	**13.3**	**18.3**	**19.7**	**18.0**

FAME from waste animal fat

A representative gas chromatogram of a biodiesel from WAF is shown in Figure 4-21. The predominant fatty acids in FAME from WAF are $C_{16:0}$, $C_{18:0}$ and $C_{18:1}$.

Additionally there are also significant amounts of $C_{14:0}$ and $C_{16:1}$ in the samples as well as quite low concentrations of $C_{15:0}$, $C_{17:0}$, $C_{17:1}$, $C_{18:3}$, $C_{20:0}$ and $C_{20:1}$. The accurate area per cents of the corresponding peaks are listed in Table 4-12.

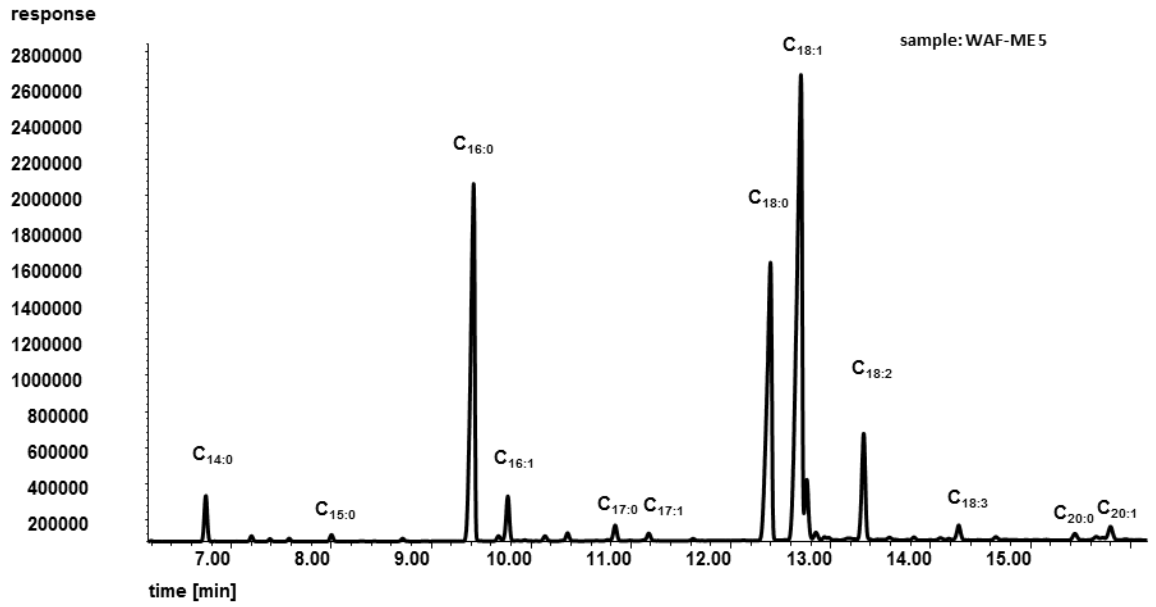

Figure 4-21 Representative gas chromatogram presenting the fatty acid profile of WAF-ME

It can easily be observed that the $C_{18:0}$ peak of WAF-ME is essentially higher that the corresponding peak of UCO-ME.

Table 4-12 Fatty acid composition of FAMEs from waste animal fat and bacon rind

	WAF-ME						BR-ME
FAME	**1**	**2**	**3**	**4**	**5**	**6**	
	[%]	**[%]**	**[%]**	**[%]**	**[%]**	**[%]**	**[%]**
$C_{10:0}$	0.11	0.10	0.09	0.10	0.06	0.05	0.09
$C_{12:0}$	0.19	0.19	0.16	0.17	0.12	0.11	0.09
$C_{12:1}$	0.03	0.03	0.03	0.03	-	-	-
$C_{14:0}$	2.55	2.44	2.49	2.57	2.12	2.02	1.48
$C_{14:1}$	0.27	0.26	0.27	0.27	0.25	0.24	-

$C_{15:0}$	0.37	0.35	0.36	0.36	0.33	0.32	0.04
$C_{15:1}$	0.18	0.17	0.17	0.17	0.15	0.15	-
$C_{16:0}$	**25.8**	**25.4**	**25.8**	**25.9**	**22.2**	**21.8**	**27.5**
$C_{16:1}$	2.82	2.72	2.80	2.84	2.29	2.24	1.77
$C_{17:0}$	**0.86**	**0.85**	**0.89**	**0.88**	**0.93**	**0.93**	**0.29**
$C_{17:1}$	0.44	0.44	0.45	0.45	0.47	0.48	0.17
$C_{18:0}$	**17.4**	**17.5**	**18.0**	**17.9**	**20.7**	**20.8**	**18.9**
$C_{18:1}$	39.1	39.2	39.1	38.8	40.6	40.9	34.3
$C_{18:2}$	8.31	8.35	7.69	7.55	5.94	6.10	12.9
$C_{18:3}$ n-6	0.79	0.87	0.83	0.73	0.14	0.16	0.54
$C_{18:3}$ n-3	-	-	-	-	0.14	1.12	0.26
$C_{20:0}$	0.20	0.19	-	0.19	0.43	0.44	-
$C_{20:1}$	-	0.44	0.48	0.45	0.99	0.10	0.62
$C_{20:2}$	0.20	0.23	0.24	0.23	0.38	0.42	0.47
$C_{20:3}$	0.09	0.24	-	0.09	0.16	0.15	0.06
$C_{20:4}$	0.23	-	-	0.26	0.42	0.44	0.18
$C_{20:3}$ n-6	-	-	-	-	0.13	0.12	0.05
$C_{20:5}$	-	-	-	-	-	-	-
$C_{22:1}$	-	-	-	-	-	-	0.01
$C_{22:2}$	-	-	-	-	-	-	-
$C_{22:4}$	-	-	-	-	0.12	-	0.10
$C_{22:5}$ n-3	-	-	-	-	-	-	0.05
$C_{22:6}$	-	-	-	-	-	-	0.03
$C_{16:0}$ + $C_{17:0}$ + $C_{18:0}$	**44.1**	**44.1**	**44.7**	**44.7**	**42.8**	**43.5**	**46.7**

FAME from bacon rind

A representative gas chromatogram of a biodiesel from bacon rind is shown in Figure 4-22. The predominant fatty acids in FAME from bacon rind are $C_{16:0}$, $C_{18:0}$, $C_{18:1}$ and $C_{18:2}$. Additionally there are also low concentrations of $C_{14:0}$ and $C_{16:1}$ in the samples as well as quite little concentrations of $C_{14:0}$, $C_{16:1}$, $C_{18:3}$, $C_{20:0}$ and $C_{20:1}$. The accurate area per cents of the corresponding peaks are listed in Table 4-12.

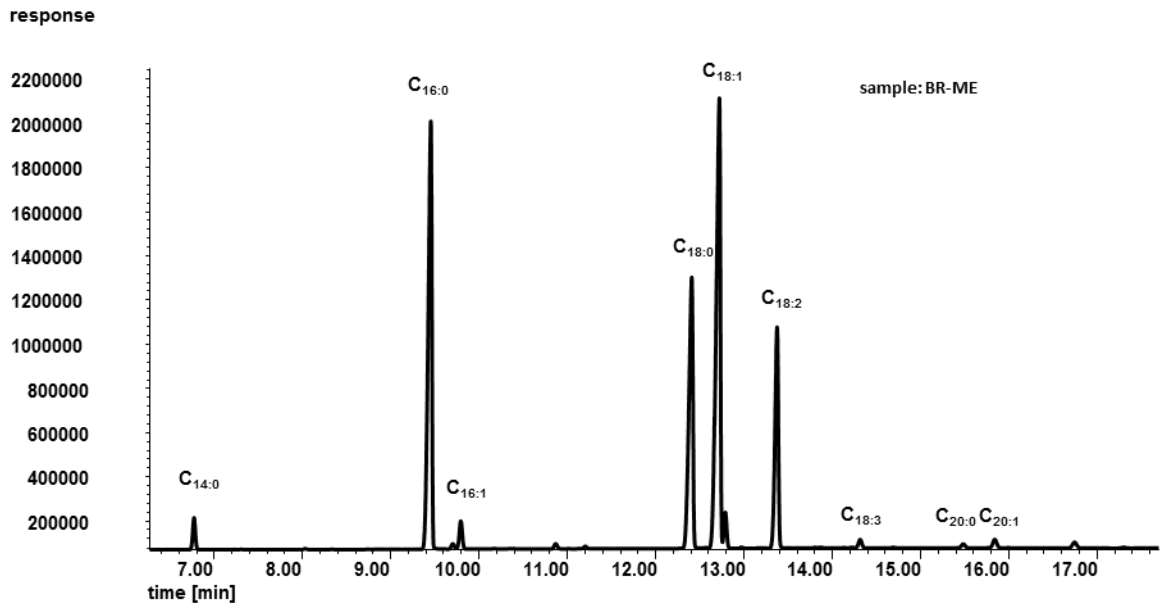

Figure 4-22 Gas chromatogram presenting the fatty acid profile of BR-ME

The fact that oleic, linoleic and linolenic acid methyl esters were found in all tested biodiesel samples allow the assumption that the unassigned peaks in the MAG quantification (Figure 4-17, Figure 4-18, Figure 4-19) indeed derive from the positional isomers of oleic, linoleic and linolenic acid methyl esters.

4.3.3 Total MAG content

MAGs, DAGs and TAGs (as well as free and total glycerol) of all biodiesel samples were determined according to the European standard method EN 14105 [37]. For this work only the total MAG results were evaluated and their saturated contents were calculated from the corresponding fatty acid profile as demonstrated in Equation 4-5.

Equation 4-5

$$1 - C_{18:0}\ calculated\ [\%] = \frac{C_{18:0}\ FAME\ [\%] \times MAG_{total}\ [\%]}{100}$$

Table 4-13 MAGs calculated from the corresponding fatty acid profile and total MAGs

		From FAME			Calculated		
Sample	**total MAG[1] [%]**	**$C_{16:0}$[2] [%]**	**$C_{17:0}$[2] [%]**	**$C_{18:0}$[2] [%]**	**1-$C_{16:0}$[3] [µg/g]**	**1-$C_{17:0}$[3] [µg/g]**	**1-$C_{18:0}$[3] [µg/g]**
UCO-ME 1	0.32	11.9	0.08	2.85	381	2.56	91.2
UCO-ME 2	0.30	15.3	0.08	3.78	459	2.40	113
UCO-ME 3	0.28	15.2	0.08	3.77	426	2.24	106
UCO-ME 4	0.31	14.3	0.08	3.82	443	2.48	118
UCO-ME 5	0.03	17.4	0.08	3.51	52.2	0.24	10.5
UCO-ME 6	0.61	8.75	0.07	4.50	872	4.27	238
UCO-ME 7	1.15	14.3	0.07	3.90	1645	8.05	449
UCO-ME 8	0.13	15.9	0.08	3.70	207	1.04	48.1
UCO-ME 9	1.07	14.5	0.09	3.40	1552	9.63	364
WAF-ME 1	0.23	25.8	0.86	17.4	593	19.8	400
WAF-ME 2	0.21	25.4	0.85	17.5	533	18.1	368
WAF-ME 3	0.24	25.8	0.89	18.0	610	21.4	432
WAF-ME 4	0.22	25.9	0.88	17.9	570	394	19.4
WAF-ME 5	0.32	22.2	0.93	20.7	710	29.8	662
WAF-ME 6	0.30	21.8	0.93	20.8	654	27.9	624
BR-ME	0.28	27.5	0.29	18.9	1843	19.4	1266

[1] total MAG contents determined with EN 14105

[2] % from FAMEs see fatty acid profile see Table 4-11, Table 4-12

[3] % MAG calculated from total MAGs and fatty acid profile

Table 4-14 Direct comparison of MAG results from the GC-MS method and the calculated results from the fatty acid profile and the total MAG contents

Sample		1-$C_{16:0}$ [µg/g]	1-$C_{17:0}$ [µg/g]	1-$C_{18:0}$ [µg/g]	Sum[3] [µg/g]	Difference[4] [%]
GC-MS[1]	**UCO-ME 1**	370	2.58	118	536	11.4
Calculated[2]	**UCO-ME 1**	381	2.56	91.2	475	
GC-MS	**UCO-ME 2**	321	2.33	96	455	26.4
Calculated	**UCO-ME 2**	459	2.40	113	575	
GC-MS	**UCO-ME 3**	318	2.39	94.6	450	18.4
Calculated	**UCO-ME 3**	426	2.24	106	533	
GC-MS	**UCO-ME 4**	435	<0	121	620	9.0
Calculated	**UCO-ME 4**	443	2.48	118	564	
GC-MS	**UCO-ME 5**	75	<0	11	97	35.1
Calculated	**UCO-ME 5**	52	0.24	10.5	63	
GC-MS	**UCO-ME 6**	958	4.94	214	1327	16.1
Calculated	**UCO-ME 6**	872	4.27	238	1114	
GC-MS	**UCO-ME 7**	1669	9.69	460	2416	13.0
Calculated	**UCO-ME 7**	1645	8.05	449	2101	
GC-MS	**UCO-ME 8**	327	<0	38.9	417	38.6
Calculated	**UCO-ME 8**	207	1.04	48.1	256	
GC-MS	**UCO-ME 9**	2057	12.7	528	3296	41.6
Calculated	**UCO-ME 9**	1552	9.63	364	1925	
GC-MS	**WAF-ME 1**	606	21.3	426	1148	9.8
Calculated	**WAF-ME 1**	593	19.8	400	1035	
GC-MS	**WAF-ME 2**	612	21.5	430	1159	20.8
Calculated	**WAF-ME 2**	533	18.1	368	918	
GC-MS	**WAF-ME 3**	637	22.3	448	1206	11.0
Calculated	**WAF-ME 3**	610	21.4	432	1073	
GC-MS	**WAF-ME 4**	583	20.5	410	1105	11.0
Calculated	**WAF-ME 4**	570	19.4	394	983	

GC-MS	**WAF-ME 5**	886	27.9	520	1569	10.6
Calculated	**WAF-ME 5**	710	29.8	662	1403	
GC-MS	**WAF-ME 6**	958	28.8	214	1327	1.6
Calculated	**WAF-ME 6**	654	27.9	624	1306	
GC-MS	**BR-ME**	1540	19.3	1326	3053	2.5
Calculated	**BR-ME**	1843	19.4	1266	3128	

[1] Results from the new developed GC-MS method

[2] Results calculated from total MAGs and fatty acid profile, see Table 4-13

[3] Sum of MAG results including the results for 2-$C_{16:0}$ determined with GC-MS

[4] Difference of sum results calculated and determined with GC-MS in per cent

Table 4-14 presents the comparison of the results for MAG quantification obtained from the GC-MS method and the calculation out of the total MAG and the fatty acid profile. At this point it has to be stated very clearly that the calculation of the MAG contents with the help of the fatty acid profile and the results from the total MAG content can only be seen as an approximation. For a direct comparison, an investigation of the detailed kinetics of the particular transesterification would be needed in order to gain information about which TAGs (precisely TAGs with what kind of fatty acid residues) are converted more likely to FAME and which TAGs tend to give a higher rate of MAGs. In general it can be stated that the calculated results have the tendency to give lower values than the results from the GC-MS analysis. This applies to all results except those of UCO-ME 1, UCO-ME 2 and BR-ME.

Although all deviations are relatively high, UCO-ME 5, UCO-ME 8 and UCO-ME 9 show especially differing results. Since the GC-MS method can be taken as the more accurate analytical procedure compared to the calculation from the fatty acid profile and the total MAG content, this might indicate that with certain samples the approximation is just not possible.

One of the reasons might be that certain TAGs are favoured for conversion to FAME as mentioned before. Possibly certain fatty acid moieties in MAGs are more likely to be successfully converted to FAME than others, which would result in a discrepancy between the levels of a specific MAG and its corresponding FAME.

Although the absolute values of the compared results differ between 1.6 and 46.1 % the two methods agree in the order of the quantitative occurrence of the MAGs. This means that no direct comparison of the results can be drawn concerning their absolute values but that as expected, the fatty acid profile of a biodiesel sample allows an approximation of the corresponding MAG composition.

By comparing the two methods it was proven that the GC-MS method is not only much more sensitive and precise but also applicable on a wide range of MAG concentrations.

5 Summary

The theoretical subject of this work dealt with the analysis of saturated monoacylglycerols (MAGs) as a contaminant in biodiesel responsible for problems at low temperature operations. The currently valid quantitative limit values for glycerol and glycerides as well as the climate-related requirements and test methods for FAME fuel were presented. After a short introduction into biodiesel synthesis, the effects of MAGs on the biodiesel quality were discussed and reports from the literature corresponding to the subject were introduced. Then an overview of approaches for removal of MAGs and analytical methods to determine saturated MAGs were presented. There is no existing method (referring to our current state of knowledge) for quantifying only saturated MAGs in biodiesel even at low concentration ranges. Therefore the experimental approach of this work was to develop a new method for the quantification of saturated monoacylglycerols in biodiesel using gas chromatography-mass spectrometry (GC-MS). The method was established on a 30 m HP-5MS column and performed a temperature programme as follows: 50°C hold for 1 minute then at a rate of 15°C/min to 275°C hold for 10 min. This ensures satisfying separation of the target MAGs. The identification and quantification of the MAGs were carried out in single ion monitoring (SIM) mode. The quantitation ions for the target MAGs were at m/z 218 (2-$C_{16:0}$), m/z 371 (1-$C_{16:0}$), m/z 385 (1-$C_{17:0}$) and 399 (1-$C_{18:0}$). The internal standard used for quantification was 1-$C_{19:0}$ with m/z at 413. The analytical procedure involved mixing the biodiesel sample with the internal standard (glyceryl monononadecanoate) and a silylating agent (N-Methyl-N-(trimethylsilyl)-trifluoracetamide) before applying GC-MS analysis. Prior to the quantification of MAGs in real biodiesel samples, based on used cooking oil and waste animal fats, the new method was validated in terms of linearity (R^2>0.99) and the limits of detection and quantification (LOD: 8 - 20 ng/g, LOQ: 26 - 61 ng/g). The MAG concentrations in the biodiesel samples, determined with this method, were also correlated with the total MAG content and the fatty acid composition of each biodiesel sample to demonstrate the relation between the fatty acid occurrence in methyl esters and MAGs. The advantage compared to other methods is the simple sample preparation which saves expenses for chemicals and materials and also time. Moreover this method enables high linear quantification, excellent

chromatographic separation as well as very low limits of detection and quantification due to the high sensitivity of GC-MS analyses performed in SIM mode.

6 Appendix

Methods

Table 6-1 Parameters for method Lena1 (preliminary tests)

Method: LENA1, HT-GC-FID	
Parameter	**Instrument**
Instrument	HP 6890 GC System with FID, HP 7683 Series Injector
Column	Agilent Technologies 123-5711 DB-5HT column (60-400°C, 15m x 320 µm x 0.1 µm)
Injection	1 µl, cold on-column
Carrier gas	H_2, 1 ml/min, 80 kPa
Temperature programme	50°C (hold 1 min), 7°C/min to 180°C 7°C/min to 230°C
Detector	380°C

Table 6-2 Parameters for method Lena lang (preliminary tests)

Method: LENA lang, HT-GC-FID	
Parameter	**Instrument**
Instrument	HP 6890 GC System with FID, HP 7683 Series Injector
Column	122-5731 DB-5HT column (30 m × 250 µm × 0.25 µm)
Injection	1 µl, cold on-column
Carrier gas	H_2, 1 ml/min, 80 kPa
Temperature programme	50°C (hold 1 min), 15°C/min to 180°C 7°C/min to 230°C (hold 10 min), 7°C/min to 250°C (hold 5 min)
Detector	380°C

Table 6-3 Parameters for method EN 14105 (determination of free- and total glycerol, MAGs, DAGs, TAGs)

Method: EN 14105, HT-GC-FID	
Parameter	**Instrument**
Instrument	HP 6890 GC System with FID, HP 7683 Series Injector
Column	Agilent Technologies 123-5711 DB-5HT column (60-400°C, 15m x 320 µm x 0.1 µm)
Injection	1 µl, cold on-column
Carrier gas	H_2, 1 ml/min, 80 kPa
Temperature programme	50°C (hold 1 min), 7°C/min to 230°C 15°C/min to 380°C (hold 10 min)
Detector	380°C

Table 6-4 Parameters for method FFAP (determination fatty acid composition)

Method: FFAP, GC-FID	
Parameter	**Instrument**
Instrument	Agilent Technologies 7890 GC System with FID, CTC Analytics Autosampler
Column	J&W Scientific 122-7031 DB-WAX PEG column (20-260°C, 30 m x 250 µm x 0.15 µm).
Injection	1 µl, split 100:1
Carrier gas	He, 0.7 ml/min, 89 kPa
Temperature programme	150°C, 7°C/min to 220°C (hold 15 min)
Detector	250°C

GC-MS chromatograms

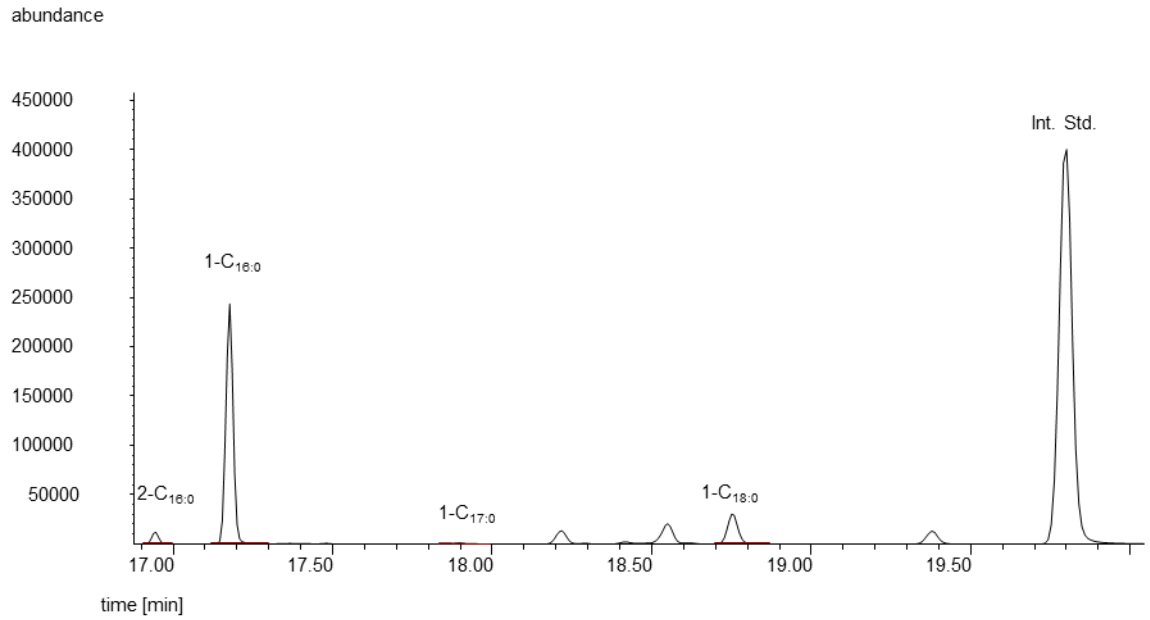

Figure 6-1 GC-MS gas chromatogramm UCO-ME 2

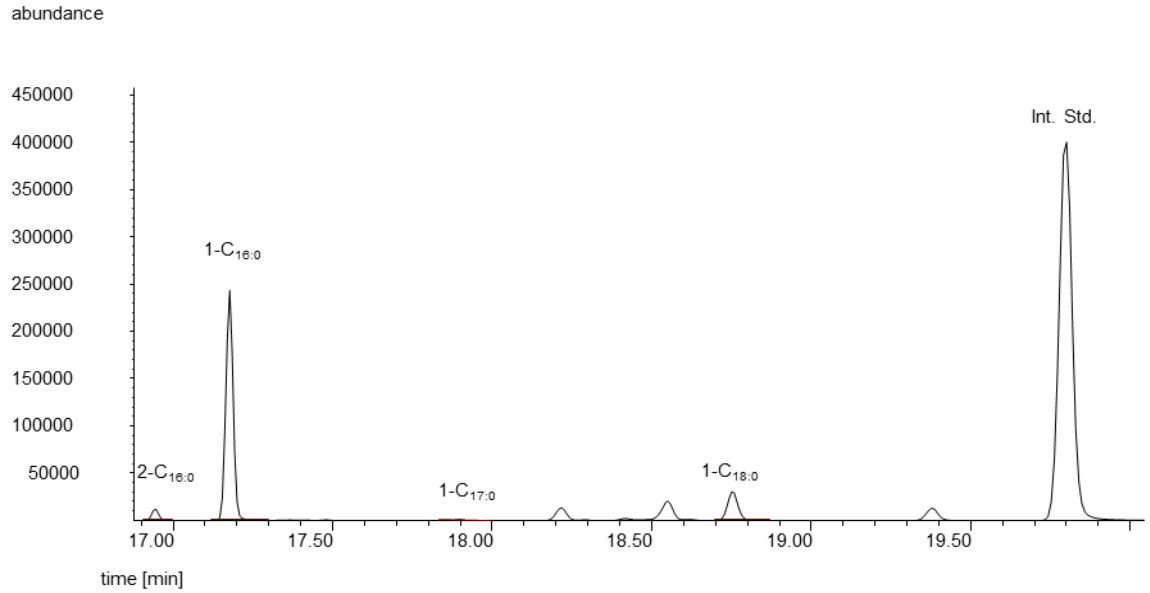

Figure 6-2 GC-MS gas chromatogramm UCO-ME 3

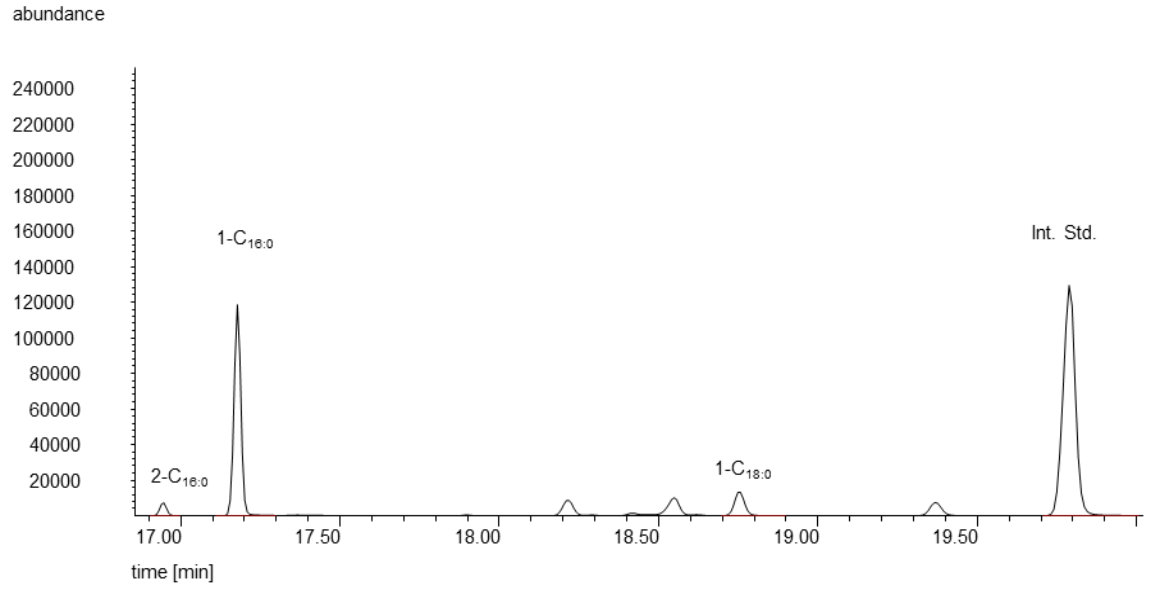

Figure 6-3 GC-MS gas chromatogramm UCO-ME 4

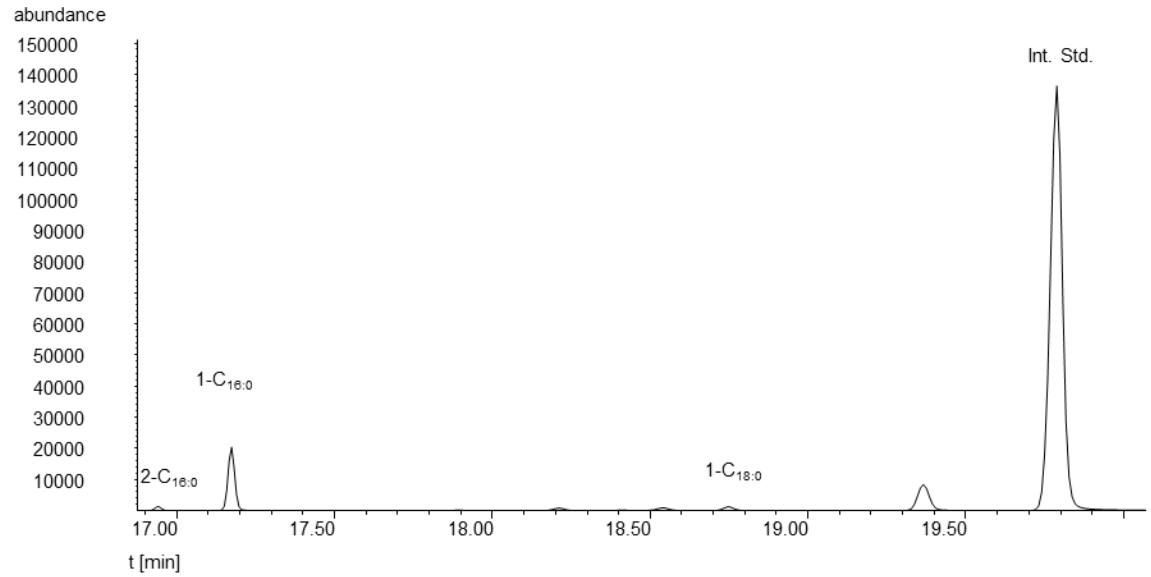

Figure 6-4GC-MS gas chromatogramm UCO-ME 5

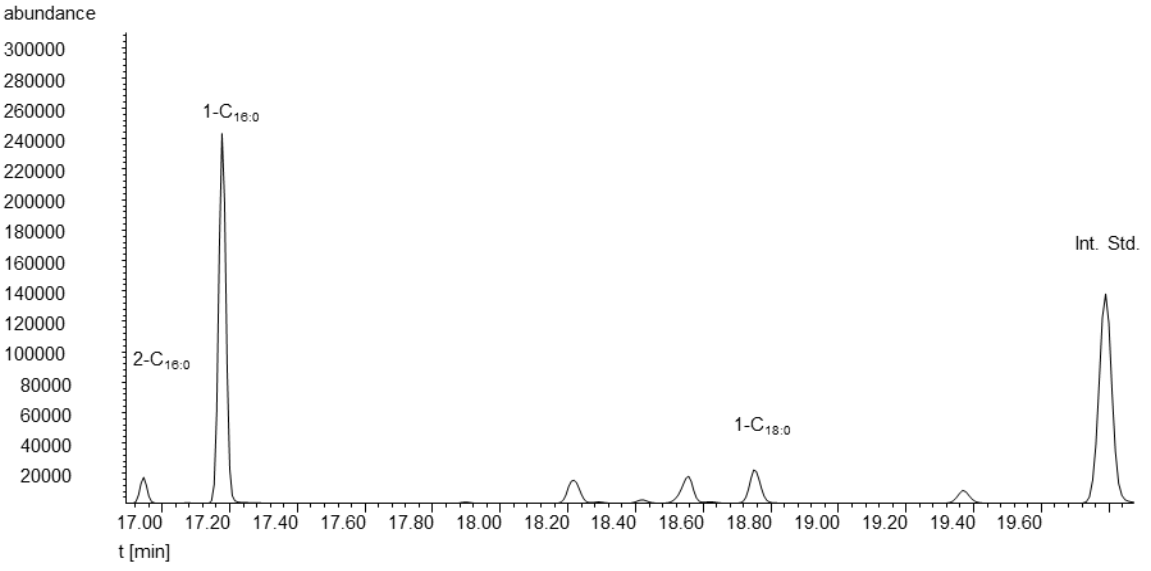

Figure 6-5 GC-MS gas chromatogramm UCO-ME 6

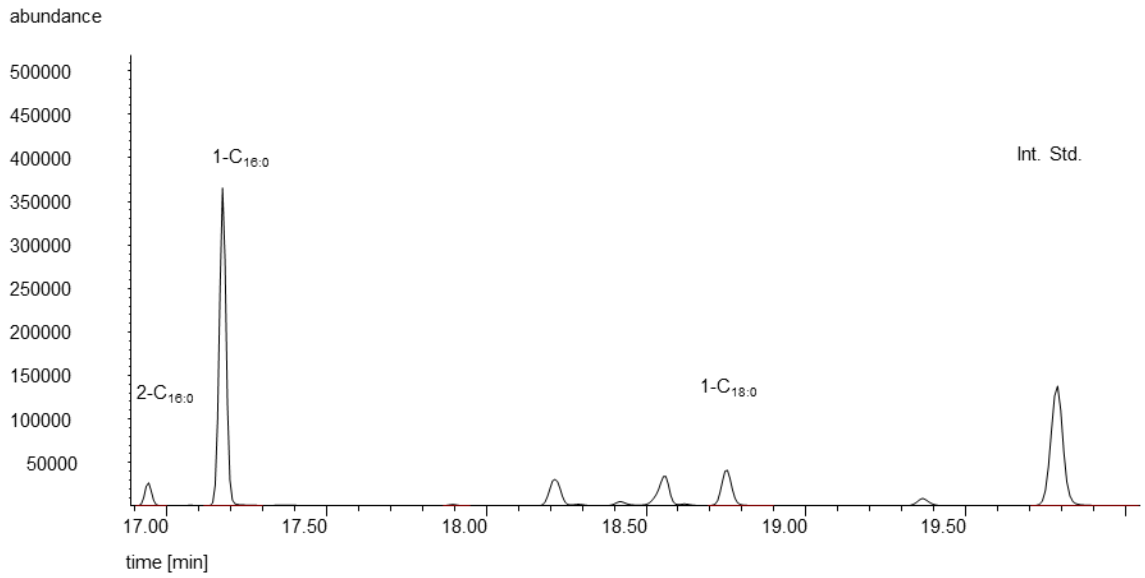

Figure 6-6 GC-MS gas chromatogramm UCO-ME 7

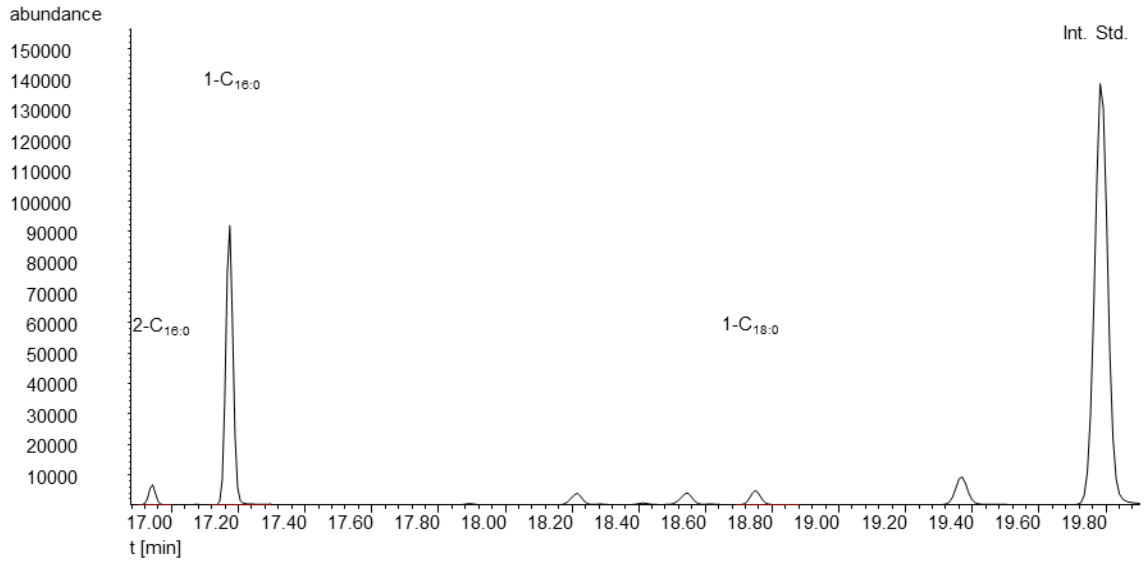

Figure 6-7 GC-MS gas chromatogramm UCO-ME 8

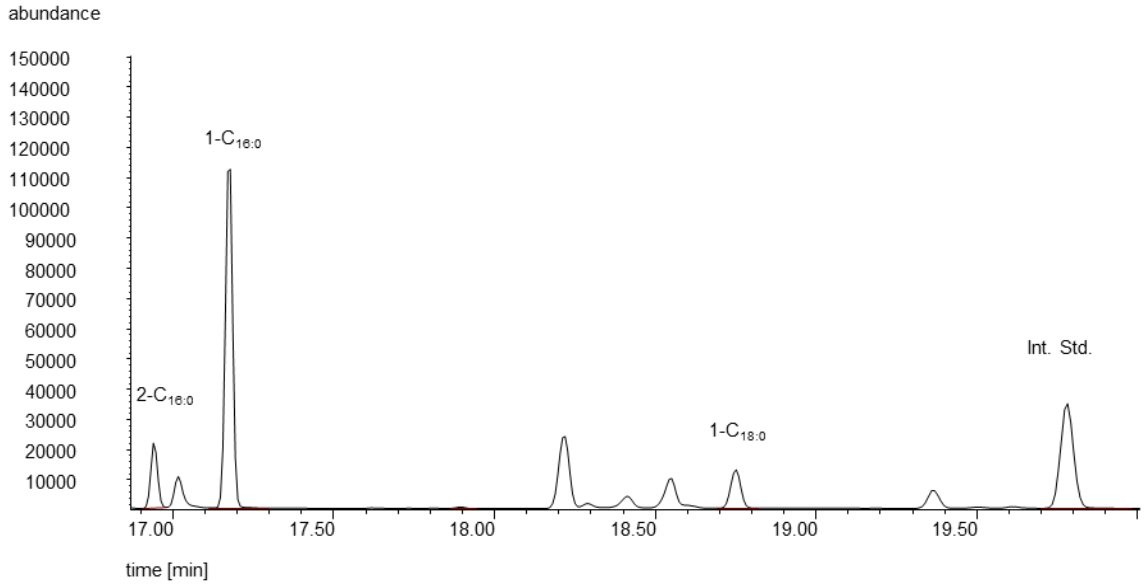

Figure 6-8 GC-MS gas chromatogramm UCO-ME 9

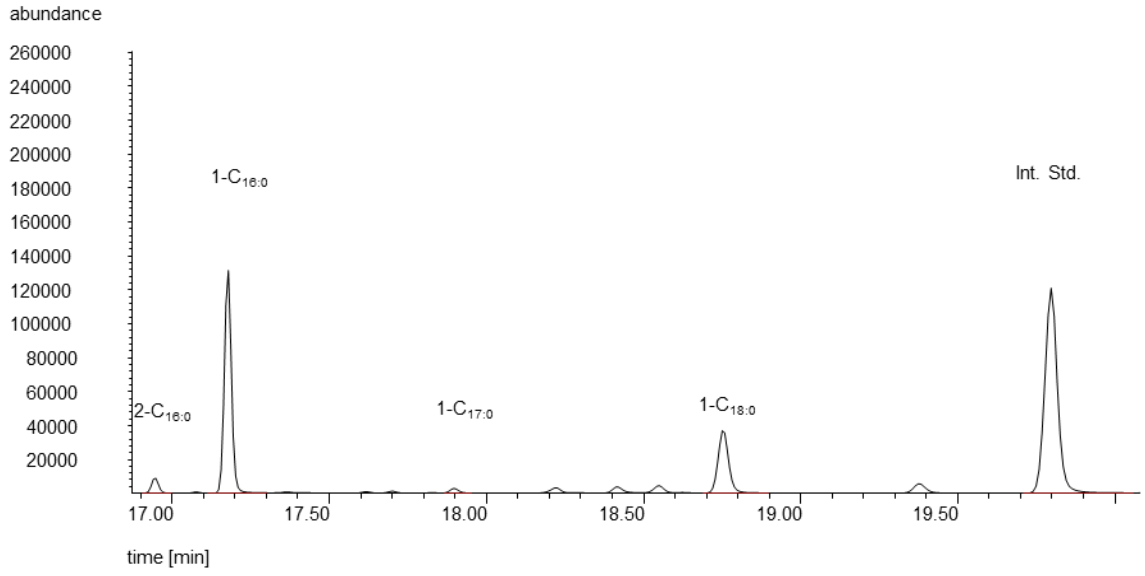

Figure 6-9 GC-MS gas chromatogramm WAF-ME 2

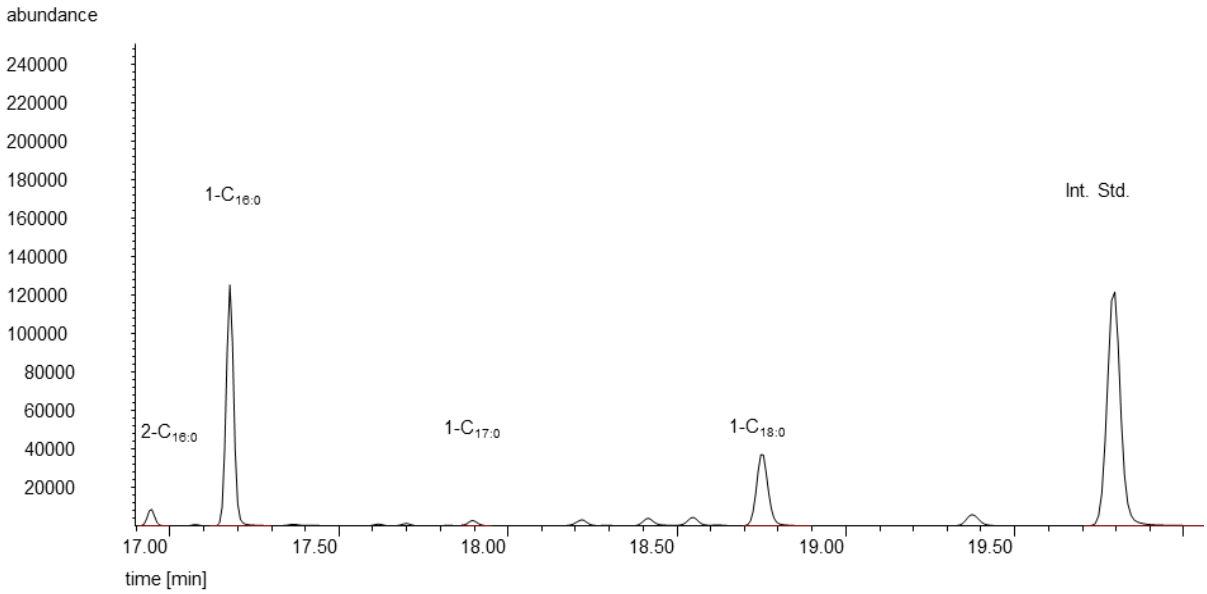

Figure 6-10 GC-MS gas chromatogramm WAF-ME 3

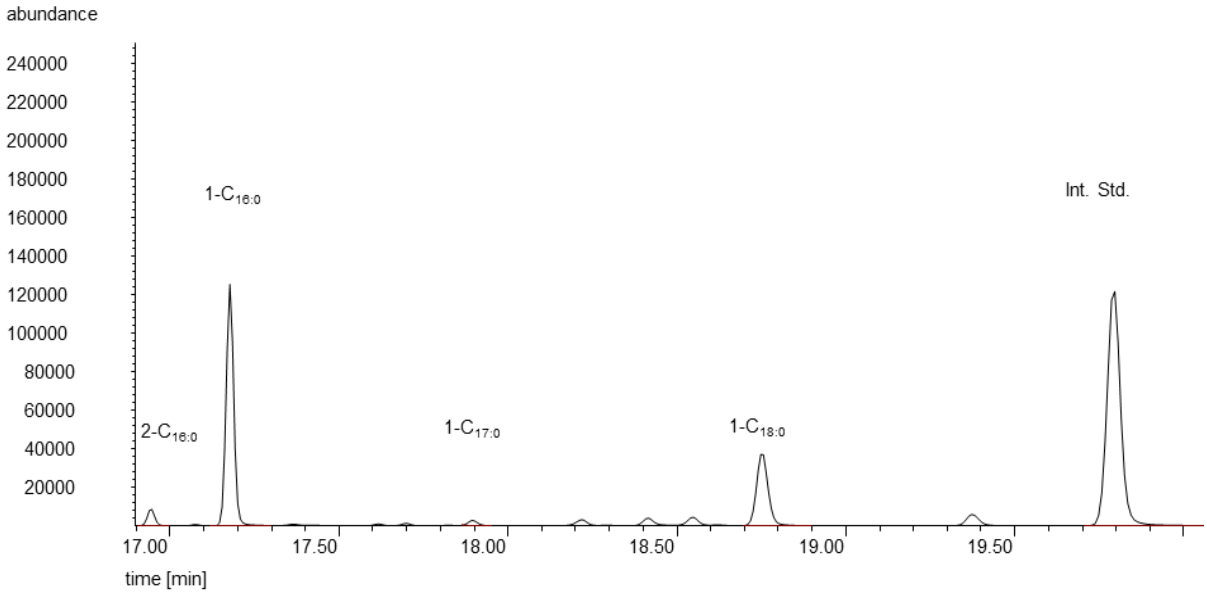

Figure 6-11 GC-MS gas chromatogramm WAF-ME 4

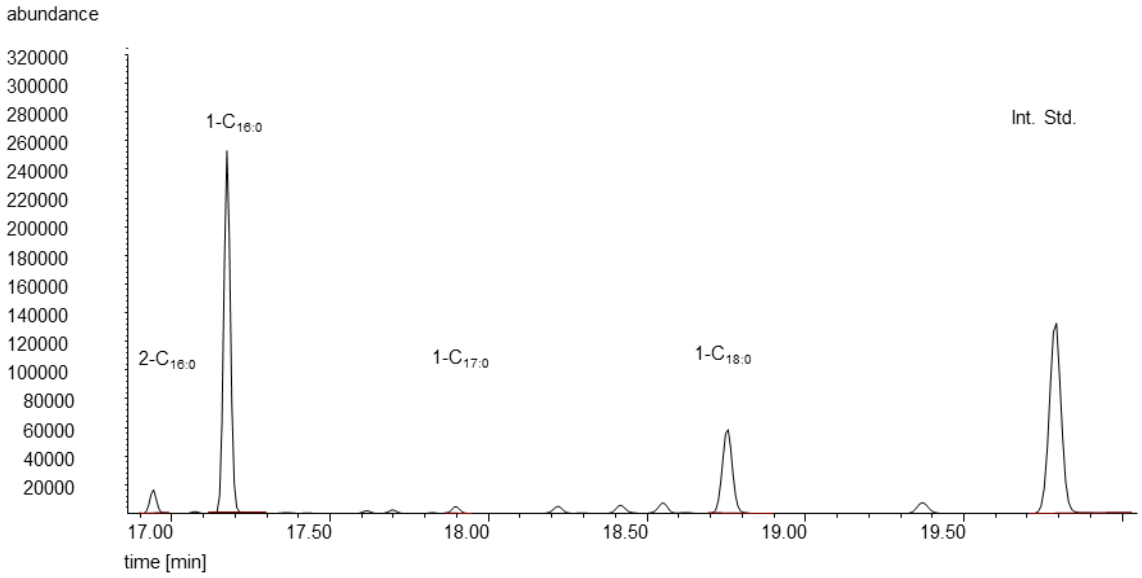

Figure 6-12 GC-MS gas chromatogramm WAF-ME 5

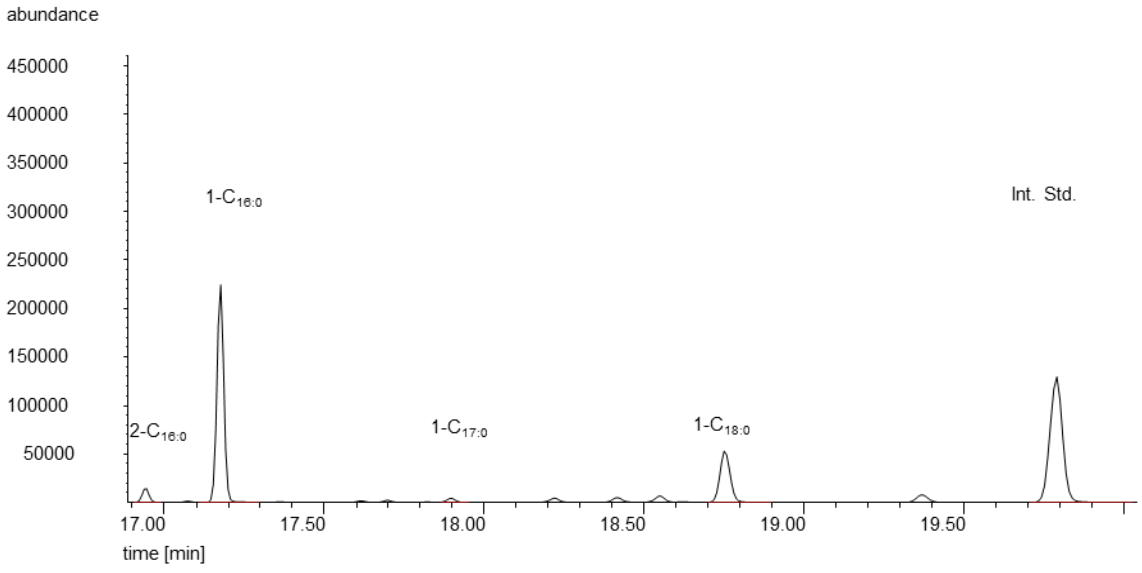

Figure 6-13 GC-MS gas chromatogramm WAF-ME 6

GC-FID chromatograms

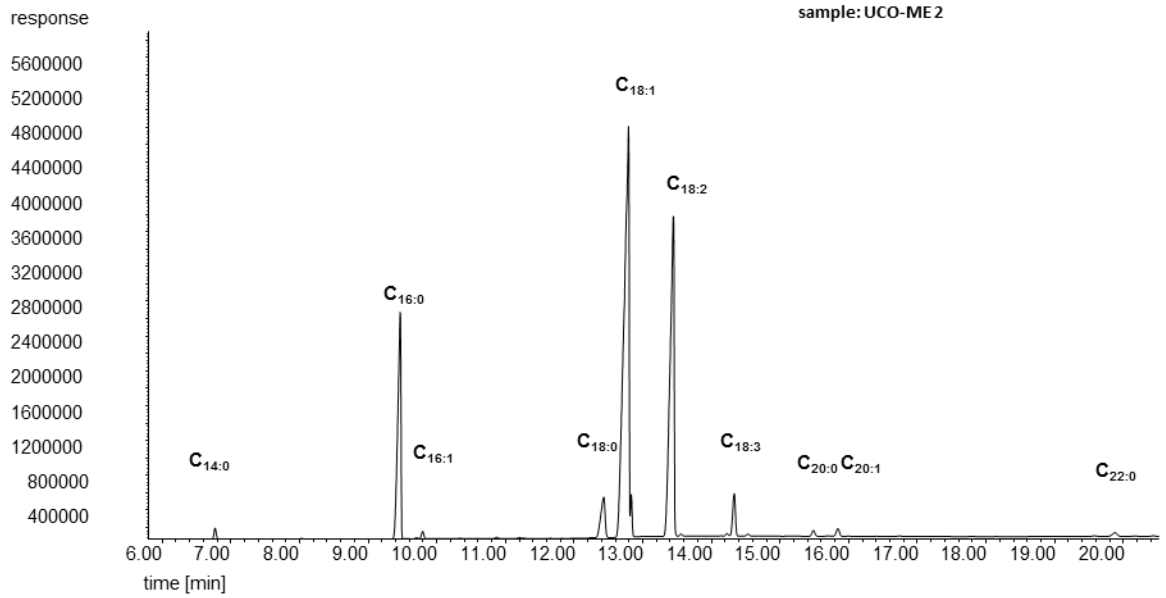

Figure 6-14 Gas chromatogram presenting the fatty acid profile of UCO-ME2

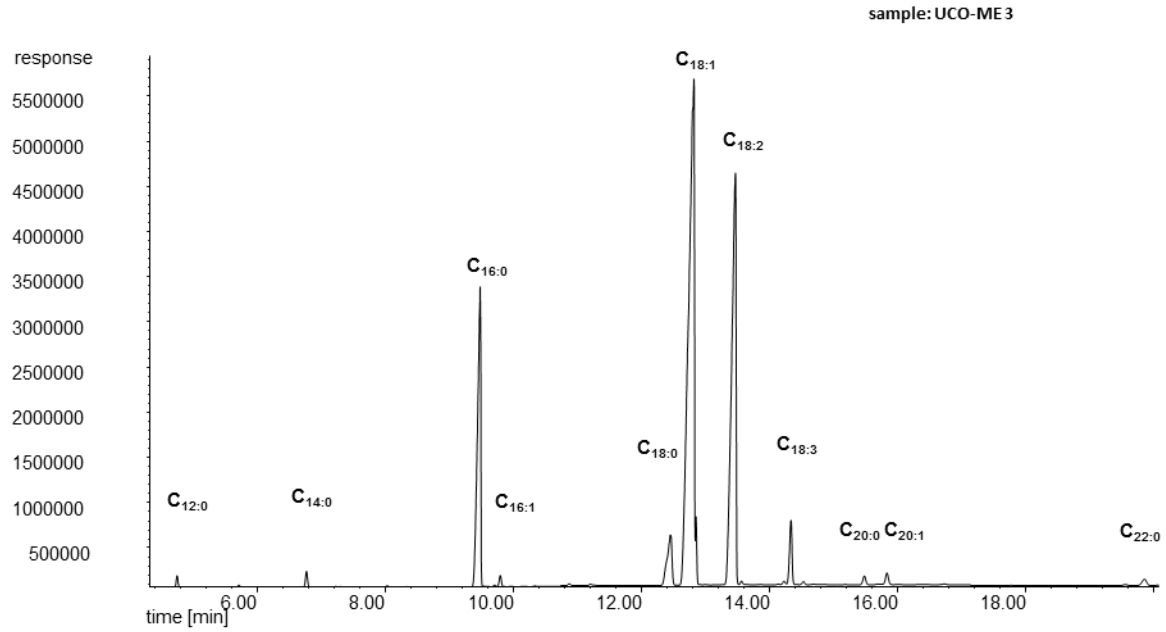

Figure 6-15 Gas chromatogram presenting the fatty acid profile of UCO-ME 3

Gas chromatograms of fatty acid composition

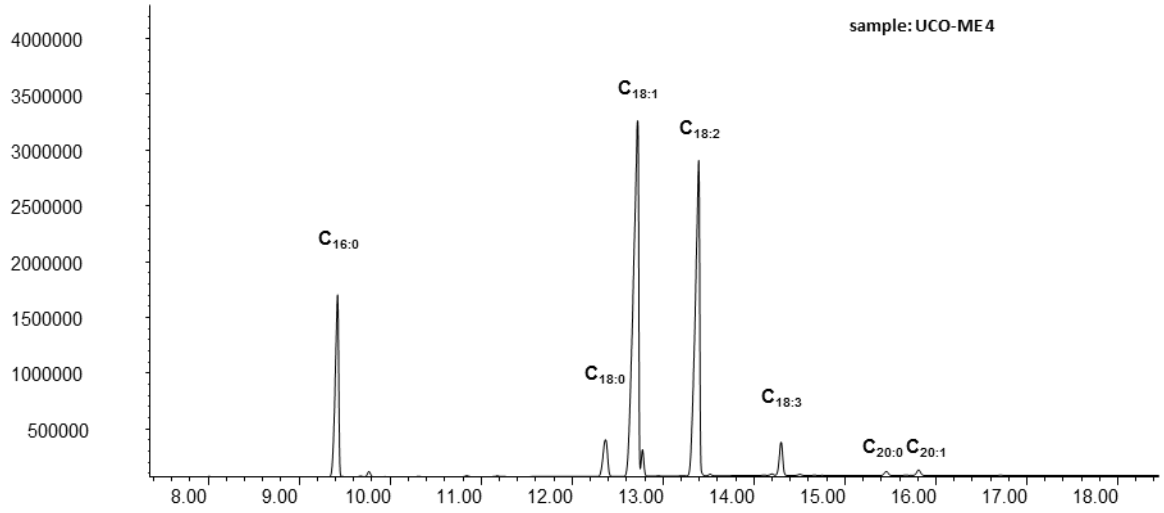

Figure 6-16 Figure 6 2 Gas chromatogram presenting the fatty acid profile of UCO-ME 4

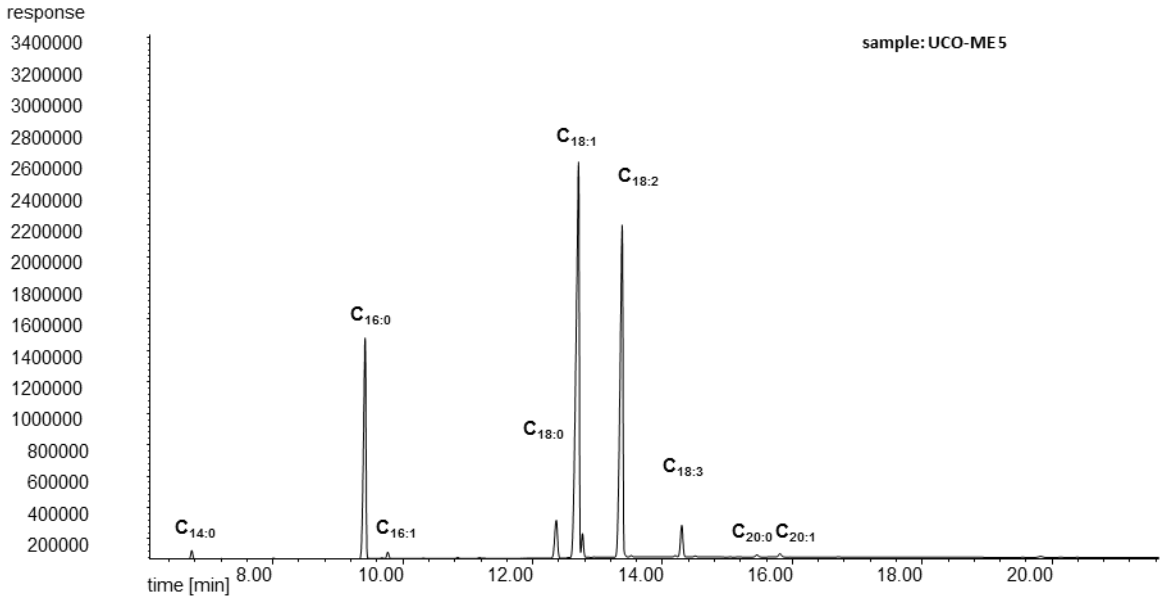

Figure 6-17 Figure 6 2 Gas chromatogram presenting the fatty acid profile of UCO-ME 5

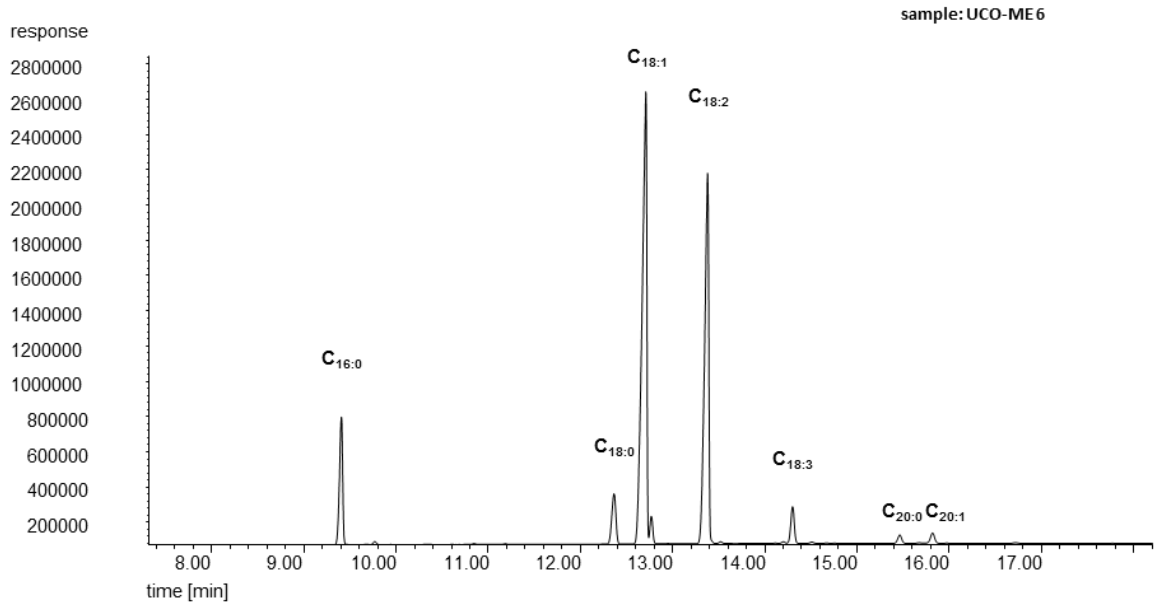

Figure 6-18 Figure 6 2 Gas chromatogram presenting the fatty acid profile of UCO-ME 6

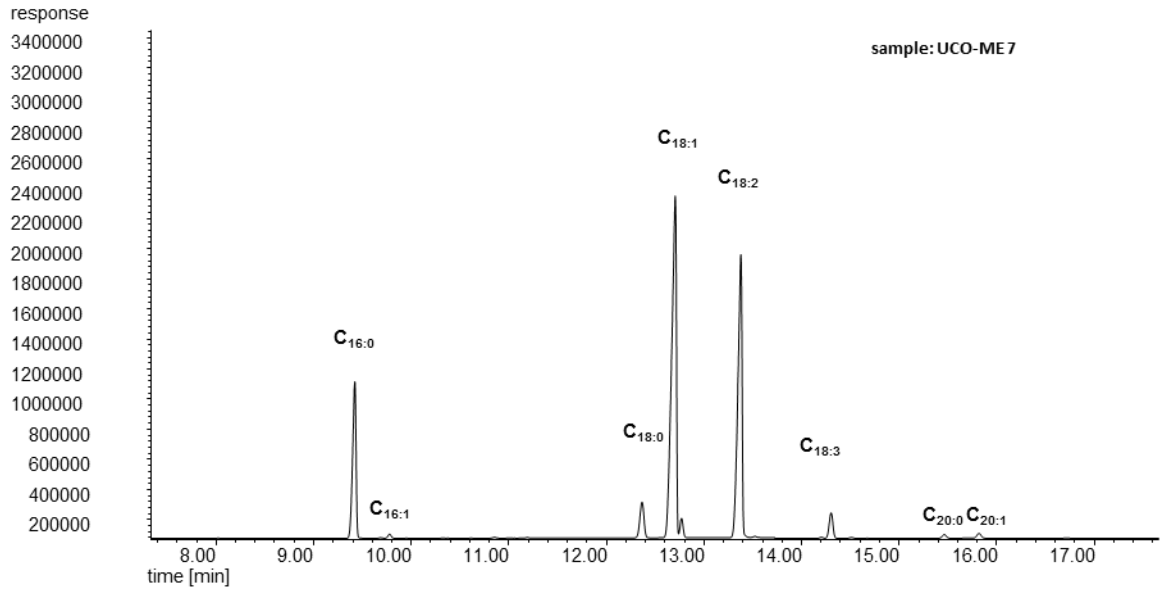

Figure 6-19 Figure 6 2 Gas chromatogram presenting the fatty acid profile of UCO-ME 7

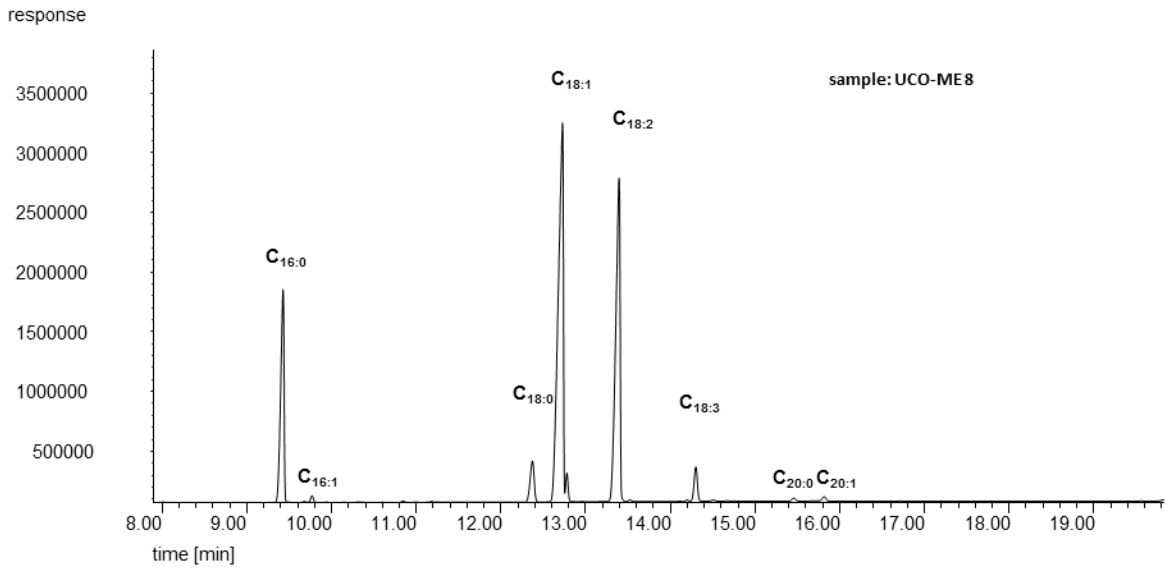

Figure 6-20 Figure 6 2 Gas chromatogram presenting the fatty acid profile of UCO-ME 8

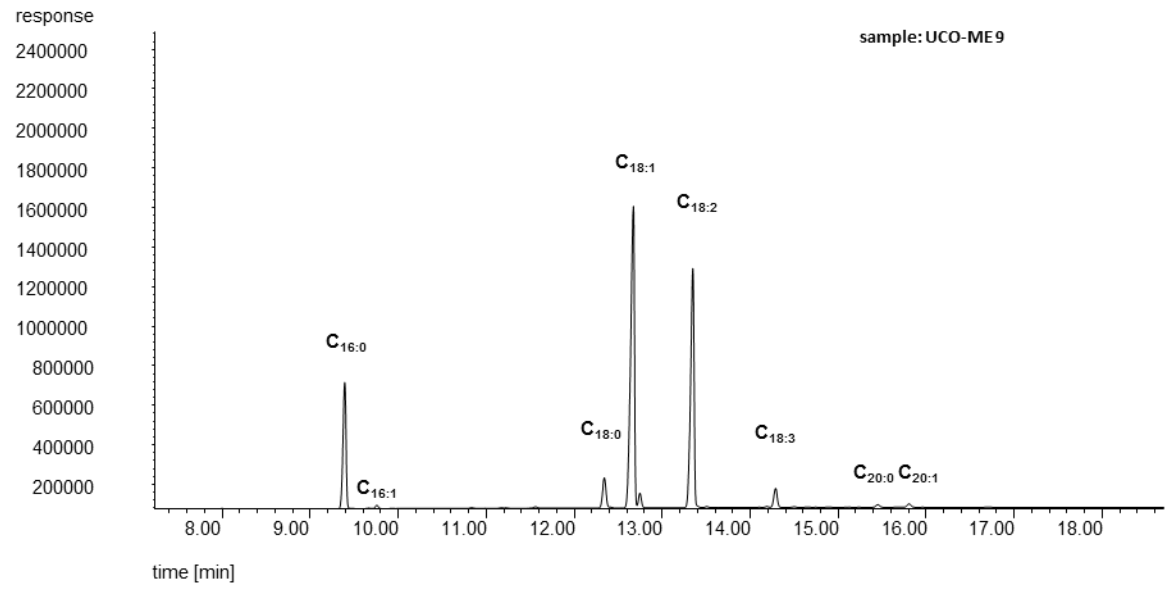

Figure 6-21 Figure 6 2 Gas chromatogram presenting the fatty acid profile of UCO-ME 9

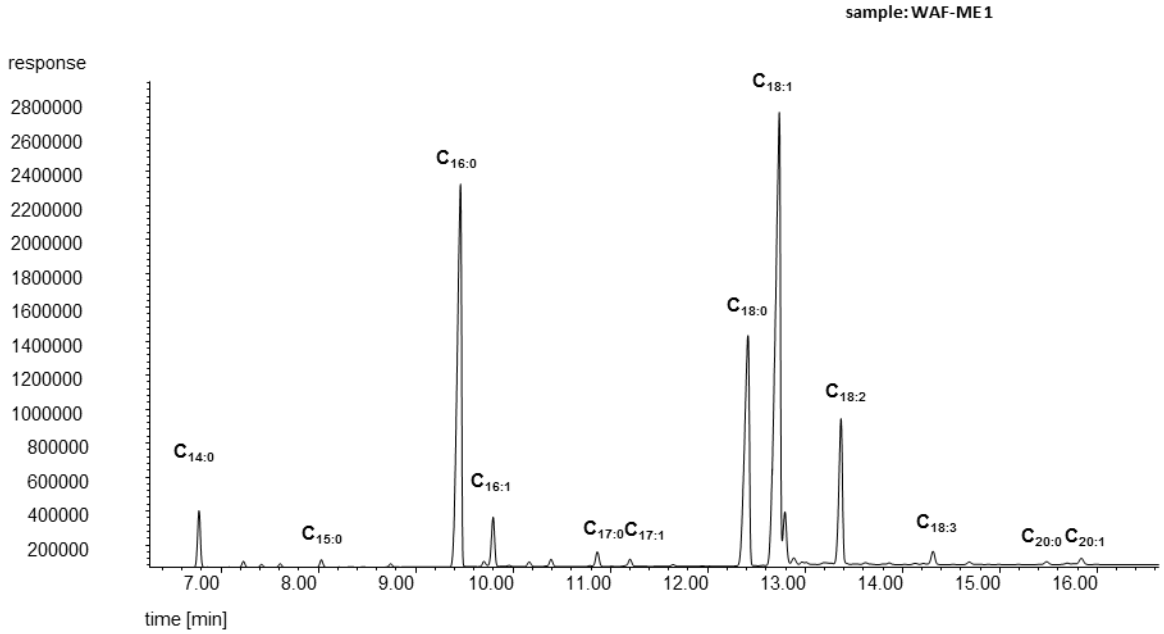

Figure 6-22 Figure 6 2 Gas chromatogram presenting the fatty acid profile of WAF-ME 1

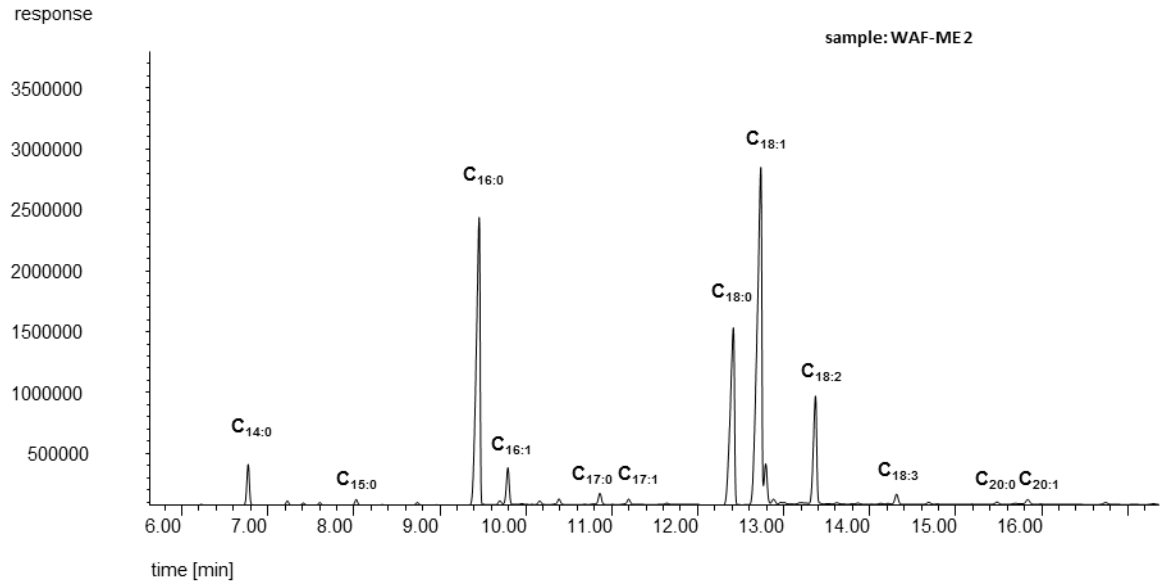

Figure 6-23 Figure 6 9 Figure 6 2 Gas chromatogram presenting the fatty acid profile of WAF-ME 2

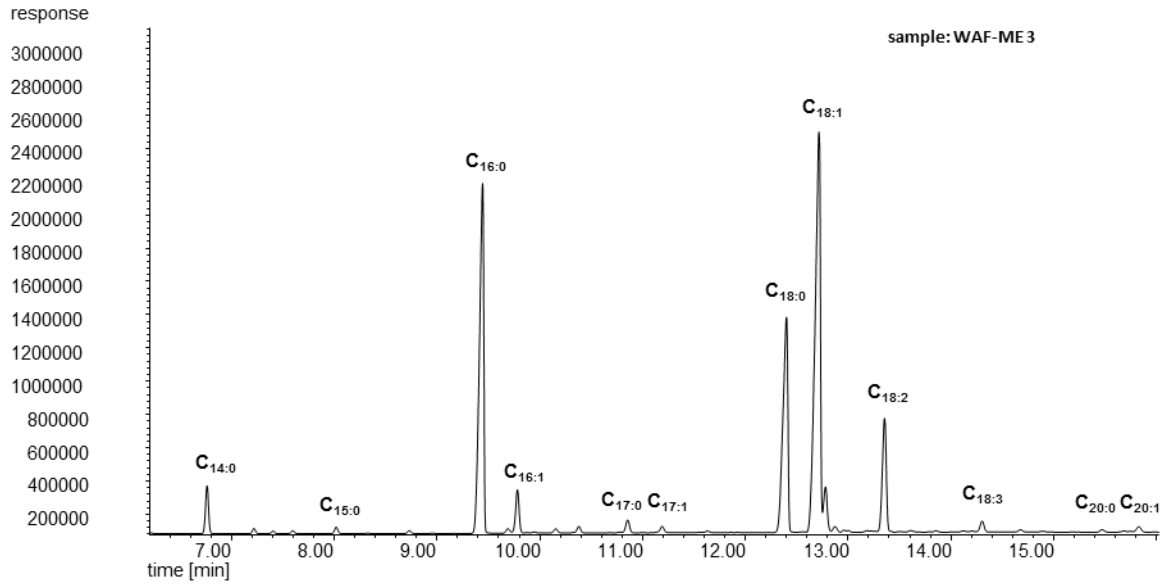

Figure 6-24 Figure 6 9 Figure 6 2 Gas chromatogram presenting the fatty acid profile of WAF-ME 3

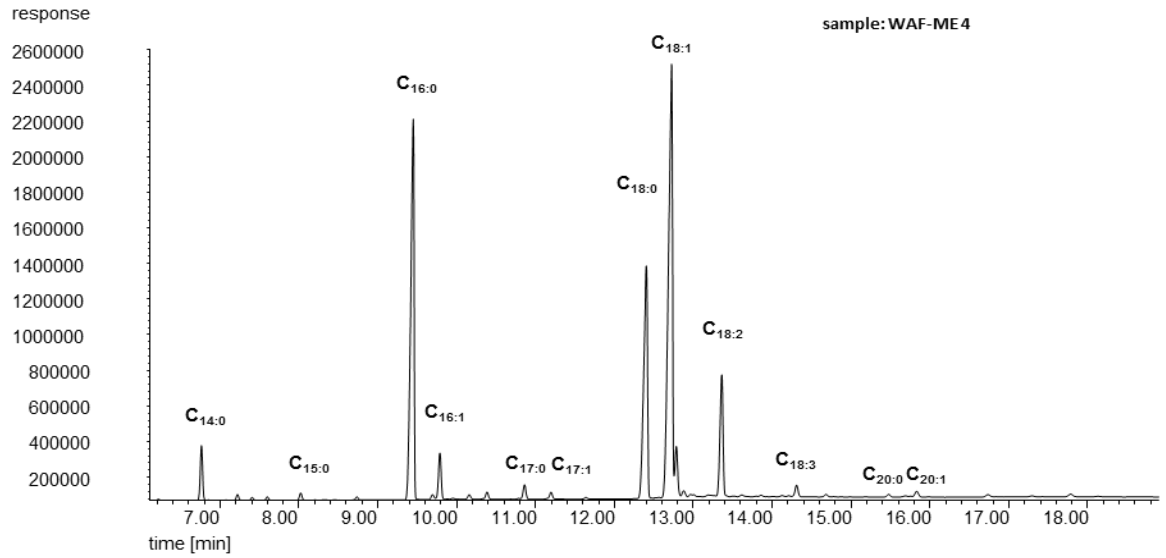

Figure 6-25 Figure 6 9 Figure 6 2 Gas chromatogram presenting the fatty acid profile of WAF-ME 5

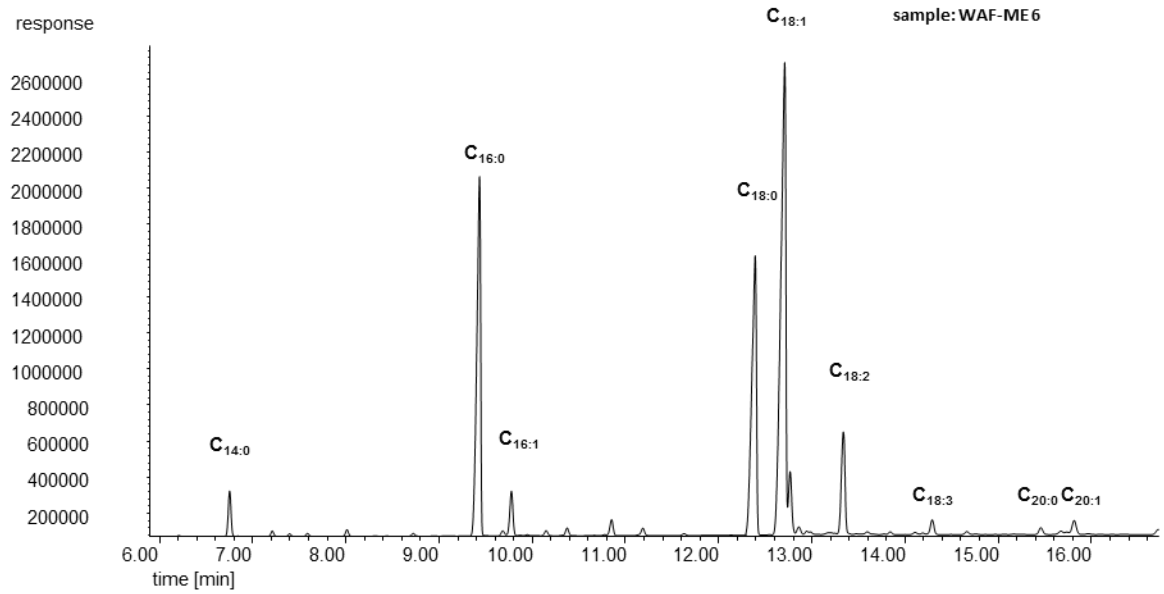

Figure 6-26 Figure 6 9 Figure 6 2 Gas chromatogram presenting the fatty acid profile of WAF-ME

References

[1] J. Van Gerpen, E. Hammond, L. Yu and A. Monyem, "Determining the Influence of Contaminants on Biodiesel Properties," Warrendale, PA, 1997.

[2] L. Pfalzgraf, L. Lee, J. Foster and G. Poppe, "Effect of Minor Components in Soy Biodiesel on Cloud Point and Filterability," *Inform supplement-biorenewable resources No. 4,* pp. 17-22, 2007.

[3] R. O. Dunn, "Effects of Minor Constituents on Cold Flow Properties and Performance of Biodiesel," *Progress in Energy and Combustion Science,* vol. 35, pp. 481-489, 2009.

[4] B. Freedman, R. O. Butterfield and E. H. Pryde, "Transesterification Kinetics of Soybean Oil," *Journal of the American Oil Chemists' Society,* vol. 63, no. 10, 1986.

[5] J. Dias, M. C. Alvim-Ferraz and M. F. Almeida, "Comparison of the Performance of Different Homogeneous Alkali Catalysts During Transesterfication of Waste and Virgin Oils and Evaluation of Biodiesel Quality," *Fuel,* vol. 87, pp. 3572-3578, 2008.

[6] R. Dunn, "Effects of Monoacylglycerols on the Cold Flow Properties," *Journal of the American Oil Chemists' Society,* vol. 89, pp. 1509-1520, 2012.

[7] "Sigma-Aldrich," [Online]. Available: http://www.sigmaaldrich.com/catalog/product/sigma/. [Accessed 14 March 2013].

[8] J. Vereecken, W. Meeussen, I. Foubert, A. Lesaffer, J. Wouters, Dewettinck and K., "Comparing the Crystallization an Polymorphic Behaviour of Saturated and Unsaturated Monoglycerides," *Food Research International,* vol. 42, pp. 1415-1425, 2009.

[9] R. Kotrba, "Bound by Determination," *Biodiesel Magazine,* vol. 3, pp. 42-50, 2006.

[10] *ÖNORM EN 14214:2012 Liquid petroleum products - Fatty Acid Methyl Esters (FAME) for Use in Diesel Engines and Heating Applications - Requirements and test methods,* 2012.

[11] S. Pinzi, L. M. Gandía, G. Arzamendi, J. J. Ruiz and M. P. Dorado, "Influence of Vegetable Oils Fatty Acid Composition in Reaction Temperature and Gylcerides Conversion on Biodiesel During Transesterification," 2011.

[12] A. Pérez, A. Casas, C. M. Fernández, M. J. Ramos and L. Rondríguez, "Winterization of Peanut Biodiesel to Improve the Cold Flow Properties," *Bioresource Technology,* vol. 101, pp. 7375-7381, 2010.

[13] *European Standard EN 116:1997 Diesel and Domestic Heating Fuels - Determination of Cold Filter Plugging Point.*

[14] G. Chupka, J. Yanowitz, G. A. T. Chiu and R. McCormick, "Effect of Saturated Monoglyceride Polymorphism on Low-Temperature Performance of Biodiesel," *Energy Fuels,* vol. 25, pp. 398-405, 2011.

[15] T. A. Foglia, L. A. Nelson, R. O. Dunn and W. Marmer, "Low-Temperature Properties of Alkyl- Esters of Tallow and Grease," *Journal of the American Oil Chemists' Society,* vol. 74, no. 8, pp. 951-955, 1997.

[16] U. Rashid and F. Anwar, "Production of Biodiesel Through Optimized Alkaline-Catalyzed Transesterification of Rapeseed Oil," *Fuel,* vol. 87, pp. 265-273, 2008.

[17] V. T. Wyatt, M. A. Hess, R. O. Dunn, T. A. Foglia, M. J. Haas and W. N. Marmer, "Fuel Properties and Nitrogen Oxide Emission Levels of Biodiesel Produced from Animal Fats," *Journal of the American Oil Chemists' Society,* vol. 82, pp. 585-591, 2005.

[18] E. Terentjev and C. H. Chen, "Aging and Metastability of Monoglycerides in Hydrophobic Solutions," *Langmuir,* vol. 25, pp. 6717-6724, 2009.

[19] E. Fredrick, I. Foubert, J. Van De Syp and K. Dewettinck, "Influence of Monoglycerides on the Crystallization Behavior of Palm Oil," *Crystal Growth & Design,* vol. 8, pp. 1833-1839, 2008.

[20] H. Tang, S. O. Salley and S. K. Y. Ng, "Fuel Properties and Precipitate Formation at Low Temperature in Soy-, Cottonseed-, and Poultry Fat- Based Biodiesel Blends," *Fuel,* vol. 87, pp. 3006-3017, 2008.

[21] H. Lin, D. M. Haagenson, D. P. Wiesenborn and S. W. Pryor, "Effect of Trace Contaminants on Cold Soak Filterability of Canola Biodiesel," *Fuel,* vol. 90, pp. 1771-1777, 2011.

[22] *ASTM 6751-08 International Designation, Standard Specification for Biodiesel Fuel Blend Stock (B100) for Middle Distillate Fuels - Annex A1.*

[23] S. K. Padhi, M. Haas and U. T. Bornscheuer, "Lipase-Catalyzed Transesterification to Remove Saturated MAG from Biodiesel," *European Journal of Lipid Science and*

Technology, vol. 114, pp. 875-879, 2012.

[24] S. Kerschbaum, G. Rinke and K. Schubert, "Winterization of Biodiesel by Micro Process Engineering," *Fuel,* no. 87, pp. 2590-2597, 2008.

[25] T. Sahalabji, H. Wichmann, H. Dieckmann, P. Jopke and M. Bahadir, "Chemical Aspects of Fractional Crystallization of Fatty acid Methyl esters Produced from Waste fats," *Clean,* vol. 35, no. 4, pp. 323-328, 2007.

[26] J. Song, M. Hou, T. Jiang, B. Han, X. Li, G. Liu and G. Yang, "Enhancing Reaction Rate of Transesterification of Glycerol Monostearate and Methanol by CO2," *Journal of Physical Chemistry A,* vol. 111, no. 47, 2007.

[27] G. Di Nicola, M. Pacetti, A. Polonaraa, G. Santori and R. Stryjekb, "Development and Optimization of a Method for Analyzing Biodiesel Mixtures with Non-Aqueous Reversed Phase Liquid Chromatography," *Journal of Chromatography A,* vol. 1190, 2008.

[28] C. Hellmuth, O. Uhl, M. Segura-Moreno, H. Demmelmair and B. Koletzko, "Determination of Acylglycerols from Biological Samples with Chromatography-Based Methods," *Journal of Separation Science,* vol. 34, pp. 3470-3483, 2011.

[29] B. Marcato and G. Cecchin, "Analysis of Mixtures Containing Free Fatty Acids and Mono-, Di- and Triglycerides by High-Performance Liquid Chromatography Coupled with Evaporative Light-Scattering Detection," *Journal of Chromatography A,* vol. 730, 1996.

[30] A. Türkan and S. Kalay, "Monitoring Liipase-Catalyzed Methanolysis of Sunflower Oil by Reversed-Phase High-Performance Lliquid Chromatography: Elucidation of the Mechanism of Lipases," *Journal of Chromatography A,* vol. 1127, pp. 34-44, 2006.

[31] G. Arzamendi, E. Arguiarena, I. Campo and L. Gandía, "Monitoring of Biodiesel Production: Simultaneous Analysis of the Transesterification Products Using Size-Exclusion Chromatography," *Chemical Engineering Journal,* vol. 122, 2006.

[32] L. Deng, N. I. and Y. Iwasaki, "Direct Separation of Regioisomers and Enantiomers of Monoacylglycerols by Tandem Column High-Performance Liquid Chromatography," *Journal of Chromatography A,* no. 1165, pp. 93-99, 2007.

[33] P. García, P. Franco, R. Álvarez and A. R. De Lera, "Separation of Regioisomers and

Enantiomers of Underivatized Saturated and Unsaturated Fatty Acid Monoacylglycerols Using Enantioselective HPLC," *Journal of Separation Science,* vol. 34, pp. 999-1003, 2011.

[34] T. Petrosino, R. Riccieri, F. Blasi, M. Brutti, G. D'Arco, A. Bosi, S. Maurelli, L. Cossignani, M. S. Simonetti and P. Dammiani, "Original Normal-Phase High Performance Liquid Chromatography Separation of Monoacylglycerol Classes from Extra Virgin Olive Oil Triacylglycerols for their Stereospecific Analysis," *Journal of AOAC International,* vol. 90, no. 6, pp. 1647-1654, 2007.

[35] M. Holcapek, P. Jandera, J. Fischer and B. Prokes, "Analytical Monitoring of Production of Biodiesel by High-Performance Liquid Chromatography with Various Detection Methods," *Journal of Chromatography A,* vol. 858, pp. 13-31, 1999.

[36] C. Plank and E. Lorbeer, "Simultaneous Determination of Glycerol, and Mono-, Dii- and triglycerides in Vegetable Oil Methyl Esters by Capillary Gas Chromatography," *Journal of Chromatography A,* no. 697, pp. 461-468, 1995.

[37] *European Standard EN 14105:2011 Fat and oil derivatives - Fatty Acid Methyl Esters (FAME) - Determination of free and total glycerol and mono-, di-, triglyceride contents.*

[38] Z. Yang, Hollebone, B. P., Z. Wang and M. Landriault, "Determination of Polar Impurities in Biodiesels Using Solid-Phase Extraction and Gas Chromatography–Mass Spectrometry," *Journal of Separation Science,* vol. 34, pp. 409-421, 2011.

[39] J. Giacametti, A. Miloševic and C. Milin, "Gas Chromatographic Determination of Fatty Acids Contained in Different Lipid Classes After their Separation by Solid-Phase Extraction," *Journal of Chromatography A,* vol. 976, pp. 47-54, 2002.

[40] P. Bondioli, L. Della Bella and G. Rivolta, "Evaluation of Total and Saturated Monoglyceride Content in Biodiesel at Low Concentration," *European Journal of Lipid Science,* 2013 submitted for publication.

[41] G. Linck, G. Teller and A. Petrovic, "Identification by Gas Chromatography and Mass Spectrometry of 1-Monoglycerides in European Hamster Brown adipose Tissue and Plasma," *European Journal of Biochemistry,* vol. 58, pp. 511-516, 1975.

[42] J. J. Myher, L. Marai and A. Kuksis, "Identification of Monoacyl- and Monoalkylglycerols by Gas-Liquid Chromatography-Mass Spectrometry Using Polar

Siloxane Liquid Phases," *Journal of Lipid Research,* vol. 15, pp. 586-592, 1974.

[43] "Deutsche Gesellschaft für Fettwissenschaft," 21 12 2011. [Online]. Available: http://www.dgfett.de/material/fszus.php. [Accessed 6 March 2013].

[44] [Online]. Available: http://www.sigmaaldrich.com/. [Accessed 06 11 2012].

[45] P. Garcia, "Separation of Regioisomers and Enantiomers of Underivatized Saturated and Unsaturated Fatty Acid Monoacylglycerols Using Enantioselective HPLC," *Journal of Separation Science,* vol. 34, pp. 999-1003, 2011.

List of figures

List of tables

Signal to Noise Report

Data Path : C:\msdchem\1\LENA\Masterarbeit\VerdünnungsreiheC\290612\NWG\y\
Data File : 0_1y.D
Acq On : 29 Jun 2012 20:07
Operator : lena
Sample : 0_1y
Misc : 0.5 ml verd-reihe C, 40 µl MSTFA sil
ALS Vial : 10 Sample Multiplier: 1

Integration File: autoint1.e

Method : C:\msdchem\1\METHODS\BENE1.M
Title :
Last Update :

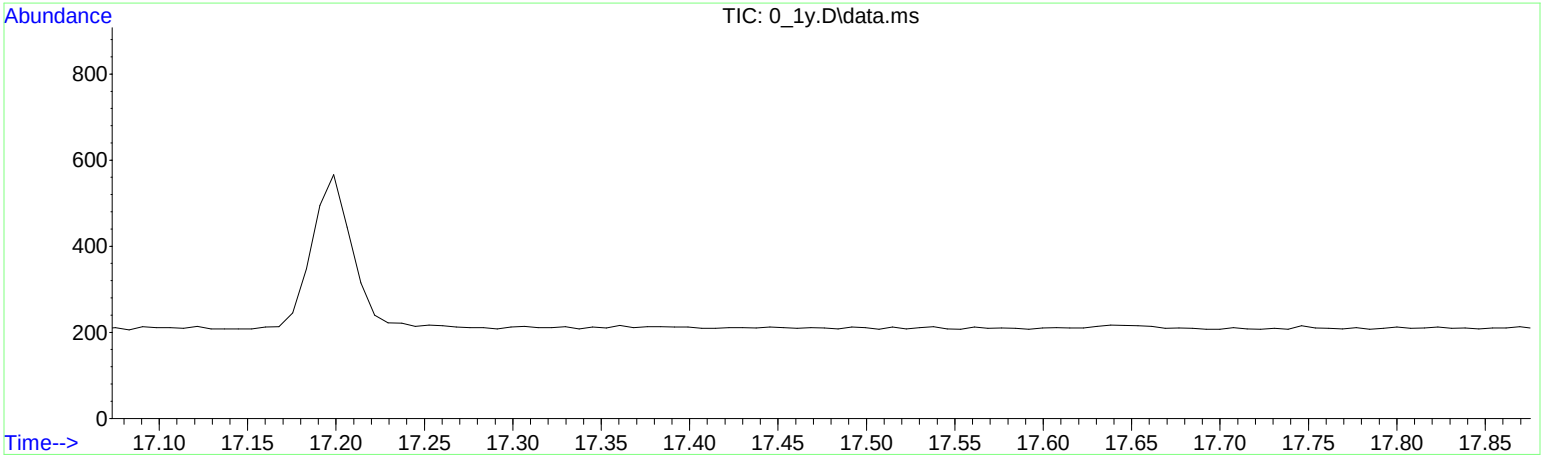

Signal region: 17.16 to 17.23 min; height: 566

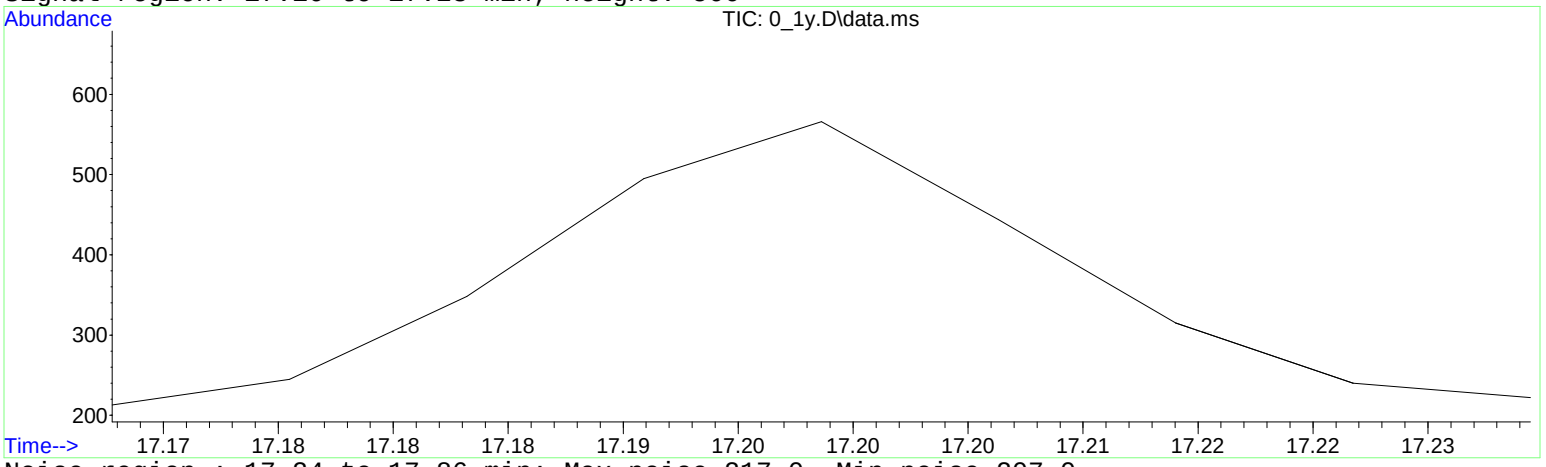

Noise region : 17.24 to 17.86 min; Max noise 217.0, Min noise 207.0

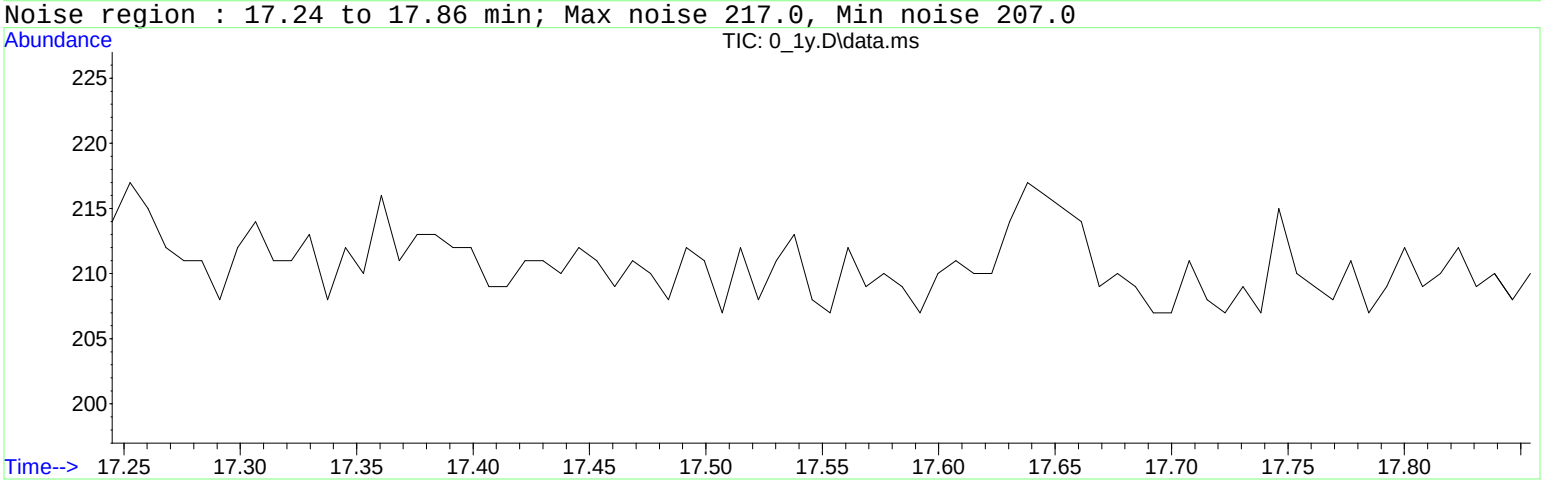

Calculations	Value
Noise Points used	80
Average noise = (sum of noise)/points	210.7
Corrected Signal = height/Average noise	355.3
Pk-pk noise = Max noise/Min noise	10.0
Pk-pk S/N = Corrected signal/Pk-pk noise	35.5
RMS noise = SQRT(sum(square(noise-avg noise))/points)	2.5
RMS S/N = Corrected signal/RMS noise	144.5

Signal to Noise Report

Data Path : C:\msdchem\1\LENA\Masterarbeit\VerdünnungsreiheC\290612\NWG\y\
Data File : 0_1y.D
Acq On : 29 Jun 2012 20:07
Operator : lena
Sample : 0_1y
Misc : 0.5 ml verd-reihe C, 40 µl MSTFA sil
ALS Vial : 10 Sample Multiplier: 1

Integration File: autoint1.e

Method : C:\msdchem\1\METHODS\BENE1.M
Title :
Last Update :

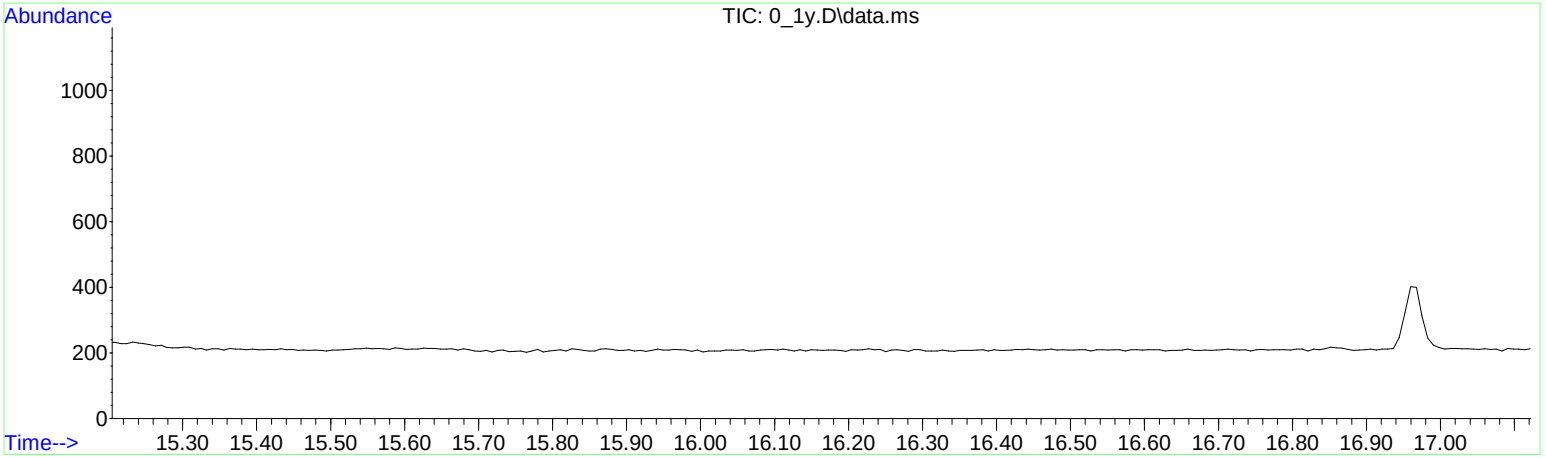

Signal region: 16.94 to 17.00 min; height: 402

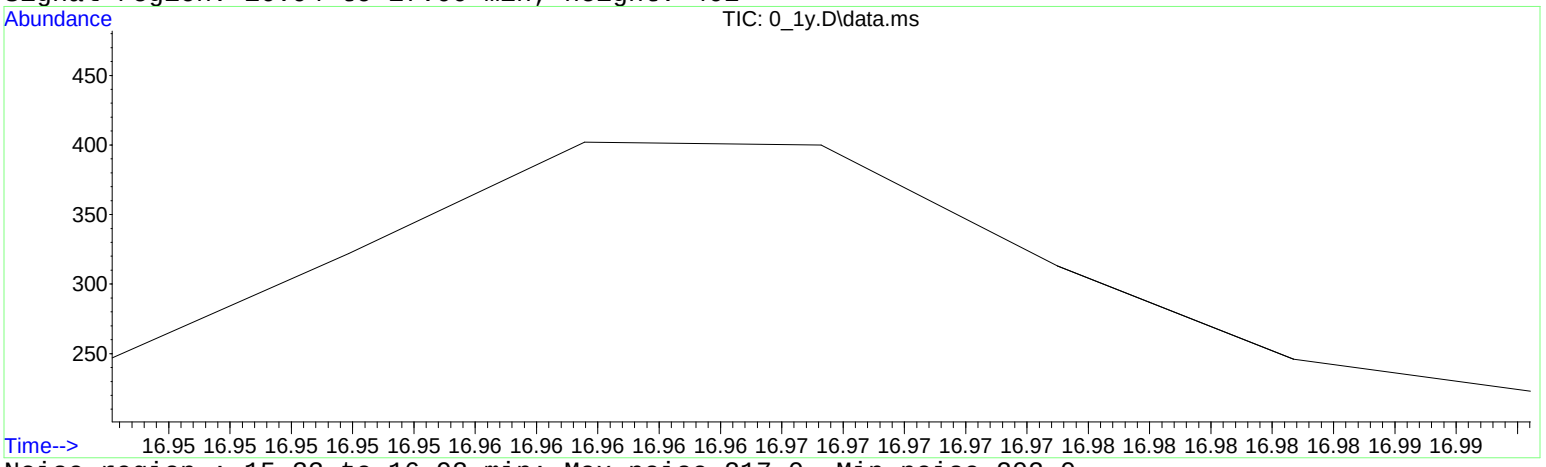

Noise region : 15.33 to 16.92 min; Max noise 217.0, Min noise 202.0

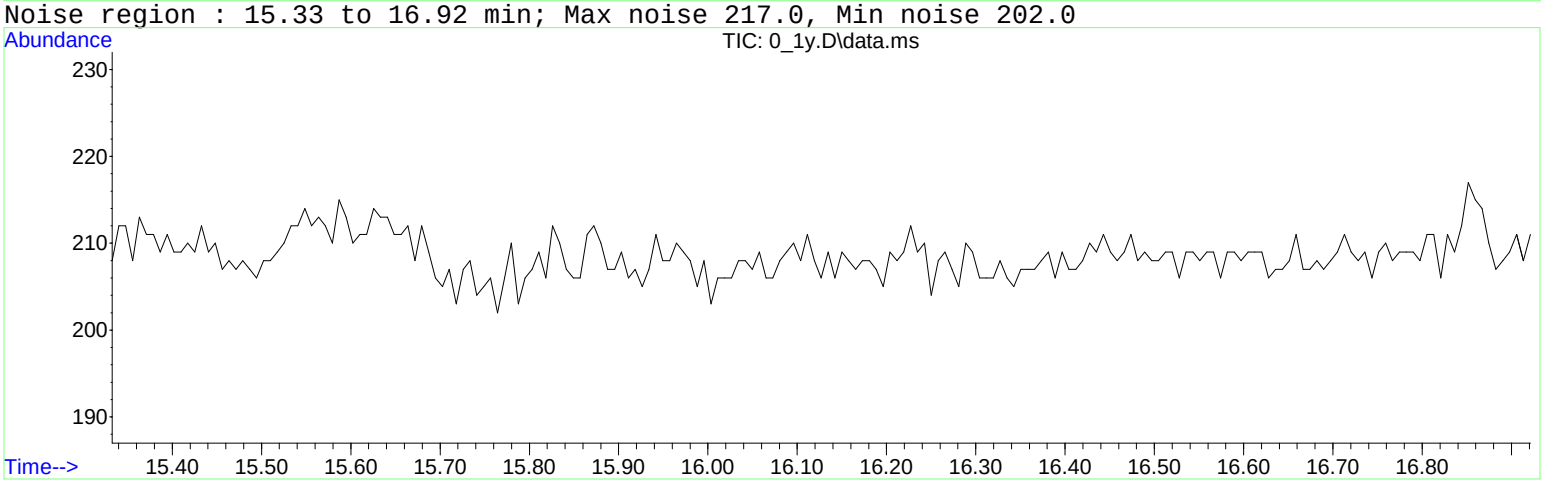

Calculations	Value
Noise Points used	207
Average noise = (sum of noise)/points	208.6
Corrected Signal = height/Average noise	193.4
Pk-pk noise = Max noise/Min noise	15.0
Pk-pk S/N = Corrected signal/Pk-pk noise	12.9
RMS noise = SQRT(sum(square(noise-avg noise))/points)	2.4
RMS S/N = Corrected signal/RMS noise	81.7

Signal to Noise Report

Data Path : C:\msdchem\1\LENA\Masterarbeit\VerdünnungsreiheC\290612\NWG\y\
Data File : 0_1y.D
Acq On : 29 Jun 2012 20:07
Operator : lena
Sample : 0_1y
Misc : 0.5 ml verd-reihe C, 40 µl MSTFA sil
ALS Vial : 10 Sample Multiplier: 1

Integration File: autoint1.e

Method : C:\msdchem\1\METHODS\BENE1.M
Title :
Last Update :

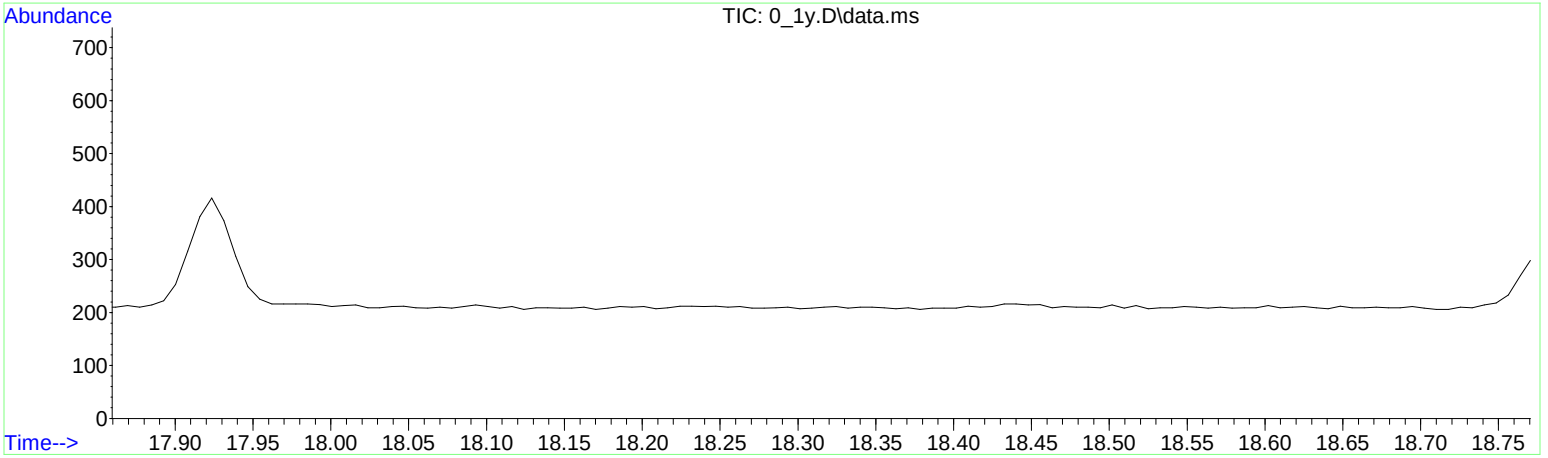

Signal region: 17.88 to 17.96 min; height: 416

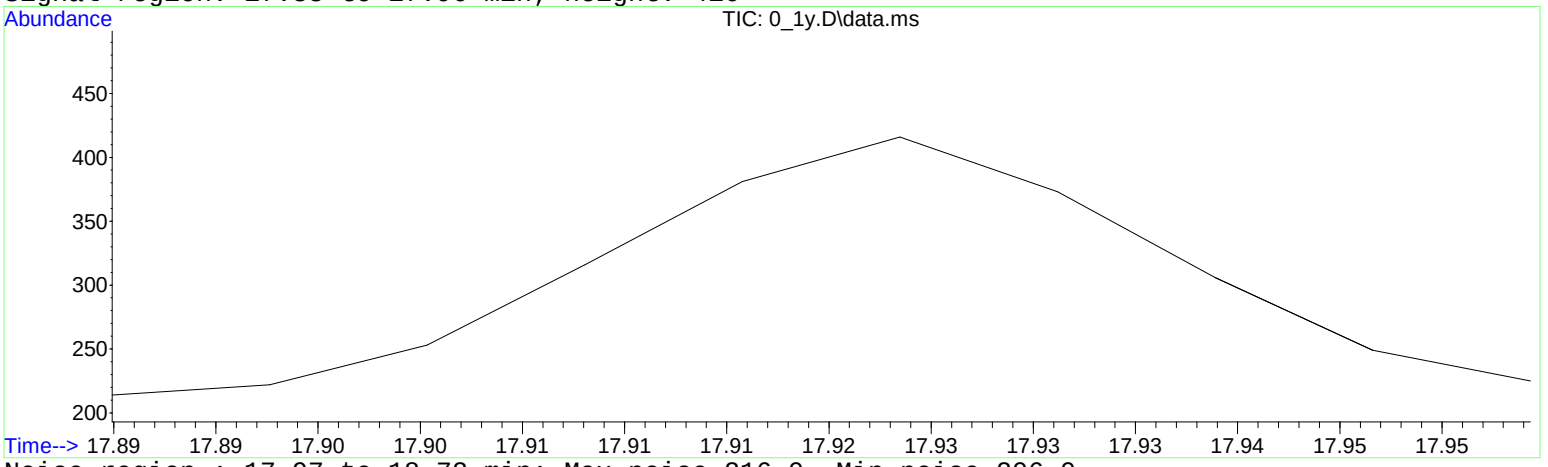

Noise region : 17.97 to 18.72 min; Max noise 216.0, Min noise 206.0

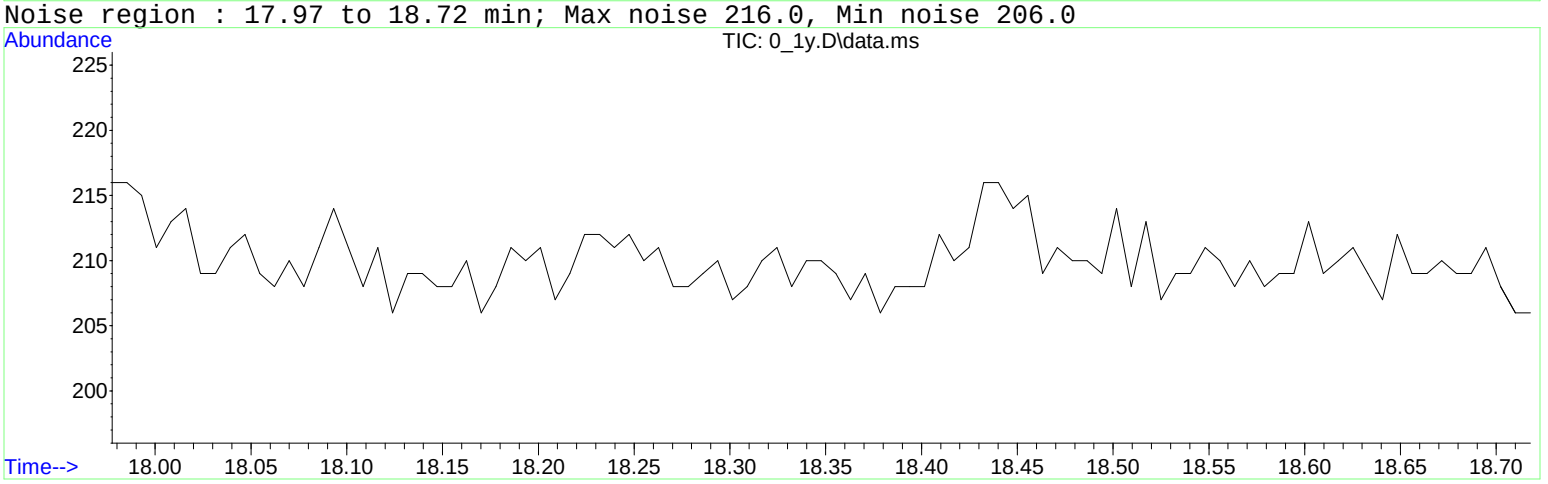

Calculations	Value
Noise Points used	97
Average noise = (sum of noise)/points	210.0
Corrected Signal = height/Average noise	206.0
Pk-pk noise = Max noise/Min noise	10.0
Pk-pk S/N = Corrected signal/Pk-pk noise	20.6
RMS noise = SQRT(sum(square(noise-avg noise))/points)	2.4
RMS S/N = Corrected signal/RMS noise	87.5

Signal to Noise Report

Data Path : C:\msdchem\1\LENA\Masterarbeit\VerdünnungsreiheC\290612\NWG\y\
Data File : 0_1y.D
Acq On : 29 Jun 2012 20:07
Operator : lena
Sample : 0_1y
Misc : 0.5 ml verd-reihe C, 40 µl MSTFA sil
ALS Vial : 10 Sample Multiplier: 1

Integration File: autoint1.e

Method : C:\msdchem\1\METHODS\BENE1.M
Title :
Last Update :

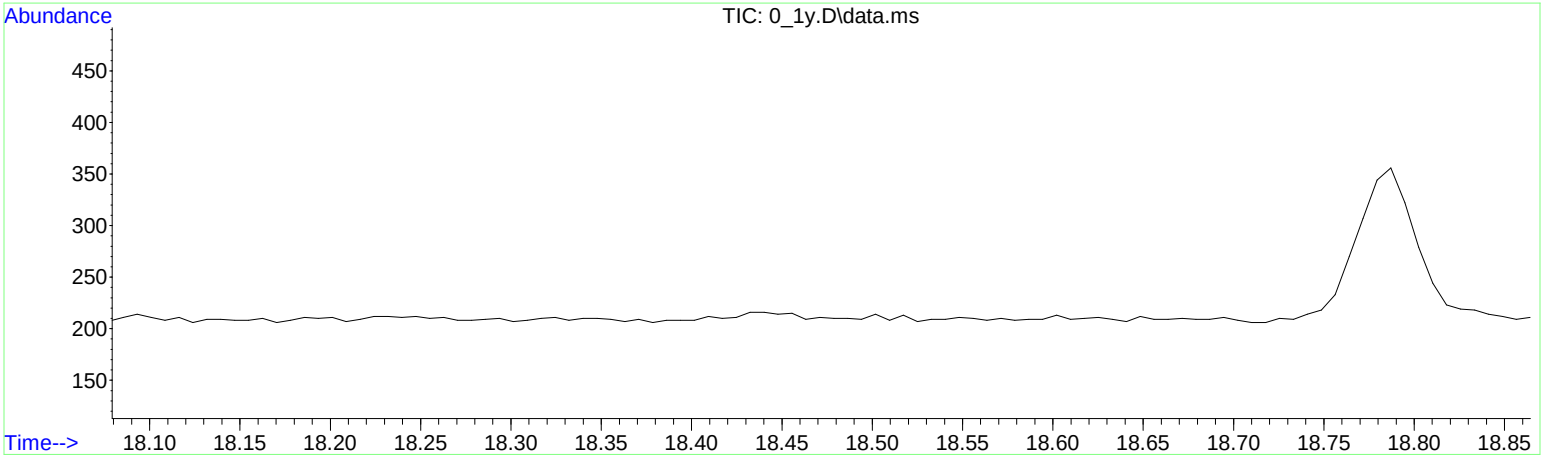

Signal region: 18.74 to 18.84 min; height: 356

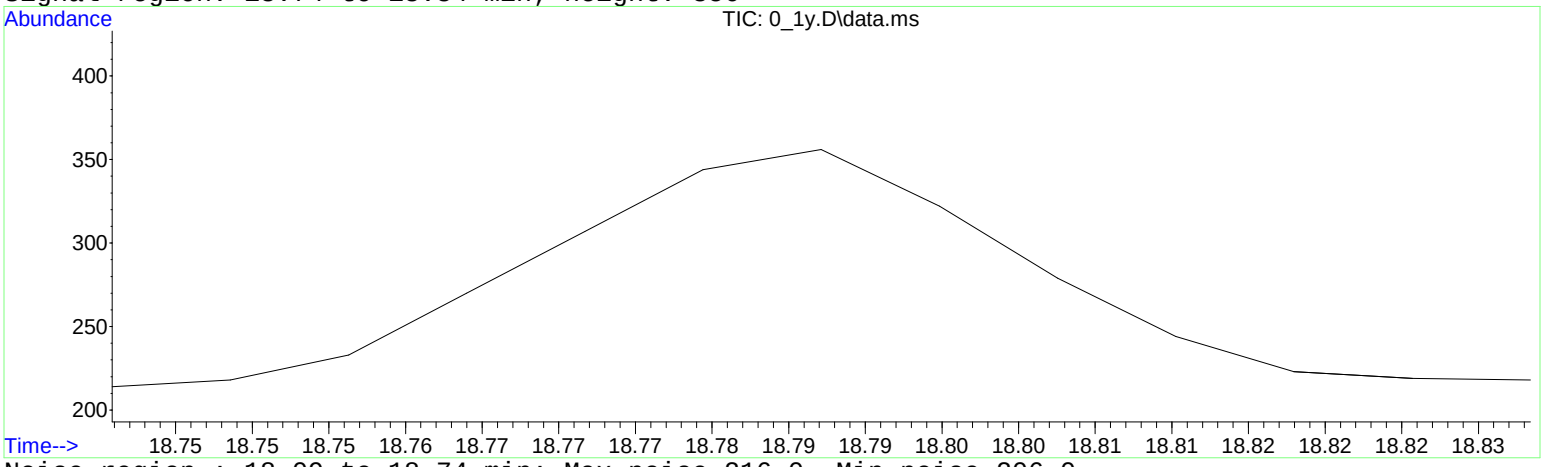

Noise region : 18.09 to 18.74 min; Max noise 216.0, Min noise 206.0

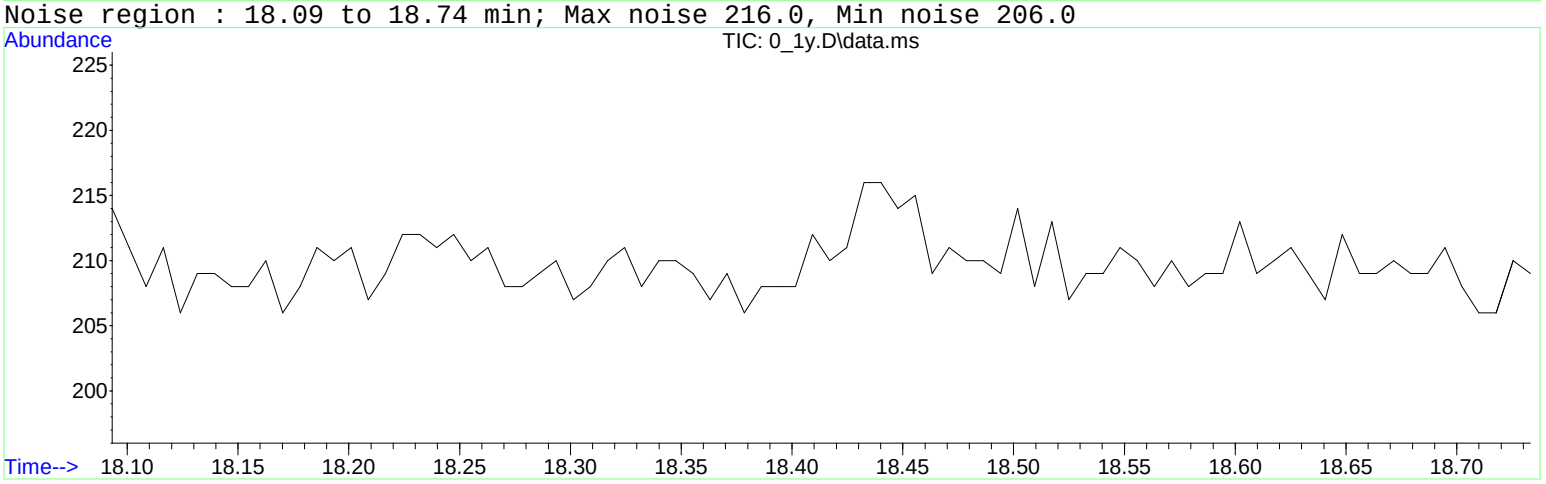

Calculations	Value
Noise Points used	84
Average noise = (sum of noise)/points	209.7
Corrected Signal = height/Average noise	146.3
Pk-pk noise = Max noise/Min noise	10.0
Pk-pk S/N = Corrected signal/Pk-pk noise	14.6
RMS noise = SQRT(sum(square(noise-avg noise))/points)	2.2
RMS S/N = Corrected signal/RMS noise	67.9